DESIGN CHARACTERISTICS OF TAPERED AND FACE GEARS IN MESH WITH CYLINDRICAL PINIONS

A Thesis Submitted
In Partial Fulfilment of the Requirements
for the Degree of
DOCTOR OF PHILOSOPHY

By
BIJENDRA SINGH BHADORIA

to the

DEPARTMENT OF MECHANICAL ENGINEERING
INDIAN INSTITUTE OF TECHNOLOGY KANPUR
AUGUST 1973

ME-1973-D-BHA-DES

CERTIFICATE

This is to certify that the work "Design Characteristics of tapered gears in mesh with cylindrical pinions" by BIJENDRA SINGH BHADORIA has been carried out under my supervision and has not been submitted elsewhere for a degree.

(Dr. J. Chakarborty)
Assistant Professor
Department of Mechanical Engineering
I.I.T. Kanpur.

ACKNOWLEDGEMENTS

The author wishes to express his gratitude to his thesis advisor, Dr. J. Chakarborty, for his expert guidance and steady encouragement throughout this work, to Mr. S.G. Dhande, for his constructive criticism, to Mr. Pradeep Wahi, Mr. M. Hariharan and Mr. A. Rajamani, for their efforts in correcting the manuscript, to Mr. Pawan Kumar for his help and friendship, to staff of I.I.T. Computer Center for making the necessary computer time available, to Mr. G.L. Misra and Mr. S.K. Tewari for their efficient typing and to all who helped in many ways, direct or indirect.

B. S. Bhadoria

August, 1973. *(B.S. Bhadoria)*

TABLE OF CONTENTS

NOMENCLATURE

a	off-set
A, B	given by equation (5.4.9)
A^*	$i_{21}a$
b	radial face width
c	clearance factor
C_f	surface condition factor
C_H	hardness ratio factor
C_L	life factor
C_ℓ	clearance between surfaces
C_s	size factor
C_T	temperature factor
C_V	dynamic load factor
DZO	$Z_o - Z_1$
E^*	$\dfrac{a(i_{21} - C\Sigma)\, i_{21} \sec\beta}{1 - 2i_{21}C\Sigma + i_{21}^2}$
E_1, E_2	young's modulii
$\underset{\sim}{e} : (e_x, e_y, e_z)$	unit normal vector
F	force
hp	horse power
i	transmission ratio
i_{o1}	Z_1/Z_o
i_{12}	Z_2/Z_1
i_{20}	Z_o/Z_2
ℓ	normal deviation

ν	angle (Figure 12)
$\nu_{1,2}$	possion's ratios
ξ	correction factor
$\hat{\rho}$	lead of the screw on screw axis
Σ	shaft angle
Σ_i	surface of ith gear
σ	angle between the principal directions
ϕ	angle of rotation
Φ_k	$\theta_k + \phi_1$
χ	curvatures
ψ	pressure angle at contact point
$\underset{\sim}{\Omega}$	angular velocity vector
ω	angular velocity

MATHEMATICAL SYMBOLS

$\rightarrow$	implies
Abs| |or| |	absolute sign
$\forall$	for all
$C\theta$ or $C(\theta)$	cos (η)
det | |	determinant sign
ϵ	number of the following set
$\ni$	such that
$\notin$	not a member of the following set
inv(θ)	tan θ - θ
$S\theta$ or $S(\theta)$	sin (θ)
$\cap$	intersection
[X,Y]	interval between X and Y

N	speed in rpm
$\underset{\sim}{N} : (N_x, N_y, N_z)$	normal vector
P	normal load
P_{rt}	rated tangential load at contact point
$\underset{\sim}{R} : (R_x, R_y, R_z)$	position vector
r	radius
r_f	radius of clearance cylinder
S	stress
S_{ac}	allowable contact stress number
$[S]$	allowable stress
$\underset{\sim}{V} : (V_x, V_y, V_z)$	velocity vector
V_T	tangential pitch line velocity
Z	number of teeth

GREEK ALPHABETS

α	pressure angle on pitch surface
β	Helix angle on base cylinder
δ	deflection
ϵ_γ	contact ratio
η	semi space width angle
Θ	scalar parameter of the surface
Θ^*	development angle of the involute curve
Θ_k^*	$\Theta_k - \lambda \tan\beta \mp \eta_1$
k^*	given by equation (5.52)
λ	scalar parameter of the surface
λ^*	$\dfrac{i_{21}\, S\Sigma\ \lambda \sec\beta}{1 - i_{21}\, C\Sigma}$

$\otimes$	set product
$S_1(x_1, y_1, z_1)$	rotating co-ordinate system fixed with pinion
$\bar{S}_1(\bar{x}_1, \bar{y}_1, \bar{z}_1)$	fixed co-ordinate system of pinion cutter
$S_2(x_2, y_2, z_2)$	rotating co-ordinate system fixed with gear
$\bar{S}_2(\bar{x}_2, \bar{y}_2, \bar{z}_2)$	fixed co-ordinate system of gear
$S(\eta, \xi, \ell)$	co-ordinate system at contact point

SUBSCRIPTS

a	related to addendum
b	base radius
B	back cone
c	contact surface
e	external dimensions
F	front cone
f	face or flank
i	internal dimensions
k	surface U and L
ℓ_c	lines of contact
MAX, max	maximum
MIN, min	minimum
m	mean
n	normal
p	pointing
r	motion on surface
s	circumfrential
t	tangent
u	undercutting

I,II	indices of curvatures of surface Σ_2
III,IV	indices of curvatures of surface Σ_2

SUBSCRIPTS

0 or o	related to cutter
1	pinion
2	gear
12	gear relative to pinion
21	pinion relative to gear
~	vector

SUPER ~~SUB~~SCRIPTS

.	total derivative with respect to time
-	related to fixed coordinate system
0 or o	related to cutter
1	pinion
2	gear
12	gear relative to pinion
21	pinion relative to gear
~	set

SYMBOLS USED IN TABLES

ABS	$2\lvert A+B\rvert$
AREA	πab
ACAP	A in (equation 49)
ASMAL	a equation 5.53
ASTAR	$a\, i_{21}$
ASTR	a* in equation 5.53

BSTR	b* in equation (5.54)
DSTR	δ* in equation (5.55)
BCAP	B in equation (5.49)
BETA	helix angle
BETA*	optimum helix angle
BSMALL	b in equation (5.54)
D1	nominal pitch dia of pinion
D2	nominal pitch diameter of cutter or pinion
DEL	δ in equation (5.55)
DZO	$Z_o - Z_1 \quad \frac{a(i_{21}-C\Sigma)i_{21}\text{Sec}\beta}{1 - 2i_{21}C\Sigma + i_{21}^2}$
E*	
FACE	b
FAIK	ϕ_k
FAI1	ϕ_1
I12	i_{12}
I21	i_{21}
KAI1, KAI2	χ_1, χ_2, etc.
L	related to surface L of figure 2
L*	λ*
LAMDA*	λ*
L1	$-1000\ \ell_1$ [table 11]
L2	$-1000\ \ell_2$ [table 11]
L1 - L2	$-1000\ (\ell_1 - \ell_2)$ [sec. 5.4.1]
M	Module
NU	ν [Figure 12 and 13]
R2U	radius of the gear at which undercutting occures

R2P	radius at which pointing occures
S	S_{max} in [equation 5.57]
SIG	σ , angle between axes of χ_I and χ_{III}
SIG1	σ_1, [Figure 12 or equation 5.47]
TAO	$\cos\tau$ [equation 5.51]
THT	θ^*
WIDTH or W	b
ZO	Z_o
Z1	Z_1
Z2P	z_{2p}
z2U	z_{2u}

LIST OF TABLES

LIST OF FIGURES

Page No.

"Design characteristics of tapered and face gears in mesh with Cylindrical pinions

A thesis submitted

in partial fulfilment of the requirements

for the Degree of

DOCTOR OF PHILOSOPHY

by

BIJENDRA SINGH BHADORIA

to the

DEPARTMENT OF MECHANICAL ENGINEERING

INDIAN INSTITUTE OF TECHNOLOGY, KANPUR.

AUGUST , 1973.

ABSTRACT

The tapered gears mating with cylindrical involute helicoid pinion mounted on skew shafts are considered in this work. The equation of contact, the equation of contact line, the equation of the surface of action and the equation of conjugate tooth surface of tapered gears has been developed. The discussion here includes the face width limitations and other design parameters like pressure angle, blank shape, contact ratios, normal curvatures, contact localization contact stress and the surface durability rating. Cases of on-center spur and spiral face gears, off-set spur and spiral face gears and on-center spur and spiral tapered gears are considered as special cases of tapered gears.

CHAPTER 1

INTRODUCTION

Gears transmit motion and energy from one shaft to another. Selection of gears to perform a desired function depends on the relative disposition of the axes, geometry of the tooth profile, demands on efficiency, load carrying capacity, restriction on space and nature of environment. The knowledge of theory of gearing is necessary to have a clear understanding of the geometry of teeth, kinematics and dynamics of gear teeth in action.

1.1 The tapered gear

A tapered gear meshes with either a cylindrical or a tapered pinion. In theory, the pinion may have any tooth profile so long as a conjugate tooth profile is achieved on the gear. The axes of the gear and pinion may be either intersecting or skew. The shaft angle may be anything, from 0° to 90° for an internal gear and from 90° to 180° for an external gear. The two limiting cases[1], of zero degree and 180 degrees are familiar internal and external cylindrical gears mounted on parallel shafts when the pinion is cylindrical. The gear tooth may be spur or spiral depending on whether the pinion is spur or helical [1] . The face gear is a particular case of the tapered gear when the angle between the shaft axes is 90 degrees. In the

---

1 Here, the shaft angle of 180° corresponds to external gear due to the particular choice of the co-ordinate system.

present dissertation discussions are confined to spiral and spur tapered and face gears in mesh with cylindrical involute pinions.

1.2 Methods of manufacture

The pinion, being a conventional involute spur or helical gear, can be manufactured on a hobbing machine or on a gear shaper. The tapered gear is generated on a gear shaper. A special fixture is used to mount the blank at the required axis-disposition and to impart the necessary generating motion. The same shaper cutter can be used to produce both the gear and the pinion.

1.3 Advantages of tapered gears

In comparison with other gears, tapered gears have the following advantages [1] [2] :

1 Cutting of the pinion of a tapered gear set requires no special operations or equipment. The tapered member requires some special fixture on the gear shaper. But, the cost of cutting operation itself is comparable to that of a cylindrical gear of the same size and module.

2 The pinion of a tapered gear set can be adjusted axially while assembling without affecting contact or backlash. Thus only one assembly parameter has to be maintained accurately against three parameters for a bevel gear. There is no axial thrust in the pinion bearings in case of spur tapered gear.

3 Generation is positive with no trial and error settings required to obtain the conjugate profile.

4 Off-set gears are produced on the same machine and with the same cutter as used to generate on-center gears. Furthermore, the cost of production is not increased by changing from on-center to hypoid gears.

The following are the disadvantages of tapered gears :

1 The face width of a tapered gear is limited by pointing and undercutting of teeth. For some combinations of the independent design parameters the gear width may be so small that the tapered gear cannot be used.

2 Shaper cutters for tapered gears are usually less versatile than the cutter blades used to produce conventional gears [2].

1.4 Practical applications

Face gears have been commercially manufactured for many years. They have been used in textile machinary, truck engines, governor drives, power mower transmissions and gear cutting machinery [2] . The use of tapered gears, in general, has not been as wide spread as their practicability warrants.

1.5 Review of existing work

A gear designer, in general, faces problems associated with the following :

1 Geometry considerations - selection of the tooth profile from the point of view of (a) ease in manufacture, (b) inspection and (c) sensitivity of the performance depending upon the assembly parameters.

2 Load considerations - choice of the independent design parameters to perform a given function.

Some information is available about the geometry of tapered and face gears. Face gears have been introduced and developed by the Fellows Gear Shaper Co. of U.S.A. One of the earliest publications in this field is by Bloomfield [3] . He devised a geometrical method to find the limiting dimensions of these gears. Bloomfield obtained the data for on-center face gears and presented it in the form of alignment charts [4] . The conclusions (in [3]) regarding the nature of the pitch surface of the hypoid face gear have been found not to conform to the laws of gearing [5] . Analytical investigations on face gears have been performed by Buckingham [6] . His method lacked generality and the proposed procedure had to be repeated for every new type of gear set.

The work of Sanborn and Bloomfield [1] in the field of tapered gears made important contributions. The authors have pointed out the effect of shaft angle on the face width of spur tapered gears. The effect of off-sets on the blanks of these gears is discussed in reference [1] . Other notable contributions in this field are by Vector Silvagi [2] and Bloomfield [7] .

An analytical investigation on on-center spur tapered gear and face gear has been presented by Litvin [8] . The kinematic method discussed by Litvin is a developed version of the methods given by Gochman [9] and Kolchin [10] . An analysis of on-center spur face gears in mesh with involute spur pinion is given in [11] . Studies on

hypoid face gears meshing with involute spur pinions have been reported in [12] . A detailed analysis of on-center tapered, hypoid tapered and face gears in mesh with cylindrical involute pinions is given in [5] . This work contains studies on the pointing and undercutting of gear teeth, variation of pressure angle and determination of contact ratio. In reference [5] , the contact ratio of face gears is found using the method suggested in [13] .

Very few authors have reported regarding the load considerations of the tapered and face gears. Some information about the surface durability ratings of the on-center spur face gears is available in reference [14] . The determination of the surface durability rating of spatial gears is a complicated task. Some of the important factors influencing the surface durability rating are given below :

1. Material characteristics of the pinion and gear
2. Reduced principal curvatures at points of contact
3. Pressure angle at contact points
4. Dynamic load factor
5. Contact ratio.

Much investigation has been done to evaluate the curvature of the tooth surface at points of contact [15][16][17][18][8] . The method given by Litvin [17] is used in the present dissertation to find the reduced normal curvatures at points of contact.

1.6 Objectives and scope of the present work

Hypoid tapered gears in mesh with cylindrical involute helical pinions are analysed in this dissertation. Off-set and on-center face

gears and on-center tapered gears are particular cases of the tapered gears considered.

The following results are obtained in this work :

For tapered gears :

1 The equation of conjugate gear tooth profile of the gear.

2 The equation of addendum surface of the gear blank

3 Equations governing pointing and undercutting of the gear teeth

4 Formulas to calculate the principal curvatures of the gear tooth surface

5 A general method to find the pressure angle in mechanisms having point or line contacts. This method is applied to tapered gears

6 The method to find the contact ratio in spatial gearing. This method is illustrated by an example.

For spur face gears with localized contact :

7 Formulas to investigate the contact localization

8 Equations for finding contact spot, contact zone and contact stress

9 A general formula to find the surface durability ratings of spatial gears having point contact

10 Formulas to find the surface durability rating of a face gear

11 Study of the effects of the independent design parameters on surface durability rating.

1.7 Presentation of contents

An equation of contact is derived using the condition that at the contact point the common normal and the relative velocity vector are perpendicular to each other. Using this condition contact lines, surface of action and conjugate btooth profile of the gear are found in chapter 2. The shape and size of the gear blank depends upon the independent parameters of meshing. Transmission ratio or velocity ratio, shaft angle, helix angle, pressure angle, off-set and the number of teeth in the pinion or cutter are considered as the independent parameters. A formula for the optional shape of the tapered gear blank is derived in chapter 2. The limiting dimensions to avoid undercutting and pointir of teeth and principal curvatures of gear surface are discussed in the same chapter.

A kinematic method to find the pressure angle in mechanisms havi line or point contacts is discussed in chapter 3. The method has been applied to find the pressure angles in tapered gear set.

A method based on elementary set theory is developed in chapter 4 to simplify the computation of contact ratios in space gear mechanisms.

Contact localization, contact spot, contact zone, contact stress and surface durability rating of spur face gear set are discussed in chapter 5.

Finally, in chapter 6, example problems are given to illustrate the use of the formulas developed in the previous chapters. The effect of independent design parameters on surface durability rating is discussed in the same chapter. The discussions and conclusions are also presented in chapter 6.

CHAPTER 2

ANALYSIS OF TAPERED GEARS

The equations developed in this chapter, unless otherwise stated, are applicable to any type of tapered gear. The equations are expressed in a general form. The use of these equations in special cases of tapered gears is given in Chapter 5.

2.1 Conjugate Action of Gear Tooth Surface

Two surfaces are conjugate if each generates or envelops the other under a specified relative motion. Thus, if a tooth surface of one gear is rigid and the mating tooth of the second gear is of a plastically deformable material, the specified relative motion will produce tooth of the second gear which is conjugate to the tooth surface of the first.

At any instant, conjugate surfaces have a line of contact which is the locus of all points of contact at that instant.

At any point of contact, the surfaces must have a common normal. As surfaces are not digging in each other or coming out of contact at the next instant, the component of the relative velocity vector in the normal direction [5][8] is zero. This is the basic requirement for gear tooth contact. Thus, the relative velocity vector is perpendicular to the common normal and lies on the tangential plane.

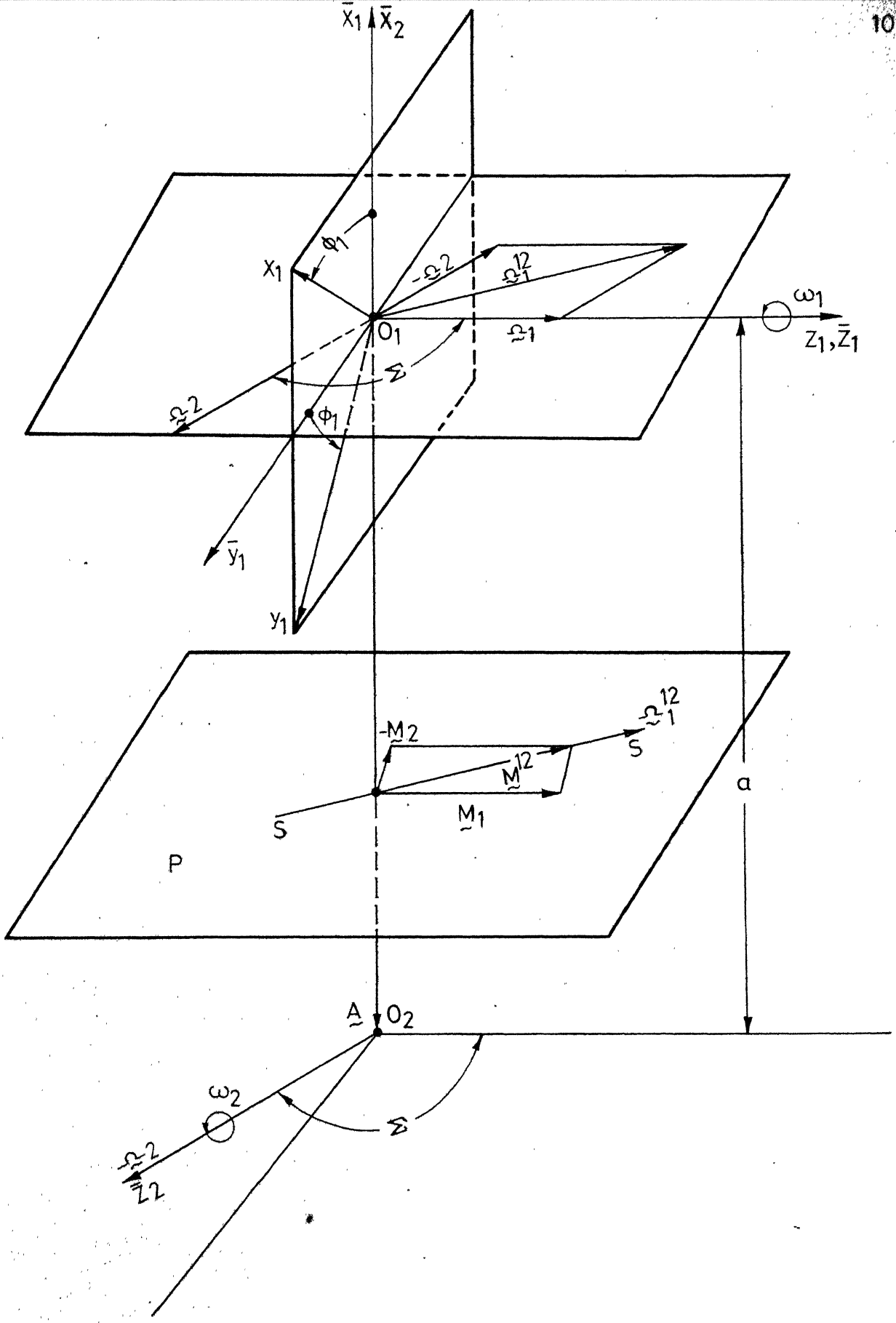

FIG.1 COORDINATE SYSTEM AND SCREW AXIS

In the process of meshing, the line of contact describes a surface in fixed space, called the surface of action.

The locus of the line of contact in the co-ordinate system of gear is the conjugate tooth surface of the pinion.

In this chapter, an investigation is made on the limitations of the face width, the pressure angle in mesh, the contact ratio and the curvatures at points of contact. The derivations will be used to find the instantaneous contact spots, contact zone, relative curvatures and the various effects of contact localization in case of spur face gears.

The profile of the pinion or cutter is described with reference to a set, s_1, of rectangular cartesian axes (x_1, y_1, z_1) which rotate with the pinion or cutter, where z_1 axis coincides with the axis of rotation [Figure 1] . There is a similar set $s_2(x_2, y_2, z_2)$ for the gear. The set $\bar{s}_i(\bar{x}_i, \bar{y}_i, \bar{z}_i)$[1] is stationary in space and coincides with $s_i(x_i, y_i, z_i)$ at some particular position. The angle of rotation of the i^{th} gear measured from this position is denoted by ϕ_i and the angular velocity $d\phi_i/dt$, by ω_i. Axes $\bar{x}_1$ and $\bar{x}_2$ are chosen along the common perpendicular to the axes of rotations, z_i's. The length of common perpendicular between the two axes, is the off-set 'a'. The angle between the axes, $\bar{z}_1$ axis and the projection of $\bar{z}_2$ axis on $\bar{y}_1 - \bar{z}_1$ plane, is denoted by Σ [Figure 1] .

---

[1] for pinion, i = 1 and for gear, i = 2.

2.2 Relative Velocity Vector, Screw Axis and Pitch Surfaces

In this section, equations governing the relative velocity vector, the screw axis and the pitch surfaces are presented. More detailed development of these equation is given in [5] . These will be needed in subsequent analysis. It will be assumed that (i) the transmission ratio is constant and (ii) the shaft angle 'Σ' and the hypoid eccentricity 'a' are known.

Relative velocity vector, $\bar{\underset{\sim}{V}}_1^{12}$, at any point R_1 on the pinion tooth with respect to the coinciding point on the gear is the difference between the instantaneous absolute velocities at this point. Thus

$$\bar{\underset{\sim}{V}}^{12} = \bar{\underset{\sim}{V}}_e^1 - \bar{\underset{\sim}{V}}_e^2 = \underset{\sim}{\Omega}_1 \times \bar{\underset{\sim}{R}}_1 - (\underset{\sim}{\Omega}_2 \times \bar{\underset{\sim}{R}}_1 + \underset{\sim}{A} \times \underset{\sim}{\Omega}_2)$$

Where $\underset{\sim}{\Omega}_1$ and $\underset{\sim}{\Omega}_2$ are angular velocity vectors of the rotation of the pinion and the gear respectively. $\underset{\sim}{A}$ is the position vector of the origin O_2 system in system S_1 [Figure 1] . It can be transformed to the rotating co-ordinate system, S_1, using transformation matrix Q_{11} and can be written as

$$\underset{\sim}{V}_1^{12} = \begin{Bmatrix} -[y_1(1-i_{21}C\Sigma) + z_1\, i_{21}\, S\Sigma\, C\phi_1 + a\, i_{21}\, C\Sigma\, S\phi_1] \\ [x_1(1 - i_{21}C\Sigma) + z_1\, i_{21}\, S\Sigma\, S\,\phi_1 - a\, i_{21}\, C\Sigma\, C\,\phi_1] \\ [i_{21}\, S\Sigma\, (x_1 C\,\phi_1 - y_1\, S\,\phi_1 + a)] \end{Bmatrix} \qquad 2.1$$

The expressions for the transformation matrices are given in Appendix I. Screw axis of the relative motion is the axis along which vectors $\bar{\underset{\sim}{V}}_1^{12}$ and $\underset{\sim}{\Omega}_{12}$ are collinear [5] [8] . Thus along this axis ,

$\underset{\sim}{\Omega}_{12} \times \underset{\sim}{\bar{V}}_1^{12} = 0$, where , $\underset{\sim}{\Omega}_{12}$ is the relative angular velocity vector.

The position and orientation of the screw axis are given by the following expressions

$$\bar{X}_1 = -a \frac{(i_{21} - C\Sigma) i_{21}}{1 - 2\, i_{21}\, C\Sigma + i_{21}^2} \qquad 2.2$$

$$\bar{Y}_1 = -\bar{Z}_1 \frac{i_{21}\, S\Sigma}{1 - i_{21} C\Sigma}$$

Lead, $\hat{\rho}$, of the screw is given by

$$\hat{\rho} = a \frac{i_{21}\, S\Sigma}{1 - 2\, i_{21}\, C\Sigma + i_{21}^2} \qquad 2.3$$

Pitch surfaces of pinion and gear are defined as the loci of the screw axis in their respective co-ordinate systems. Transforming equation (2.2) to the co-ordinate system S_1 and eliminating ϕ_1 from the resulting equations, we get pitch surface of the pinion as

$$x_1^2 + y_1^2 - D^2 z_1^2 = C^2 \qquad 2.4$$

where

$$C = a \frac{(i_{21} - C\Sigma) i_{21}}{1 - 2\, i_{21}\, C\Sigma + i_{21}^2} \quad \text{and} \quad D = \frac{i_{21}\, S\Sigma}{1 - i_{21}\, C\Sigma}$$

Similarly, we get pitch surface of the gear as

$$x_2^2 + y_2^2 - F^2 z_2^2 = E^2 \qquad 2.5$$

$$E = \frac{a(1 - i_{21}\, C\Sigma)}{1 - 2\, i_{21}\, C\Sigma + i_{21}^2} \quad \text{and} \quad F = \frac{S\Sigma}{i_{21} - C\Sigma}$$

Equations (2.4) and (2.5) represent hyperboloids of revolution. The lead of the screw can be zero only in the following cases: (i) $\Sigma = 0$ or π and (ii) $a = 0$. They correspond to gears having parallel and intersecting axes respectively. For these cases, the relative velocity will be zero on the screw axis. The pitch surfaces will be in pure rolling. Further, it may be seen from equations (2.4) and (2.5) that corresponding pitch surfaces are either cylinders or cones.

It should be noted that pitch surfaces do not depend on the type of the tooth profile but only on the relative disposition of shafts and their specified relative motion.

The pitch surface is generally used as a basis for designing gear blank. Thus conical blanks are used for bevel gears and cylindrical blanks for spur and helical gears. When this is not done, practical disadvantages like pointed teeth or under cutting may become apparent. In the case of tapered gears since the gear teeth are not positioned more or less symmetrically around the pitch surfaces, these disadvantages are inherent in the gears under consideration.

2.3 Tooth surfaces of the cutter and the pinion.

Tooth surfaces of the pinion and the cutter are needed for subsequent development of the conjugate tooth surface on the gear. It may be noted that tapered and face gears the number of teeth of the cutter may be different from that of the pinion. Basically

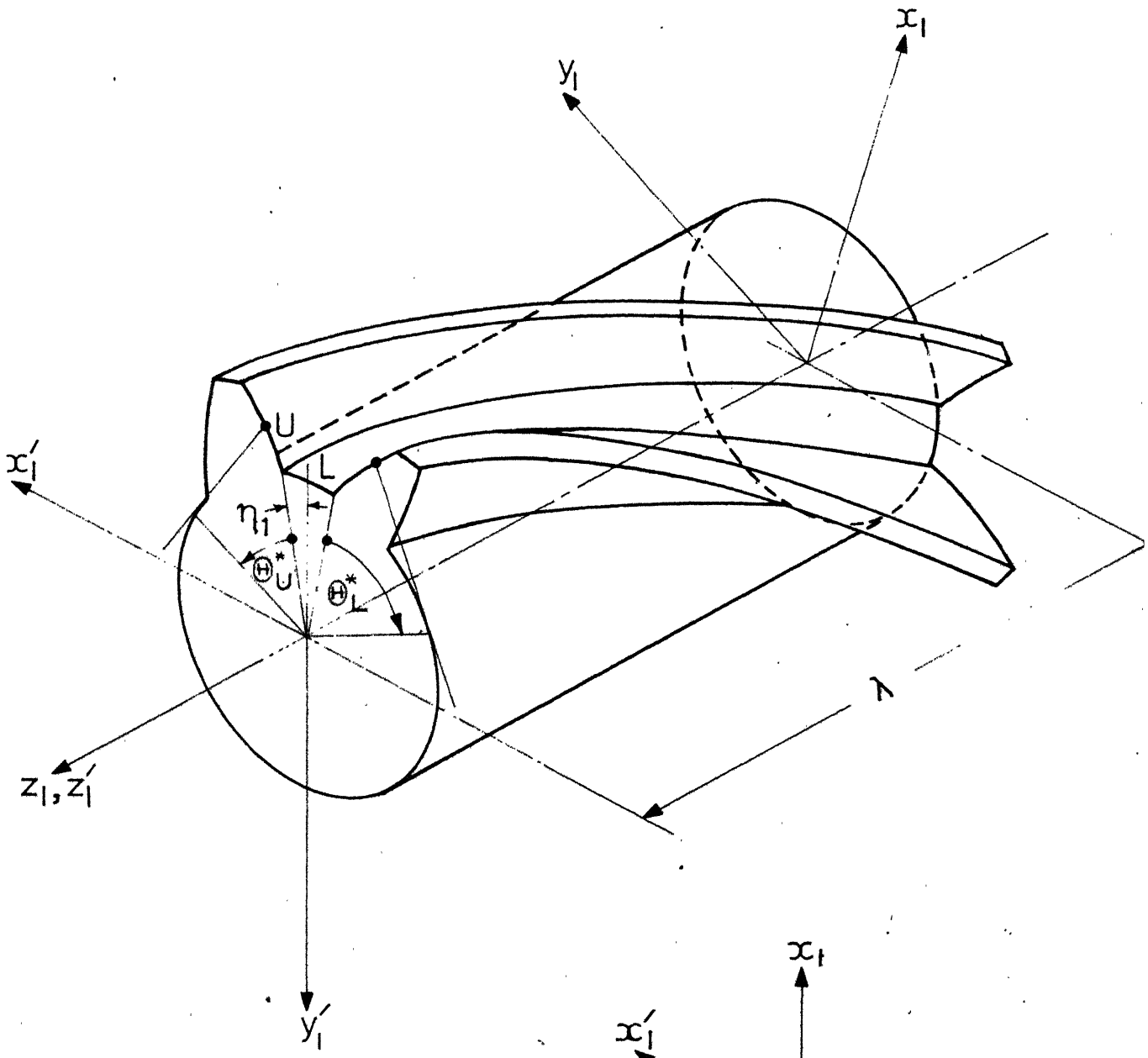

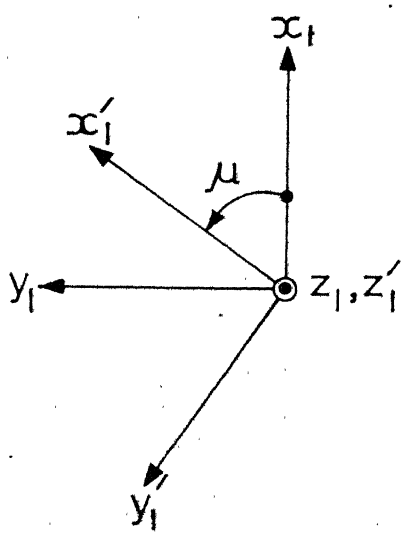

$\Theta_K = \lambda \tan\beta \pm (\Theta^*_K + \eta_1)$

$\mu = \lambda \tan\beta$

β - helix angle

both the tooth surfaces are involute helicoid the spur gear being a special case when the helix angle is equal to zero.

An involute helicoid is the surface generated by the helical motion of an involute curve about the axis of the base cylinder Figire 2. To non-dimensionalize all quantities with respect to the radius of the base cylinder of pinion, the radius of the base cylinder is taken to be unity. The equation of the pinion surface can be written as[1] [5][11]

$$\underset{\sim}{R}_1(\theta_k,\lambda) = [\{S\theta_k - \theta^* C\,\theta_k\}, -\{C\theta_k + \theta_k^* S\,\theta_k\}, \lambda]^T;\ k = U,L \qquad 2.6$$

where $\theta_k^* = \theta_k - \lambda \tan\beta \mp \eta_1$,

$\beta \neq (2n+1)\pi/2$; $n = 0,1,2,3,\ldots$

β is the helix angle on base cylinder,

θ_k,λ are the parameters of the surface,

and η_1 is the semi space-width angle.

The upper and lower signs respectively correspond to the surfaces U and L in Figure 2.

In general, equation (2.6) represents an involute helicoid. The surface of a straight tooth pinion can be obtained by substituting $\beta = 0$ in this equation.

The tooth surface of the pinion will be identical to that of the cutter if the number of teeth, the pressure angle and the

---

[1] Subscript 1 corresponds to the surface of gear cutter/pinion in this case.

correction factor are the same. Otherwise, the tooth surface of the former can be obtained from the following equation

$$\underset{\sim}{R}_1 = i_{o1}[\{S\theta_k - \theta_k^* \; C \; \theta_k\}, -\{C\theta + \theta_k^* \; S \; \theta_k\}, \lambda]^T \qquad 2.7$$

where,

$$\theta_k^* = \theta_k - \lambda \tan \beta \mp \eta_1$$

$$i_{o1} = Z_1/Z_o$$

and $$\eta_1 = \pi/2Z_1 - \text{inv}\, \alpha_{1s} - \frac{2\,\xi_{1s}}{Z_1 \tan \alpha_{1s}}$$

To get the semi space width angle of the cutter, subscript '1' should be replaced by the subscript '0'.

In the case of standard cutters and pinions $\xi_{0s} = 0$ and $\xi_{1s} = 0$ respectively.

The normal vector to any surface, $\underset{\sim}{R}_1 = \underset{\sim}{R}_1 (\theta, \lambda)$, is given by $\underset{\sim}{N} = \frac{\partial \underset{\sim}{R}_1}{\partial \theta_k} \times \frac{\partial \underset{\sim}{R}_1}{\partial \lambda}$. Here θ and λ are the parameters of the surface. In the case of involute helicoid surface, it can be written as

$$\underset{\sim}{N}_1 = [-\theta_k^* \; C \; \theta_k, \; - \theta_k^* \; S \; \theta_k, \; \theta_k^* \tan \beta]^T \qquad 2.8$$

So the unit normal vector is

$$\underset{\sim}{e}_1 = [-C \; \theta_k \; C\beta \; , \; - S \; \theta_k \; C\beta, \; S\beta]^T \qquad 2.9$$

2.4 The conjugate tooth profile.

Some of the methods to determine the equation of contact and subsequently, the conjugate tooth profile are mentioned below:

1. The classical differential geometry method
2. The method of Gokhman [9]
3. The kinematic method [8] .

In the present disertation, the kinematic method is used.

The conjugate tooth profile of the meshing gear can be found by transforming the contact lines to the co-ordinate system of the gear. Hence, at the outset, contact lines on the pinion are to be found. In order that a point on the tooth surface of the pinion be a contact point, certain conditions must be satisfied. The conditions can be obtained by the following considerations.

Let tooth surfaces Σ_1 and Σ_2 , while moving in space relative to each other, make contact at the point P at any instant and let $\underset{\sim}{V}_1^{12}$ be the relative velocity vector of the two surfaces at the point P. For conjugate action this vector must lie on the common tangent plane through P. Otherwise surfaces will be either digging in or coming out of contact at the next instant [5] [8] [18] [19] [20] . In other words, if $\underset{\sim}{N}_1$ is the common normal, then vectors $\underset{\sim}{V}_1^{12}$ and $\underset{\sim}{N}_1$ will be mutually perpendicular. Or

$$\underset{\sim}{V}_1^{12} \cdot \underset{\sim}{N}_1 = 0 \qquad 2.10$$

The above condition results in a mathematical expression relating different parameters. This is known as the equation of contact and is given as

$$f(\theta,\lambda,\phi_1) = 0 \qquad (2.11)$$

θ, λ are parameters of the pinion surface and ϕ_1 is the parameter of motion of the surface Σ_1.

It is seen that the equation of contact gives the condition which must be satisfied by the parameters at all contact points. This is the fundamental requirement for the gear tooth contact. As the contact point lies on the tooth surface the condition given in equation (2.11) must be satisfied at this point. The contact point is found from equations (2.6) and (2.11) by eliminating one of the two independent parameters, θ or λ. Thus we get the equation of a space curve which is the contact line for the angle of rotation ϕ_1. By eliminating λ from equations (2.6) and (2.11), the equation of the contact line is obtained in the form ,

$\underset{\sim}{R}_{\ell c} = \underset{\sim}{R}_{\ell c}(\theta,\phi_1)$.

The locus of the lines of contact in the co-ordinate system S_2 of the gear gives the conjugate gear tooth surface. The conjugate surface Σ_2 of the gear can thus be found by transforming $\underset{\sim}{R}_{\ell c}$ to the co-ordinate system S_2, using the relation $\underset{\sim}{R}_2 = \underset{\sim}{R}_2(\theta,\phi_1) = Q_{21}\,\underset{\sim}{R}_{\ell c}$, where Q_{21} is the transformation matrix.

2.5 General equation of contact for tapered gears.

Let the cutter be of involute helicoid form. The angle between the axes of the cutter and the gear is Σ and the eccentricity is 'a'. The equation of contact is obtained from equations (2.1), (2.8) and (2.10). After simplification the equation of contact takes the form

$$\lambda\, i_{21} S\Sigma C\Phi_k \sec^2\beta - [1 - i_{21} C\Sigma - a\, i_{21} C\Sigma S\Phi_k - i_{21} S\Sigma \tan\beta (S\Phi_k - (\theta_k \mp \eta) C\Phi_k + a)] = 0 \qquad 2.12$$

It can also be written as $f = f(\theta, \lambda, \phi_1)$ where, $\Phi_k = \theta_k + \Phi_1$; k = U,L.

Equation (2.12) is the general equation of contact for the hypoid tapered gears in mesh with the involute helicoid pinions. This equation has been derived earlier in a different form [5] .

For the external spur gear set, $\beta = 0$ and $\Sigma = \pi$. The equation of contact in this case takes the form

$$S\,\Phi_k = -(1 + i_{21})/i_{21}\, a \qquad 2.13$$

For involute helicoid worm gear set $\Sigma = \pi/2$ and $\beta \neq 0$, the equation of contact is

$$i_{21}\, \lambda\, C\,\Phi_k = 1 - i_{21} \tan\beta (\bar{x}_1 + a)$$

Similar expressions were derived previously by Kolchin [10] and Palit [21] following the method of Gochman [9] .

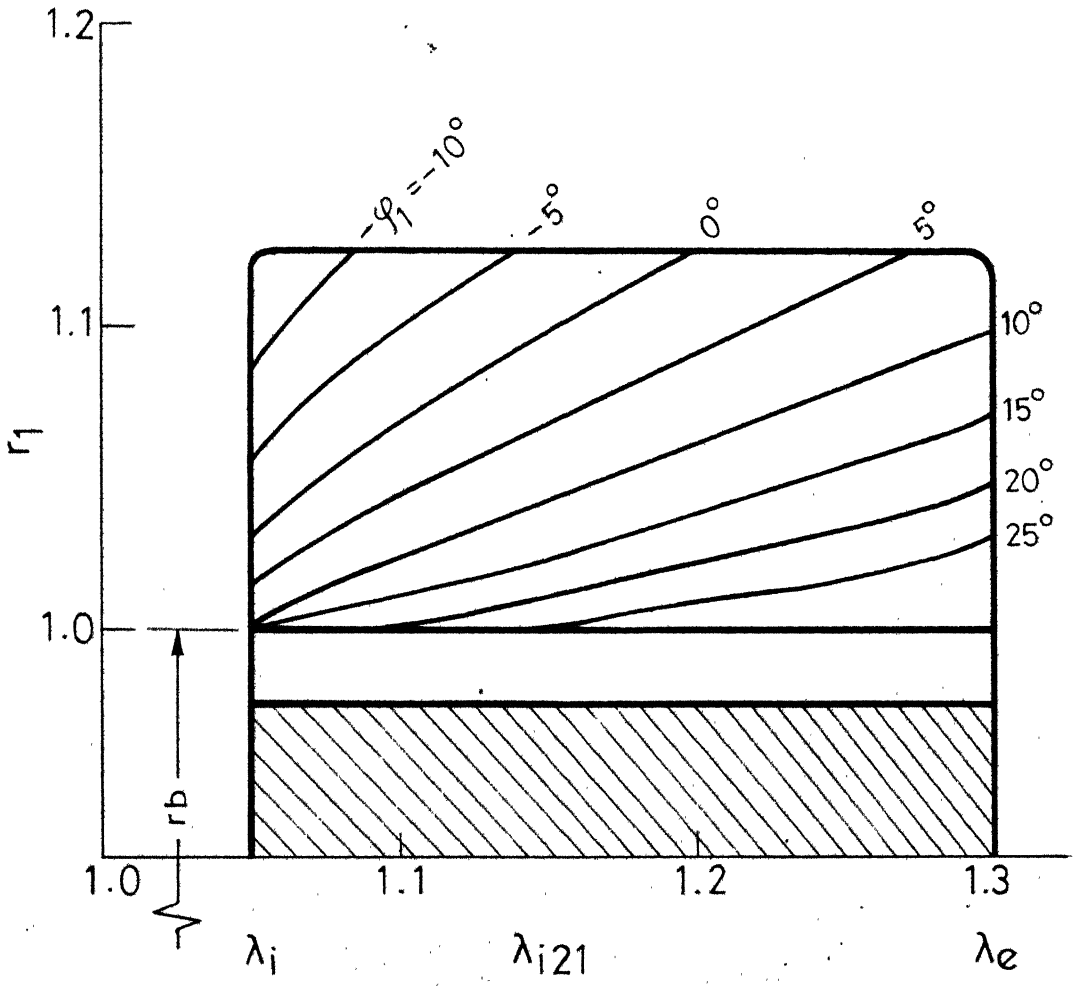

FIG. 3 LINES OF CONTACT ON PINION TOOTH.

(ON-CENTER FACE GEAR: $\Sigma=\pi/2, \beta=0, Z_1=20$ AND $\alpha_0=20°$)

2.6 Contact line, surface of action and the conjugate tooth surface

In the present section, equation of the contact line, the contact surface and the conjugate tooth profile for tapered gears are developed.

The equation of contact is rewritten in a different form

$$\lambda = \lambda(\Theta_k,\phi_1) = \frac{1-i_{21}C\Sigma-ai_{21}C\Sigma S\Phi_k-i_{21}S\Sigma \tan\beta(S\Phi_k-(\Theta_k\mp\eta)C\Phi_k+a)}{i_{21}\, S\Sigma\, C\,\Phi_k \sec^2\beta} \qquad 2.14$$

where, $\Phi_k = \Theta_k + \phi_1$

and $\Sigma \neq n\pi$; $n = 0,1,2,\ldots$

When equation (2.14) is used to eliminate λ from equation (2.6), we get equation of the line of contact as

$$\underset{\sim}{R}_{\ell c}(\Theta_k,\phi_1) = [\{S\Theta_k-\Theta_k^*C\Theta_k\},-\{C\Theta_k+\Theta_k^*S\Theta_k\},\lambda(\Theta_k,\phi_1)]^T;\ k = U,L \qquad 2.15$$

where,

$$\Theta_k^* = \Theta_k - \lambda(\Theta_k,\phi_1)\tan\beta \mp \eta_1 .$$

The lines of contact for an on-center face gear ($\Sigma = \frac{\pi}{2}$, $\beta=0$, $a = 0$) are shown in Figure 3. The locus of the line of contact in the fixed co-ordinate system $\bar{S}_1$ is the contact surface or the surface of action [5] [18] [19] .

One can transform $\underset{\sim}{R}_{\ell c}$ into the co-ordinate system $\bar{S}_1$ using the expression, $\underset{\sim}{\bar{R}}_c = Q_{11}^{-}\, \underset{\sim}{R}_{\ell c}$. On transformation, we get

$$\underset{\sim}{R}_c(\theta_k,\phi_1) = [\{S\Phi_k-\theta_k^*C\Phi_k\},-\{C\Phi_k+\theta_k^*S\Phi_k\},\ \lambda(\theta_k,\phi_1)]^T \qquad 2.16$$

The tooth profile $\underset{\sim}{R}_{2k}$ of the meshing gear is the locus of the contact line in the co-ordinate system, S_2. Transforming $\underset{\sim}{R}_{\ell c}$ to the system S_2, we get

$$\underset{\sim}{R}_{2k}(\theta_k,\phi_1) = \left\{\begin{array}{l} [(S\phi_k-\theta_k^*C\phi_k)C\phi_2-(C\Phi_k+\theta_k^*S\Phi_k)C\Sigma S\phi_2-\lambda S\Sigma S\phi_2+aC\phi_2] \\ -[(S\Phi_k-\theta_k^*C\phi_k)S\phi_2+(C\Phi_k+\theta_k^*S\phi_k)C\Sigma C\phi_2+\lambda S\Sigma C\phi_2+aS\phi_2] \\ [-(C\Phi_k+\theta_k^*S\Phi_k)S\Sigma+\lambda C\Sigma] \end{array}\right\} \qquad 2.17$$

2.7 Shape of blanks for tapered gears:

The optional blank shape of the tapered gear varies with the offset and the shaft angle. The maximum practicable offset in tapered gears can be as small as one-fourth of the nominal pitch diameter of the gear for $\Sigma = \frac{\pi}{2}$ i.e. for face gears. And it can be as large as the sum of the nominal pitch radii in gears having small shaft angles. In the latter case, the taper-effect practically disappears and the blank becomes almost cylindrical [1] . For an on-center gear the blank is conical while for a face gear the blank is in the form of a disc having teeth on the face. Determination of the actual size and shape of the gear blank is a prerequisite to the investigation of pointing and evaluation of the contact ratio. In the absence of a standard practice to fix the shape of the tapered gear blank, it is assumed that the blank always maintains a constant clearance with the root cylinder of the pinion. The clearance

cylinder is a cylinder coaxial with the pinion and having a radius r_f, which is equal to the sum of the radius of the root cylinder of the pinion and the radial clearance [Figure 5.] . $r_f=(1-2f_{1s}/Z_1)/\cos\alpha_{1s}$. The problem here is to find a surface of revolution on the axis of the gear which always touches the clearance cylinder.

The equation of the cylinder of radius r_f in the co-ordinate system $\bar{S}_2$ is written as

$$\underset{\sim}{R}(\theta,\lambda) = [\{r_f C\theta+a\},-\{r_f S\theta C\Sigma+\lambda S\Sigma\},\{-r_f S\theta S\Sigma+\lambda C\Sigma\}]^T \qquad 2.18$$

Here, θ and λ are parameter of the surface. It may be noted that λ is the parameter along the z_1 axis. Now, considering the intersection of this cylinder with a plane perpendicular to z_2 axis, we get intersection curve,

$$\bar{x}_2 + \bar{y}_2 = R_f^2 = (r_f C\theta+a)^2 + (r_f S\theta C\Sigma + \lambda S\Sigma)^2 \qquad 2.19$$

where $\lambda = (z_2 + r_f S\theta S\Sigma)/C\Sigma$ 2.20

Equation (2.19) can be written as

$$C^2\Sigma R_f^2 = C^2\Sigma (r_f C\theta + a)^2 + (r_f S\theta + z_2 S\Sigma)^2 \qquad 2.21$$

As the ideal or optimal blank surface touches the intersection curve the condition for touching is given by $dR_f/d\theta = 0$. Differentiating equation (2.21) with respect to θ , we get

$$r_f S\theta C\theta S^2\Sigma - a S\theta C^2\Sigma + z_2 S\Sigma C\theta = 0 \qquad 2.22$$

Here, z_2 is assumed to be constant. From equations (2.22) and (2.20), one can write

$$\tan \theta = \lambda \tan \Sigma/a \qquad 2.23$$

The equation for the optimal blank shape is obtained by eliminating θ from equation (2.21) using the expression (2.23). This equation is given below

$$(\bar{x}_2^2 + \bar{y}_2^2)C^2\Sigma = Ra^2C^2\Sigma = C^2\Sigma\,(r_fC\theta + a)^2 + (r_f S\theta + z_2 S\Sigma)^2 \qquad 2.24$$

$$\text{where, } S\theta = \lambda S\Sigma / [\lambda^2S^2\Sigma + a^2C^2\Sigma]^{1/2}, C\theta = aC\Sigma/[\lambda^2S^2\Sigma+a^2C\Sigma]^{1/2}, \qquad 2.25$$

and Ra is the radius of the gear blank for a specified value of z_2. The addemdum surface of face gears, on-center tapered gears and cylindrical gears are special cases of the above surface.

In case of the face gear ($\Sigma = \pi/2$) the equation (2.24) takes the form

$$r_f + z_2 = 0 \qquad 2.26$$

This plane is called tip plane of the face gear. Here, the off-set 'a' may or may not be equal to zero.

For on-center tapered gears, off set 'a' is equal to zero. In this case the equation (2.24) takes the form of the equation of a cone

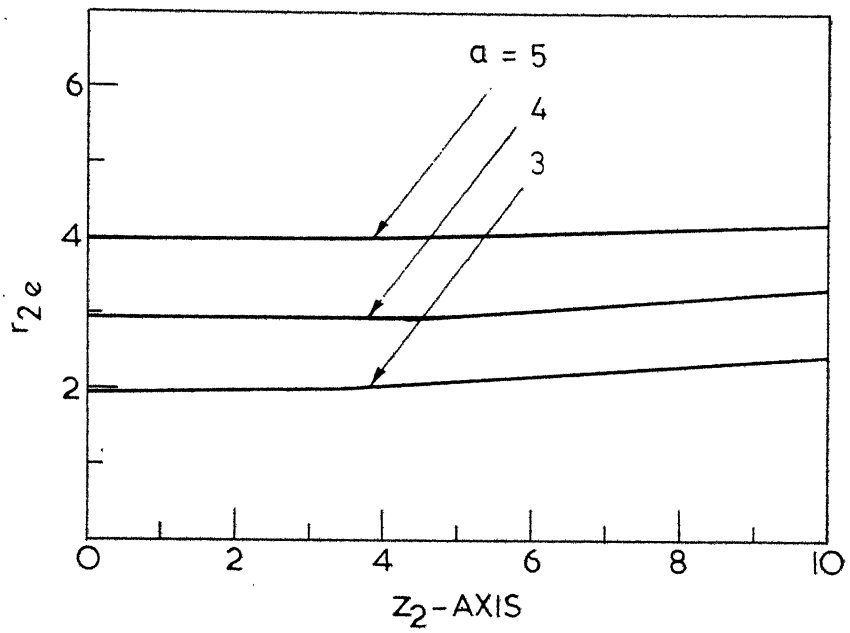

(Off-set tapered gears $\Sigma = 17/18\ \pi$ & $r_f = 1$)

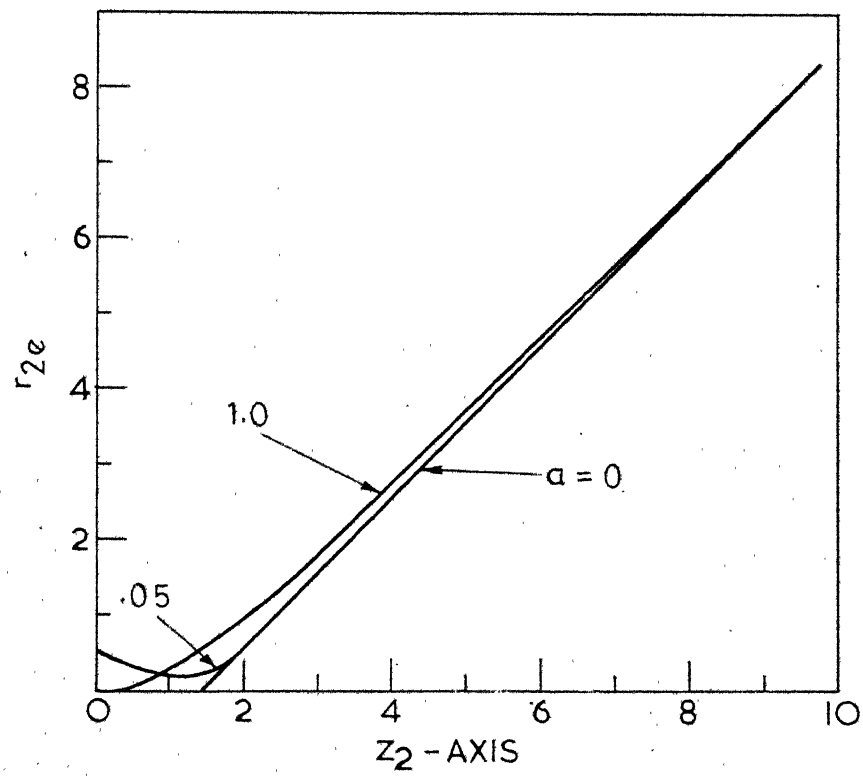

(Off-set tapered gears $\Sigma = 3\pi/4$ & $r_f = 1$)

FIG. 4 OPTIMUM BLANK SHAPE FOR TAPERED GEARS

(ACTUAL BLANK SHAPES ARE SURFACES OF REVOLUTION GENERATED BY ROTATING CURVES ABOUT z_2 - AXES)

$$(\bar{x}_2^2 + \bar{y}_2^2)C^2\Sigma = (r_f + z_2 S\Sigma)^2 \qquad 2.27$$

For external cylindrical gears, the blank shape can be derived from equation (2.24) after substituting $\Sigma = \pi$. This gives

$$\bar{x}_2^2 + \bar{y}_2^2 = (a - r_f)^2 \qquad 2.28$$

For off set tapered gears, it is seen from equation (2.24) that the optimal blank shape is not conical. However, for ease of manufacture and inspection, the blank should be conical although it means a loss of some portion of the surface of action. The procedure for obtaining the most suitable conical blank shape is out line below.

Figure 4 shows the plots of the surfaces for a few specific cases. It can be seen that the optimal blank surface is of the concave nature. We can find a cone which just touches this surface and is wholly within it. Such a cone will not interfer with the clearance cylinder of the pinion. In order to use the maximum tooth width and height one can find a cone which touches this surface at the middle of the tooth width.

It is assumed, that the distances from the origin of the small end, z_{2F}, and the large end, z_{2B}, of the blank along the z_2 axis are known [Figure 5] . To avoid undercutting and pointing, inequalities ($|z_{2F}| \geq |z_{2u}|$) and ($|z_{2B}| \leq |z_{2p}|$) must be

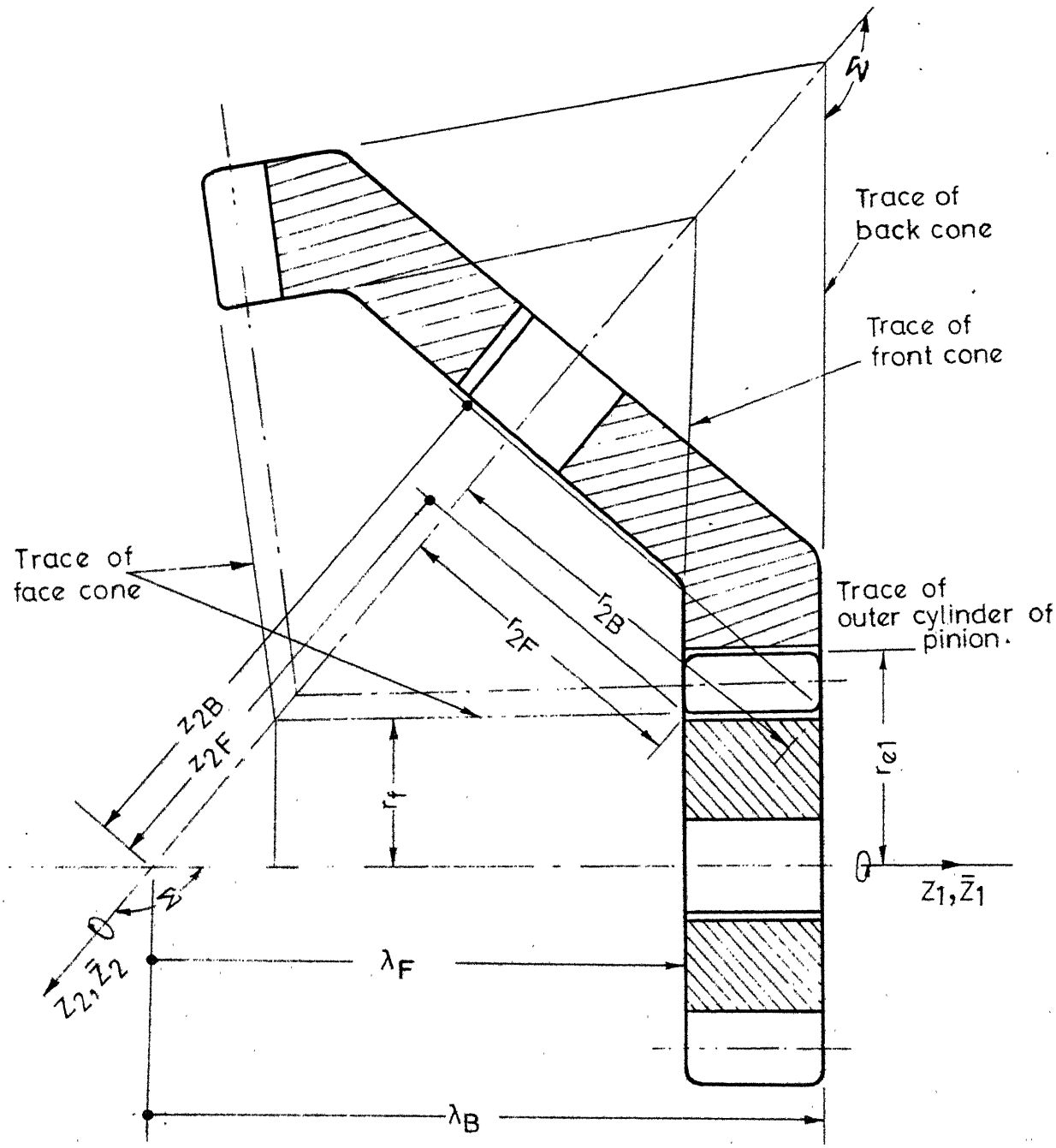

FIG. 5 SPUR ON-CENTER TAPERED GEAR.

satisfied. Here z_{2u} and z_{2p} are the respective distances where undercutting and pointing of the teeth occur . Estimation of these limiting parameters will be discussed later. The following steps are followd for calculating the conical blank size.

i. The middle of the tooth width is found, using

$$z_{2m} = (z_{2F} + z_{2B})/2 \qquad 2.29$$

ii. The semicone angle, δ_a , of the blank is obtained using the expression

$$\tan \delta_a = \left.\frac{d R_a}{dz_2}\right|_{z_{2m}} \qquad 2.30$$

iii. From equation (2.24), we compute

$$\left.\frac{dR_a}{dz_2}\right|_{z_{2m}} = \frac{\tan \Sigma \cdot \text{Num}}{[(r_f C\theta + a)^2 + (r_f S\theta C\Sigma + \lambda S\Sigma)^2]^{1/2}} \qquad 2.31$$

where, $$\text{Num} = r_f S\theta C\Sigma + \lambda S\Sigma + \frac{[\lambda S\Sigma C\theta - aC\Sigma S\theta] r_f C\theta}{aC\theta C^2\Sigma + \lambda S\Sigma C\Sigma - r_f S^2\Sigma C^2\theta} \qquad 2.32$$

θ is given by

$$S\Sigma C\theta [r_f S\theta \, S\Sigma - a \tan \theta C^2 \Sigma + z_{2m}] = 0 \qquad 2.33$$

and λ is given by

$$\tan \theta = \lambda \tan \Sigma / a. \qquad 2.34$$

iv. The equation of the cone is now written as

$$\bar{x}_2^2 + \bar{y}_2^2 = [r_{2m} + (z_2 - z_{2m}) \tan \delta_a]^2 \qquad 2.35$$

The radii of the small and large end are given by

$$r_{2F} = r_{2m} + (z_{2F} - z_{2m}) \tan \delta_a$$

$$r_{2B} = r_{2m} + (z_{2B} - z_{2m}) \tan \delta_a \qquad 2.36$$

The radius r_{2m} is obtained from equation (2.24) with $z_2 = z_{2m}$ and using the solutions of equations (2.33) and (2.34). The face width of blank is obtained considering

$$b = |(z_{2B} - z_{2F})| / \cos \delta_a \qquad 2.37$$

From equations (2.33) , (2.31) and (2.32) it can be observed that for an on-center tapered gear ($a = 0$) the semi cone angle $\delta_a = \Sigma$. Figure 4b shows that for gears with low transmission ratio and low off-sets, the semicone angle approaches the shaft angle.

2.8 Pointing of gear tooth.

On a conventional bevel gear of octoidal form the face width can theoritically be increased indefinitely. The tool and machine are the limiting factors. The pitch and height increase in proportion to the diameter but the pressure angle on the pitch surface remains constant. In case of tapered gears, the pitch and the height of pinion tooth remains constant but the pressure angle varies along the face. This makes gear teeth to become pointed towards the larger end of the blank.

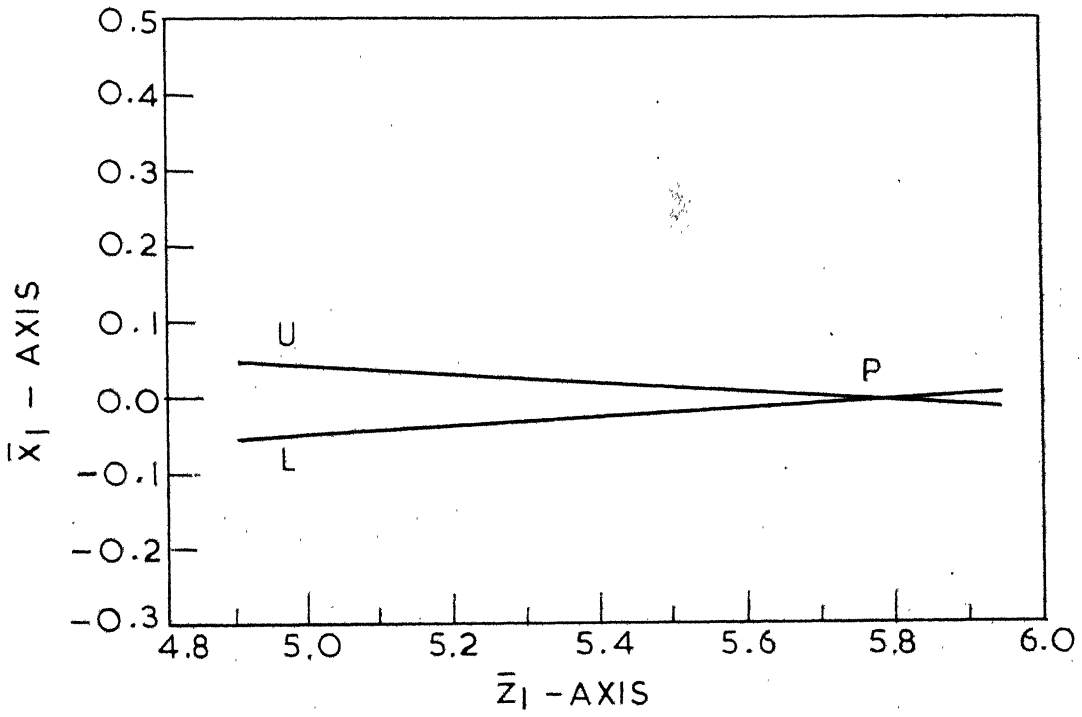

FIG. 6 TRACE OF TOOTH SURFACES ON TIP PLANE.

(ON-CENTER FACE GEAR: $\Sigma = \pi/2, \beta = 0°, a = 0, Z_1 = 20,$ $i_{21} = 0.2$ AND $\alpha_0 = 20°$).

Let the addandum surface of the gear intersect the tooth surfaces, U and L. There will be two curves of intersection corresponding to the surface, U and L. Gear tooth will appear to be pointed where these two curves meet together on the addandum surface [Figure 6].

The condition of interpretation of the addendum surface of the gear with the tooth surfaces, U and L is given by

$$(R_{x2k}^2+R_{y2k}^2)C^2\Sigma-C^2\Sigma(r_fC\theta+a)^2+(r_fS\theta+R_{z2k}S\Sigma)^2=0;\ k = U,L \qquad 2.39$$

where, $\underset{\sim}{R}_{2k} = [R_{x2k}, R_{y2k}, R_{z2k}]^T$, is given by equation (2.15)

$$S\theta = \frac{\lambda_k S\Sigma}{[\lambda_k^2S^2\Sigma+a^2C^2\Sigma]^{1/2}}\ ,\ C\theta = \frac{aC\Sigma}{[\lambda^2S^2\Sigma+a^2C^2\Sigma]^{1/2}}$$

$$\lambda_kS\Sigma = \frac{[1-i_{21}C\Sigma-ai_{21}C\Sigma S\Phi_k-i_{21}S\Sigma\tan\beta\{S\Phi_k-(\theta_k\bar{+}\eta)C\Phi_k+a\}]}{i_{21}C\Phi_k\sec^2\beta}$$

and, $\Phi_k = \theta_k + \phi_{1k}$

As the point at which pointing of the tooth occurs in common to tooth surfaces, U and L, one can write

$$R_{x2U} - R_{x2L} = 0$$
$$R_{y2U} - R_{x2L} = 0 \qquad 2.40$$

Pointing occurs, if equations (2.39) and (2.40) are satisfied simultaneously at that point. This set of equations can be represented in vectorial form as

$$\underset{\sim}{F}_p(\underset{\sim}{\theta}) = \underset{\sim}{0},\ \text{where},\ \underset{\sim}{\theta} = [\theta_U, \phi_{1U}, \theta_L, \phi_{1L}]^T \qquad 2.41$$

BLE 1 POSITION AT WHICH POINTING OCCURES IN TAPERED GEARS

. .I21.	1	1/2	1/3	1/4	1/5	1/6	1/7	1/8	1/9	1/10
1.ASTAR.										

HAFT ANGLE 105 HELIX ANGLE 0.0

7. 0.00	1.217	2.377	3.540	4.705	5.870	7.036	8.201	9.367	10.533	11.698R2
	-1.240	-1.551	-1.863	-2.175	-2.487	-2.799	-3.112	-3.424	-3.736	-4.049Z2
0.05	1.218	2.378	3.543	4.708	5.874	7.041	8.207	9.374	10.540	11.707
	-1.240	-1.551	-1.863	-2.175	-2.487	-2.799	-3.112	-3.424	-3.736	-4.049
0.10	1.220	2.383	3.550	4.718	5.887	7.056	8.225	9.394	10.563	11.732
	-1.240	-1.551	-1.862	-2.174	-2.487	-2.799	-3.111	-3.423	-3.736	-4.048
0.15	1.223	2.390	3.561	4.734	5.907	7.080	8.254	9.427	10.601	11.775
	-1.240	-1.551	-1.862	-2.174	-2.486	-2.798	-3.110	-3.423	-3.735	-4.047
0.20	1.227	2.400	3.578	4.756	5.936	7.115	8.295	9.474	10.654	11.834
	-1.240	-1.550	-1.862	-2.173	-2.485	-2.797	-3.109	-3.421	-3.734	-4.046
0.25	1.233	2.413	3.599	4.785	5.972	7.159	8.347	9.534	10.722	11.910
	-1.239	-1.550	-1.861	-2.173	-2.484	-2.796	-3.108	-3.420	-3.732	-4.044
0.30	1.239	2.429	3.624	4.820	6.016	7.213	8.410	9.607	10.804	12.001
	-1.239	-1.549	-1.860	-2.171	-2.483	-2.795	-3.106	-3.418	-3.730	-4.042
0.35	1.247	2.448	3.654	4.861	6.068	7.276	8.484	9.692	10.900	12.109
	-1.238	-1.548	-1.859	-2.170	-2.482	-2.793	-3.105	-3.416	-3.728	-4.039
0.40	1.256	2.469	3.688	4.907	6.127	7.348	8.569	9.790	11.011	12.232
	-1.238	-1.547	-1.858	-2.169	-2.480	-2.791	-3.102	-3.414	-3.725	-4.036
0.45	1.266	2.493	3.726	4.959	6.194	7.429	8.664	9.899	11.134	12.369
	-1.237	-1.546	-1.857	-2.167	-2.478	-2.789	-3.100	-3.411	-3.722	-4.033
0.50	1.277	2.520	3.768	5.017	6.267	7.518	8.769	10.019	11.270	12.521
	-1.236	-1.545	-1.855	-2.165	-2.476	-2.786	-3.097	-3.408	-3.718	-4.029
8. 0.00	1.211	2.367	3.526	4.686	5.847	7.008	8.170	9.331	10.493	11.654
	-1.245	-1.554	-1.865	-2.176	-2.487	-2.798	-3.109	-3.420	-3.732	-4.043
0.05	1.212	2.368	3.528	4.689	5.851	7.013	8.176	9.338	10.500	11.663
	-1.245	-1.554	-1.865	-2.176	-2.487	-2.798	-3.109	-3.420	-3.732	-4.043
0.10	1.213	2.372	3.535	4.699	5.864	7.028	8.193	9.358	10.523	11.688
	-1.245	-1.554	-1.865	-2.176	-2.487	-2.798	-3.109	-3.420	-3.731	-4.042
0.15	1.216	2.380	3.547	4.715	5.884	7.053	8.222	9.392	10.561	11.731
	-1.244	-1.554	-1.864	-2.175	-2.486	-2.797	-3.108	-3.419	-3.730	-4.041
0.20	1.221	2.390	3.563	4.738	5.913	7.088	8.263	9.439	10.614	11.790
	-1.244	-1.553	-1.864	-2.174	-2.485	-2.796	-3.107	-3.418	-3.729	-4.040
0.25	1.226	2.403	3.584	4.766	5.949	7.132	8.316	9.499	10.682	11.866
	-1.244	-1.553	-1.863	-2.174	-2.484	-2.795	-3.106	-3.416	-3.727	-4.038
0.30	1.233	2.419	3.609	4.801	5.994	7.186	8.379	9.572	10.765	11.958
	-1.243	-1.552	-1.862	-2.172	-2.483	-2.793	-3.104	-3.415	-3.725	-4.036
0.35	1.240	2.438	3.639	4.842	6.046	7.249	8.453	9.657	10.861	12.066
	-1.243	-1.551	-1.861	-2.171	-2.481	-2.792	-3.102	-3.412	-3.723	-4.033
0.40	1.249	2.459	3.673	4.889	6.105	7.322	8.538	9.755	10.972	12.189
	-1.242	-1.550	-1.860	-2.170	-2.480	-2.790	-3.100	-3.410	-3.720	-4.030
0.45	1.259	2.483	3.711	4.941	6.172	7.402	8.633	9.864	11.096	12.327
	-1.241	-1.549	-1.859	-2.168	-2.478	-2.788	-3.097	-3.407	-3.717	-4.027
0.50	1.270	2.509	3.754	4.999	6.245	7.492	8.739	9.985	11.232	12.479
	-1.240	-1.548	-1.857	-2.166	-2.476	-2.785	-3.095	-3.404	-3.713	-4.023

ABLE 1 POSITICN AT WHICH POINTING OCCURES IN TAPERED GEARS

. .I21.	I	I	I	I	I	I	I	I	I	I
. . . 1	I 1/2	I 1/3	I 1/4	I 1/5	I 1/6	I 1/7	I 1/8	I 1/9	I 1/10	I
. . .	I	I	I	I	I	I	I	I	I	I
Z1.ASTAR.	I	I	I	I	I	I	I	I	I	I

SHAFT ANGLE 105 HELIX ANGLE 10.0

17.	0.00	1.215	2.376	3.540	4.705	5.870	7.036	8.202	9.368	10.533	11.699
		-1.238	-1.549	-1.861	-2.173	-2.486	-2.798	-3.110	-3.423	-3.735	-4.048
	0.05	1.208	2.360	3.514	4.670	5.827	6.983	8.140	9.297	10.454	11.611
	0.05	1.208	2.360	3.514	4.670	5.827	6.983	8.140	9.297	10.454	11.611
		-1.236	-1.544	-1.854	-2.163	-2.473	-2.782	-3.092	-3.402	-3.712	-4.021
	0.10	1.202	2.346	3.494	4.643	5.792	6.941	8.091	9.240	10.390	11.539
		-1.234	-1.540	-1.846	-2.153	-2.460	-2.767	-3.074	-3.381	-3.688	-3.995
	0.15	1.198	2.336	3.478	4.622	5.765	6.909	8.053	9.197	10.341	11.486
		-1.232	-1.535	-1.838	-2.142	-2.446	-2.751	-3.055	-3.359	-3.663	-3.968
	0.20	1.195	2.329	3.468	4.607	5.747	6.888	8.028	9.169	10.309	11.450
		-1.229	-1.529	-1.830	-2.132	-2.433	-2.734	-3.036	-3.337	-3.639	-3.940
	0.25	1.193	2.325	3.462	4.600	5.738	6.877	8.015	9.154	10.293	11.432
		-1.227	-1.524	-1.822	-2.121	-2.419	-2.718	-3.016	-3.315	-3.614	-3.912
	0.30	1.192	2.324	3.461	4.599	5.738	6.876	8.015	9.154	10.294	11.433
		-1.225	-1.519	-1.814	-2.109	-2.405	-2.701	-2.996	-3.292	-3.588	-3.884
	0.35	1.192	2.327	3.465	4.605	5.746	6.887	8.028	9.169	10.310	11.451
		-1.222	-1.513	-1.805	-2.098	-2.391	-2.684	-2.976	-3.269	-3.562	-3.855
	0.40	1.194	2.332	3.474	4.618	5.763	6.908	8.052	9.198	10.343	11.488
		-1.219	-1.508	-1.797	-2.086	-2.376	-2.666	-2.956	-3.246	-3.536	-3.826
	0.45	1.197	2.340	3.488	4.638	5.788	6.939	8.090	9.240	10.391	11.543
		-1.216	-1.502	-1.788	-2.075	-2.361	-2.648	-2.935	-3.222	-3.509	-3.796
	0.50	1.202	2.352	3.507	4.664	5.822	6.980	8.139	9.297	10.456	11.615
		-1.214	-1.496	-1.779	-2.062	-2.346	-2.630	-2.914	-3.198	-3.482	-3.766
18.	0.00	1.211	2.371	3.534	4.697	5.862	7.026	8.190	9.355	10.519	11.684
		-1.247	-1.557	-1.869	-2.181	-2.493	-2.805	-3.117	-3.429	-3.741	-4.053
	0.05	1.204	2.355	3.509	4.663	5.818	6.973	8.129	9.284	10.440	11.595
		-1.244	-1.553	-1.861	-2.171	-2.480	-2.789	-3.098	-3.408	-3.717	-4.026
	0.10	1.199	2.342	3.488	4.635	5.783	6.931	8.079	9.228	10.376	11.524
		-1.242	-1.548	-1.854	-2.160	-2.467	-2.773	-3.080	-3.387	-3.693	-4.000
	0.15	1.194	2.332	3.473	4.614	5.757	6.899	8.042	9.185	10.328	11.471
		-1.240	-1.543	-1.846	-2.150	-2.453	-2.757	-3.061	-3.365	-3.669	-3.973
	0.20	1.191	2.325	3.462	4.600	5.739	6.878	8.017	9.156	10.296	11.435
		-1.238	-1.537	-1.838	-2.139	-2.440	-2.741	-3.042	-3.343	-3.644	-3.945
	0.25	1.189	2.321	3.456	4.593	5.730	6.867	8.005	9.142	10.280	11.418
		-1.235	-1.532	-1.830	-2.128	-2.426	-2.724	-3.023	-3.321	-3.619	-3.917
	0.30	1.188	2.320	3.455	4.592	5.729	6.867	8.005	9.142	10.280	11.418
		-1.233	-1.527	-1.822	-2.117	-2.412	-2.707	-3.003	-3.298	-3.594	-3.889
	0.35	1.189	2.322	3.460	4.598	5.738	6.877	8.017	9.157	10.297	11.437
		-1.230	-1.521	-1.813	-2.105	-2.398	-2.690	-2.983	-3.275	-3.568	-3.860
	0.40	1.190	2.327	3.469	4.611	5.755	6.898	8.042	9.186	10.330	11.474
		-1.227	-1.516	-1.805	-2.094	-2.383	-2.673	-2.962	-3.252	-3.541	-3.831
	0.45	1.193	2.336	3.483	4.631	5.780	6.930	8.079	9.229	10.379	11.529
		-1.225	-1.510	-1.796	-2.082	-2.368	-2.655	-2.941	-3.228	-3.515	-3.801
	0.50	1.198	2.347	3.501	4.657	5.814	6.971	8.128	9.286	10.443	11.601
		-1.222	-1.504	-1.787	-2.070	-2.353	-2.637	-2.920	-3.204	-3.487	-3.771

TABLE 1 POSITICN AT WHICH POINTING OCCURES IN TAPERED GEARS

. .I21.	I	I	I	I	I	I	I	I	I	I
. . . 1	I 1/2	I 1/3	I 1/4	I 1/5	I 1/6	I 1/7	I 1/8	I 1/9	I 1/1	
. . .	I	I	I	I	I	I	I	I	I	
Z1.ASTAR.	I	I	I	I	I	I	I	I	I	

SHAFT ANGLE 135 HELIX ANGLE 0

17. 0.00 1.265 2.432 3.598 4.764 5.930 7.096 8.262 9.428 10.594 11.7
-2.513-3.680-4.847-6.013-7.179-8.345-9.511-10.677-11.843-13.0
0.05 1.265 2.432 3.599 4.765 5.932 7.098 8.265 9.431 10.598 11.7
-2.513-3.680-4.845-6.011-7.176-8.342-9.508-10.673-11.839-13.0
0.10 1.266 2.434 3.602 4.770 5.938 7.106 8.274 9.441 10.609 11.7
-2.512-3.677-4.841-6.006-7.170-8.334-9.498-10.662-11.826-12.9
0.15 1.267 2.437 3.607 4.777 5.948 7.118 8.288 9.458 10.628 11.7
-2.510-3.673-4.835-5.997-7.158-8.320-9.482-10.644-11.805-12.9
0.20 1.268 2.441 3.615 4.788 5.961 7.135 8.308 9.482 10.655 11.8
-2.508-3.667-4.826-5.984-7.143-8.301-9.460-10.618-11.776-12.9
0.25 1.270 2.447 3.624 4.801 5.979 7.156 8.334 9.512 10.689 11.8
-2.504-3.659-4.814-5.968-7.122-8.276-9.431-10.585-11.739-12.8
0.30 1.272 2.453 3.635 4.818 6.000 7.183 8.366 9.548 10.731 11.9
-2.500-3.650-4.799-5.948-7.097-8.246-9.395-10.544-11.693-12.8
0.35 1.275 2.461 3.649 4.837 6.025 7.214 8.403 9.591 10.780 11.9
-2.495-3.639-4.782-5.925-7.068-8.210-9.353-10.496-11.638-12.7
0.40 1.278 2.470 3.664 4.859 6.054 7.250 8.445 9.641 10.836 12.0
-2.490-3.627-4.762-5.898-7.033-8.169-9.304-10.440-11.575-12.7
0.45 1.282 2.481 3.682 4.884 6.087 7.290 8.493 9.696 10.900 12.1
-2.483-3.612-4.740-5.867-6.994-8.121-9.249-10.376-11.503-12.6
0.50 1.286 2.492 3.701 4.912 6.123 7.335 8.546 9.758 10.970 12.1
-2.476-3.596-4.714-5.832-6.950-8.068-9.186-10.304-11.421-12.5
18. 0.00 1.257 2.419 3.581 4.743 5.905 7.067 8.228 9.390 10.552 11.7
-2.514-3.676-4.838-6.000-7.162-8.324-9.485-10.647-11.809-12.9
0.05 1.257 2.420 3.582 4.745 5.907 7.069 8.231 9.393 10.556 11.7
-2.513-3.676-4.837-5.998-7.160-8.321-9.482-10.643-11.805-12.9
0.10 1.257 2.422 3.585 4.749 5.913 7.076 8.240 9.403 10.567 11.7
-2.512-3.673-4.833-5.993-7.153-8.313-9.473-10.632-11.792-12.9
0.15 1.259 2.425 3.591 4.757 5.922 7.088 8.254 9.420 10.586 11.7
-2.510-3.669-4.827-5.984-7.142-8.299-9.456-10.614-11.771-12.9
0.20 1.260 2.429 3.598 4.767 5.936 7.105 8.275 9.444 10.613 11.7
-2.508-3.663-4.817-5.972-7.126-8.280-9.434-10.588-11.742-12.8
0.25 1.262 2.434 3.607 4.780 5.954 7.127 8.300 9.474 10.647 11.8
-2.504-3.655-4.805-5.955-7.105-8.255-9.405-10.555-11.704-12.8
0.30 1.264 2.441 3.619 4.797 5.975 7.154 8.332 9.510 10.689 11.8
-2.500-3.646-4.791-5.936-7.080-8.225-9.369-10.514-11.658-12.8
0.35 1.267 2.449 3.632 4.816 6.000 7.185 8.369 9.554 10.738 11.9
-2.495-3.635-4.774-5.912-7.050-8.189-9.327-10.465-11.603-12.7
0.40 1.270 2.458 3.648 4.838 6.029 7.220 8.412 9.603 10.795 11.9
-2.490-3.622-4.754-5.885-7.016-8.147-9.278-10.409-11.540-12.6
0.45 1.274 2.468 3.665 4.863 6.062 7.261 8.460 9.659 10.858 12.0
-2.483-3.608-4.731-5.854-6.977-8.099-9.222-10.344-11.467-12.5
0.50 1.278 2.480 3.685 4.891 6.098 7.306 8.513 9.721 10.929 12.1
-2.476-3.592-4.705-5.819-6.932-8.046-9.159-10.272-11.385-12.4

TABLE 1 POSITION AT WHICH POINTING OCCURES IN TAPERED GEARS

Z1.	ASTAR.	1	1 1/2	1 1/3	1 1/4	1 1/5	1 1/6	1 1/7	1 1/8	1 1/9	1 1/10
SHAFT ANGLE 135										HELIX ANGLE 10.	
17.	0.00	1.280	2.450	3.617	4.784	5.951	7.117	8.283	9.450	10.616	11.78
		-3.98	-6.01	-8.03	-10.05	-12.07	-14.09	-16.11	-18.13	-20.15	-22.1
	0.05	1.279	2.446	3.612	4.776	5.940	7.105	8.269	9.432	10.596	11.76
		-3.98	-6.00	-8.02	-10.03	-12.05	-14.06	-16.08	-18.09	-20.11	-22.1
	0.10	1.277	2.443	3.607	4.770	5.932	7.094	8.256	9.419	10.581	11.74
		-3.97	-5.99	-8.00	-10.00	-12.01	-14.02	-16.02	-18.03	-20.04	-22.0
	0.15	1.276	2.441	3.603	4.764	5.925	7.086	8.247	9.408	10.569	11.72
		-3.97	-5.97	-7.97	-9.97	-11.96	-13.96	-15.96	-17.95	-19.95	-21.9
	0.20	1.275	2.439	3.600	4.761	5.921	7.081	8.241	9.401	10.560	11.72
		-3.96	-5.95	-7.94	-9.92	-11.91	-13.89	-15.87	-17.85	-19.84	-21.8
	0.25	1.275	2.438	3.598	4.758	5.918	7.078	8.237	9.397	10.556	11.71
		-3.95	-5.93	-7.90	-9.87	-11.84	-13.80	-15.77	-17.74	-19.70	-21.6
	0.30	1.274	2.437	3.598	4.758	5.917	7.077	8.236	9.396	10.555	11.71
		-3.94	-5.90	-7.85	-9.80	-11.75	-13.70	-15.65	-17.60	-19.55	-21.5
	0.35	1.274	2.437	3.598	4.758	5.918	7.079	8.239	9.399	10.559	11.71
		-3.93	-5.87	-7.80	-9.73	-11.66	-13.59	-15.52	-17.44	-19.37	-21.3
	0.40	1.274	2.437	3.599	4.760	5.921	7.083	8.244	9.405	10.566	11.72
		-3.91	-5.83	-7.74	-9.65	-11.56	-13.46	-15.36	-17.27	-19.17	-21.0
	0.45	1.274	2.438	3.601	4.764	5.926	7.089	8.251	9.414	10.576	11.73
		-3.89	-5.79	-7.68	-9.56	-11.44	-13.32	-15.19	-17.07	-18.95	-20.8
	0.50	1.274	2.440	3.604	4.769	5.933	7.098	8.262	9.426	10.591	11.75
		-3.88	-5.75	-7.60	-9.46	-11.31	-13.15	-15.00	-16.85	-18.70	-20.5
18.	0.00	1.272	2.438	3.602	4.766	5.928	7.091	8.254	9.417	10.579	11.74
		-3.98	-6.00	-8.02	-10.03	-12.05	-14.06	-16.07	-18.09	-20.10	-22.1
	0.05	1.271	2.435	3.597	4.757	5.918	7.079	8.239	9.399	10.560	11.72
		-3.98	-5.99	-8.00	-10.01	-12.02	-14.03	-16.04	-18.05	-20.05	-22.0
	0.10	1.270	2.432	3.592	4.751	5.910	7.068	8.227	9.386	10.544	11.70
		-3.97	-5.98	-7.98	-9.99	-11.99	-13.99	-15.99	-17.99	-19.99	-21.9
	0.15	1.268	2.429	3.588	4.746	5.903	7.061	8.218	9.375	10.532	11.68
		-3.97	-5.96	-7.96	-9.95	-11.94	-13.93	-15.92	-17.91	-19.90	-21.8
	0.20	1.268	2.428	3.585	4.742	5.899	7.055	8.211	9.368	10.524	11.68
		-3.96	-5.94	-7.92	-9.90	-11.88	-13.86	-15.83	-17.81	-19.79	-21.7
	0.25	1.267	2.426	3.583	4.740	5.896	7.052	8.208	9.364	10.520	11.67
		-3.95	-5.92	-7.89	-9.85	-11.81	-13.77	-15.73	-17.69	-19.65	-21.6
	0.30	1.266	2.426	3.583	4.739	5.895	7.051	8.207	9.363	10.519	11.67
		-3.94	-5.89	-7.84	-9.79	-11.73	-13.67	-15.61	-17.56	-19.50	-21.4
	0.35	1.266	2.425	3.583	4.740	5.896	7.053	8.210	9.366	10.523	11.67
		-3.93	-5.86	-7.79	-9.71	-11.64	-13.56	-15.48	-17.40	-19.32	-21.2
	0.40	1.266	2.426	3.584	4.742	5.899	7.057	8.215	9.372	10.530	11.68
		-3.91	-5.83	-7.73	-9.63	-11.53	-13.43	-15.33	-17.22	-19.12	-21.0
	0.45	1.266	2.427	3.586	4.745	5.904	7.063	8.222	9.381	10.540	11.69
		-3.89	-5.78	-7.66	-9.54	-11.41	-13.28	-15.15	-17.02	-18.89	-20.7
	0.50	1.266	2.428	3.589	4.750	5.911	7.072	8.233	9.394	10.555	11.71
		-3.88	-5.74	-7.59	-9.44	-11.28	-13.12	-14.96	-16.80	-18.64	-20.4

The solution, $\underset{\sim}{\theta}_p$ of equation (2.41) when substituted in equation (2.15) gives the point on the gear surface at which pointing occurs. The radius and the distances along z_2 and z_1 axis at which pointing occurs can be determined from the following expressions:

$$r_{2p} = [R^2_{x2U} + R^2_{y2U}]^{1/2} \cos \alpha_{os} = [R^2_{x2L} + R^2_{y2L}]^{1/2} \cos \alpha_{os}$$

$$z_{2p} = R_{z2U} \cos \alpha_{os} = R_{z2L} \cos \alpha_{os}$$

and $$z_{1p} = \lambda_U \cos \alpha_{os} = \lambda_L \cos \alpha_{os} \qquad 2.42$$

where $$\underset{\sim}{R}_{2k} = [R_{x2k}(\theta_{kp}, \phi_{1kp}),\ R_{y2k}(\theta_{kp}, \phi_{1kp}), R_{z2k}(\theta_{kp}, \phi_{1kp})]^T$$

Here, r_{2p}, z_{2p} and z_{1p} are non-dimensionalized with respect to nominal pitch radius of the cutter. It can be seen that the above limiting dimensions depend on Z_o, α_{os}, i_{20}, f_{os}, ξ_{os}, Σ, β and a. Equation (2.41) may be solved for different sets of these parameters. A few samples of the results of computation are tabulated in Table 1.[1]

2.9 Undercutting of gear teeth.

Undercutting of gear tooth is due to the appearance of the cuspoidal points on its surface [8] During generation a portion of the tooth surface is removed below these points. Physical boundaries of gear blanks are so chosen that these special points are avoided from the region of mesh [19] . In this section, the

---

[1] For more results, see [22]

equation to find the limiting dimensions of tapered gear to avoid undercutting are developed.

The condition for undercutting is expressed in the following form. This condition holds good at cuspoidal points. [Appendix II]

$$\det \begin{vmatrix} \frac{\partial f}{\partial \Theta_k} & \frac{\partial f}{\partial \lambda} & \frac{\partial f}{\partial \phi_1}\frac{d\phi_1}{dt} \\ \frac{\partial R_{x1}}{\partial \Theta_k} & \frac{\partial R_{x1}}{\partial \lambda} & V_{x1}^{12} \\ \frac{\partial R_{z1}}{\partial \Theta_k} & \frac{\partial R_{z1}}{\partial \lambda} & V_{z1}^{12} \end{vmatrix} = 0 \qquad 2.43$$

where $\frac{d\phi_1}{dt} = 1$

Expanding the determinant, we can write

$$U = U(\Theta_k, \lambda, \phi_1) \qquad 2.44$$

where, $$\underset{\sim}{R}_1 = \underset{\sim}{R}_1(\Theta_k, \lambda) \qquad 2.6$$

is the generating surface and

$$f = f(\Theta_k, \lambda, \phi_1) \qquad 2.11$$

is the equation of contact. The interest lies in finding the cuspoidal points corresponding to the tip of the cutter. The equation of the tip of the cutter is given by

$$B(\Theta_k, \lambda) = 0 \qquad 2.45$$

In case of the involute helical cutter equation (2.45) is expressed as

$$\theta_k^* = \theta_{ke}^* = (r_{oe}^2 - 1)^{1/2} \qquad 2.46$$

where, $$r_{oe} = [1 + 2(f_{os} + c_{os})/Z_c]/\cos \alpha_{os} \qquad 2.47$$

Here, the cutter is assumed to be unconnected, that is, $\xi_{os} = 0$.

To obtain the condition of undercutting for tapered gears the expressions for $\frac{\partial f}{\partial \lambda}$, $\frac{\partial f}{\partial \theta_k}$, $\frac{\partial R_{x1}}{\partial \lambda}$, $\frac{\partial R_{z1}}{\partial \theta_k}$, $\frac{\partial R_{z1}}{\partial \theta_k}$, V_{1x}^{12} and V_{1y}^{12} derived from equations (2.6 , 2.13, R-1, and 2.46) are substituted in equation (2.43). As a result the following condition is obtained

$$[ai_{21}C\Sigma+i_{21}S\Sigma \tan \beta(S\phi_k+a)S\phi_k-(1-i_{21}C\Sigma)S\phi_k][(1-i_{21}C\Sigma)S\phi_k+i_{21}C\Sigma C\phi_k\theta_{ke}^*-ai_{21}C\Sigma-$$

$$-i_{21}S\Sigma \tan \beta\, S\phi_k(R_{cx}+a)]+i_{21}S\Sigma C^3\phi_k\theta_{ke}^* \tan \beta - i_{21}^2S^2\Sigma C^3\phi_k\theta_{ke}^* \sec^2\beta(R_{cx}+a)=0 \qquad 2.48$$

where

$$R_{cx} = S\phi_k - \theta_{ke}^* C \phi_k$$

This can be written as

$$F_u(\phi_k) = 0 \qquad 2.49$$

For spur face gears, above equation takes a simpler from

$$S^2 \phi_k + i_{21}^2 \theta_{ke}^*(S\phi_k - \theta_{ke}^* C\phi_k + a)C^3 \phi_k = 0$$

similar expressions have been derived earlier [5] [8] [12] . The limiting dimension of the gear to avoid undercutting can be found by the following consideration.

TABLE 2 POSITICN AT WHICH UNDERCUTTING OCCURES IN TAPERED GEARS

Z1 ASTAR	1	1/2	1/3	1/4	1/5	1/6	1/7	1/8	1/9	1/10
SHAFT ANGLE 105									HELIX ANGLE	0.0
17. 0.00	1.009	1.947	2.878	3.810	4.743	5.678	6.613	7.550	8.486	9.424
	-1.393	-1.608	-1.834	-2.067	-2.306	-2.548	-2.792	-3.038	-3.285	-3.533
0.05	1.019	1.967	2.904	3.840	4.777	5.714	6.652	7.590	8.529	9.468
	-1.399	-1.620	-1.848	-2.084	-2.324	-2.567	-2.811	-3.058	-3.305	-3.553
0.10	1.029	1.988	2.934	3.877	4.819	5.761	6.703	7.646	8.589	9.532
	-1.405	-1.630	-1.861	-2.098	-2.339	-2.582	-2.828	-3.074	-3.321	-3.569
0.15	1.040	2.012	2.968	3.919	4.869	5.818	6.767	7.716	8.666	9.615
	-1.410	-1.639	-1.873	-2.111	-2.352	-2.596	-2.842	-3.088	-3.335	-3.583
0.20	1.052	2.038	3.005	3.967	4.927	5.886	6.844	7.801	8.759	9.716
	-1.414	-1.647	-1.883	-2.122	-2.364	-2.609	-2.854	-3.101	-3.348	-3.596
0.25	1.065	2.066	3.047	4.021	4.993	5.963	6.931	7.900	8.868	9.836
	-1.418	-1.654	-1.892	-2.132	-2.375	-2.619	-2.865	-3.112	-3.359	-3.607
0.30	1.078	2.096	3.092	4.081	5.066	6.049	7.031	8.012	8.992	9.973
	-1.421	-1.661	-1.900	-2.141	-2.384	-2.629	-2.875	-3.122	-3.369	-3.617
0.35	1.092	2.127	3.141	4.146	5.146	6.145	7.141	8.137	9.132	10.126
	-1.424	-1.666	-1.907	-2.149	-2.393	-2.638	-2.884	-3.130	-3.377	-3.625
0.40	1.106	2.161	3.193	4.216	5.234	6.249	7.262	8.274	9.285	10.296
	-1.426	-1.671	-1.913	-2.156	-2.400	-2.645	-2.891	-3.138	-3.385	-3.632
0.45	1.121	2.197	3.249	4.291	5.328	6.361	7.393	8.423	9.452	10.480
	-1.428	-1.676	-1.919	-2.163	-2.407	-2.652	-2.898	-3.144	-3.391	-3.639
0.50	1.136	2.234	3.308	4.371	5.428	6.481	7.533	8.583	9.632	10.680
	-1.430	-1.679	-1.924	-2.168	-2.413	-2.658	-2.904	-3.150	-3.397	-3.644
18. 0.00	1.006	1.945	2.876	3.808	4.741	5.676	6.612	7.548	8.485	9.423
	-1.387	-1.603	-1.830	-2.064	-2.303	-2.546	-2.790	-3.036	-3.283	-3.531
0.05	1.016	1.965	2.903	3.840	4.775	5.717	6.656	7.596	8.535	9.476
	-1.393	-1.614	-1.844	-2.080	-2.320	-2.564	-2.809	-3.055	-3.303	-3.551
0.10	1.026	1.985	2.931	3.874	4.816	5.758	6.701	7.644	8.586	9.530
	-1.398	-1.624	-1.857	-2.094	-2.335	-2.579	-2.825	-3.071	-3.319	-3.567
0.15	1.038	2.009	2.964	3.916	4.866	5.815	6.764	7.713	8.663	9.612
	-1.403	-1.633	-1.868	-2.107	-2.349	-2.593	-2.838	-3.085	-3.332	-3.581
0.20	1.049	2.034	3.002	3.964	4.923	5.882	6.840	7.798	8.755	9.713
	-1.407	-1.641	-1.878	-2.118	-2.360	-2.605	-2.850	-3.097	-3.345	-3.593
0.25	1.062	2.062	3.043	4.017	4.989	5.958	6.927	7.896	8.864	9.831
	-1.411	-1.648	-1.886	-2.127	-2.370	-2.615	-2.861	-3.108	-3.355	-3.603
0.30	1.075	2.092	3.088	4.076	5.061	6.044	7.026	8.007	8.988	9.968
	-1.414	-1.655	-1.894	-2.136	-2.380	-2.625	-2.871	-3.117	-3.365	-3.613
0.35	1.088	2.123	3.136	4.141	5.141	6.139	7.136	8.132	9.126	10.121
	-1.417	-1.660	-1.901	-2.144	-2.388	-2.633	-2.879	-3.126	-3.373	-3.621
0.40	1.103	2.157	3.188	4.211	5.228	6.243	7.256	8.268	9.279	10.290
	-1.419	-1.665	-1.907	-2.151	-2.395	-2.640	-2.886	-3.133	-3.380	-3.628
0.45	1.117	2.192	3.244	4.285	5.322	6.355	7.387	8.417	9.446	10.474
	-1.421	-1.669	-1.913	-2.157	-2.401	-2.647	-2.893	-3.140	-3.387	-3.634
0.50	1.133	2.229	3.302	4.365	5.422	6.475	7.527	8.576	9.625	10.673
	-1.423	-1.673	-1.918	-2.162	-2.407	-2.652	-2.898	-3.145	-3.392	-3.639

TABLE 2 POSITION AT WHICH UNDERCUTTING OCCURES IN TAPERED GEARS

Z1	ASTAR	1	1/2	1/3	1/4	1/5	1/6	1/7	1/8	1/9	1/10
SHAFT ANGLE 105										HELIX ANGLE 10.0	
17.	0.00	1.052	2.017	2.963	3.904	4.842	5.780	6.718	7.656	8.594	9.531
		-1.418	-1.649	-1.883	-2.121	-2.362	-2.606	-2.850	-3.097	-3.344	-3.591
	0.05	1.038	1.989	2.923	3.854	4.783	5.713	6.642	7.572	8.502	9.432
		-1.412	-1.637	-1.866	-2.101	-2.339	-2.579	-2.822	-3.065	-3.310	-3.555
	0.10	1.026	1.964	2.888	3.810	4.733	5.656	6.579	7.503	8.427	9.352
		-1.405	-1.624	-1.848	-2.079	-2.314	-2.551	-2.791	-3.032	-3.275	-3.518
	0.15	1.014	1.941	2.857	3.773	4.691	5.609	6.529	7.450	8.371	9.293
		-1.398	-1.609	-1.828	-2.055	-2.286	-2.521	-2.758	-2.997	-3.236	-3.477
	0.20	1.003	1.920	2.832	3.752	4.672	5.592	6.513	7.471	8.357	9.279
		-1.390	-1.593	-1.810	-2.036	-2.267	-2.500	-2.735	-2.871	-3.210	-3.449
	0.25	0.992	1.930	2.858	3.783	4.707	5.632	6.557	7.536	8.406	9.332
		-1.382	-1.598	-1.818	-2.044	-2.273	-2.505	-2.738	-2.851	-3.209	-3.445
	0.30	1.000	1.951	2.888	3.820	4.752	5.682	6.613	7.618	8.474	9.404
		-1.387	-1.604	-1.824	-2.049	-2.277	-2.507	-2.739	-2.833	-3.205	-3.439
	0.35	1.010	1.973	2.921	3.864	4.804	5.743	6.682	7.716	8.558	9.496
		-1.390	-1.609	-1.829	-2.053	-2.280	-2.508	-2.737	-2.816	-3.199	-3.431
	0.40	1.021	1.997	2.958	3.913	4.864	5.814	6.763	7.830	8.659	9.606
		-1.393	-1.612	-1.833	-2.056	-2.281	-2.507	-2.734	-2.800	-3.192	-3.421
	0.45	1.031	2.023	2.999	3.967	4.931	5.894	6.855	7.959	8.775	9.735
		-1.394	-1.615	-1.835	-2.057	-2.280	-2.505	-2.730	-2.784	-3.183	-3.410
	0.50	1.043	2.051	3.043	4.027	5.006	5.983	6.959	8.102	8.907	9.880
		-1.395	-1.617	-1.837	-2.057	-2.279	-2.501	-2.724	-2.769	-3.172	-3.397
18.	0.00	1.049	2.013	2.959	3.900	4.838	5.777	6.714	7.652	8.590	9.528
		-1.412	-1.644	-1.878	-2.116	-2.358	-2.602	-2.847	-3.093	-3.340	-3.588
	0.05	1.035	1.986	2.920	3.850	4.780	5.709	6.639	7.569	8.499	9.429
		-1.406	-1.631	-1.861	-2.096	-2.335	-2.576	-2.819	-3.062	-3.307	-3.553
	0.10	1.023	1.960	2.885	3.807	4.730	5.653	6.577	7.501	8.425	9.350
		-1.399	-1.618	-1.843	-2.075	-2.310	-2.548	-2.788	-3.030	-3.272	-3.515
	0.15	1.011	1.938	2.854	3.771	4.688	5.607	6.527	7.448	8.369	9.291
		-1.392	-1.604	-1.824	-2.051	-2.283	-2.518	-2.755	-2.994	-3.234	-3.475
	0.20	1.000	1.917	2.830	3.750	4.670	5.590	6.512	7.433	8.355	9.278
		-1.384	-1.588	-1.806	-2.032	-2.263	-2.497	-2.733	-2.970	-3.208	-3.447
	0.25	0.989	1.928	2.855	3.781	4.705	5.630	6.554	7.479	8.404	9.330
		-1.375	-1.593	-1.814	-2.040	-2.270	-2.502	-2.735	-2.971	-3.206	-3.443
	0.30	0.998	1.948	2.885	3.817	4.749	5.680	6.610	7.541	8.471	9.402
		-1.381	-1.598	-1.820	-2.045	-2.273	-2.504	-2.736	-2.968	-3.202	-3.436
	0.35	1.008	1.970	2.918	3.860	4.801	5.740	6.678	7.617	8.555	9.493
		-1.384	-1.603	-1.824	-2.049	-2.276	-2.504	-2.734	-2.965	-3.196	-3.428
	0.40	1.018	1.994	2.955	3.909	4.860	5.810	6.759	7.707	8.655	9.602
		-1.386	-1.607	-1.828	-2.051	-2.276	-2.503	-2.730	-2.959	-3.188	-3.418
	0.45	1.029	2.020	2.995	3.963	4.927	5.890	6.851	7.811	8.771	9.730
		-1.388	-1.609	-1.830	-2.052	-2.275	-2.500	-2.726	-2.952	-3.179	-3.406
	0.50	1.040	2.048	3.039	4.022	5.002	5.979	6.954	7.929	8.902	9.876
		-1.389	-1.611	-1.831	-2.052	-2.274	-2.496	-2.719	-2.943	-3.168	-3.393

TABLE 2 POSITION AT WHICH UNDERCUTTING OCCURES IN TAPERED GEARS

Z1.ASTAR.	1	1/2	1/3	1/4	1/5	1/6	1/7	1/8	1/9	1/10

SHAFT ANGLE 135 HELIX ANGLE 0.0

17.	0.00	0.967	1.906	2.842	3.779	4.716	5.654	6.592	7.531	8.469	9.408
		-2.468	-3.361	-4.270	-5.189	-6.114	-7.042	-7.973	-8.906	-9.840	-10.775
	0.05	0.971	1.914	2.854	3.793	4.732	5.671	6.610	7.550	8.489	9.429
		-2.474	-3.373	-4.286	-5.207	-6.133	-7.062	-7.993	-8.926	-9.860	-10.795
	0.10	0.975	1.923	2.867	3.809	4.751	5.693	6.634	7.576	8.518	9.460
		-2.479	-3.382	-4.297	-5.218	-6.144	-7.073	-8.003	-8.935	-9.868	-10.801
	0.15	0.980	1.933	2.882	3.828	4.774	5.720	6.665	7.610	8.556	9.501
		-2.483	-3.389	-4.304	-5.225	-6.149	-7.076	-8.004	-8.933	-9.864	-10.795
	0.20	0.984	1.944	2.899	3.850	4.801	5.752	6.702	7.652	8.601	9.551
		-2.486	-3.393	-4.307	-5.225	-6.147	-7.071	-7.995	-8.921	-9.848	-10.775
	0.25	0.989	1.956	2.917	3.875	4.832	5.789	6.745	7.700	8.655	9.611
		-2.488	-3.394	-4.306	-5.221	-6.138	-7.057	-7.978	-8.899	-9.820	-10.742
	0.30	0.995	1.969	2.937	3.903	4.867	5.830	6.793	7.755	8.717	9.679
		-2.488	-3.393	-4.300	-5.211	-6.123	-7.036	-7.951	-8.866	-9.781	-10.697
	0.35	1.000	1.983	2.959	3.933	4.905	5.877	6.847	7.817	8.787	9.757
		-2.488	-3.389	-4.291	-5.195	-6.101	-7.007	-7.914	-8.822	-9.730	-10.638
	0.40	1.006	1.997	2.983	3.966	4.947	5.927	6.907	7.886	8.864	9.843
		-2.486	-3.382	-4.278	-5.174	-6.072	-6.970	-7.869	-8.768	-9.667	-10.567
	0.45	1.012	2.012	3.008	4.001	4.992	5.982	6.971	7.960	8.949	9.937
		-2.483	-3.372	-4.260	-5.148	-6.036	-6.925	-7.813	-8.703	-9.592	-10.481
	0.50	1.018	2.028	3.035	4.038	5.040	6.041	7.041	8.041	9.040	10.039
		-2.479	-3.360	-4.238	-5.116	-5.993	-6.871	-7.748	-8.626	-9.504	-10.382
18.	0.00	0.966	1.905	2.842	3.778	4.716	5.653	6.592	7.530	8.469	9.407
		-2.460	-3.355	-4.265	-5.185	-6.110	-7.039	-7.971	-8.904	-9.838	-10.773
	0.05	0.970	1.913	2.853	3.792	4.731	5.670	6.609	7.549	8.488	9.428
		-2.467	-3.367	-4.281	-5.202	-6.129	-7.058	-7.990	-8.923	-9.858	-10.793
	0.10	0.974	1.922	2.866	3.808	4.750	5.691	6.633	7.575	8.517	9.459
		-2.472	-3.376	-4.292	-5.214	-6.140	-7.069	-8.000	-8.932	-9.865	-10.799
	0.15	0.979	1.932	2.880	3.827	4.773	5.718	6.664	7.609	8.554	9.499
		-2.476	-3.382	-4.298	-5.220	-6.144	-7.071	-8.000	-8.930	-9.860	-10.791
	0.20	0.983	1.943	2.897	3.849	4.800	5.750	6.700	7.650	8.600	9.549
		-2.478	-3.386	-4.301	-5.220	-6.142	-7.066	-7.991	-8.917	-9.844	-10.771
	0.25	0.988	1.955	2.915	3.874	4.831	5.787	6.743	7.698	8.654	9.609
		-2.480	-3.387	-4.299	-5.215	-6.133	-7.052	-7.973	-8.894	-9.816	-10.738
	0.30	0.993	1.968	2.936	3.901	4.865	5.828	6.791	7.753	8.715	9.677
		-2.480	-3.385	-4.294	-5.205	-6.117	-7.031	-7.945	-8.861	-9.776	-10.692
	0.35	0.999	1.981	2.957	3.931	4.903	5.874	6.845	7.815	8.785	9.754
		-2.480	-3.381	-4.284	-5.189	-6.095	-7.001	-7.909	-8.817	-9.725	-10.633
	0.40	1.004	1.995	2.981	3.964	4.945	5.925	6.904	7.883	8.862	9.840
		-2.478	-3.374	-4.271	-5.168	-6.065	-6.964	-7.863	-8.762	-9.661	-10.561
	0.45	1.010	2.011	3.006	3.998	4.990	5.980	6.969	7.958	8.946	9.934
		-2.475	-3.365	-4.253	-5.141	-6.029	-6.918	-7.807	-8.696	-9.586	-10.475
	0.50	1.016	2.026	3.032	4.036	5.038	6.038	7.039	8.038	9.037	10.036
		-2.471	-3.352	-4.231	-5.109	-5.986	-6.864	-7.742	-8.620	-9.498	-10.376

TABLE 2 POSITICN AT WHICH UNDERCUTTING OCCURES IN TAPERED GEARS

Z1.ASTAR.	1	1 1/2	1 1/3	1 1/4	1 1/5	1 1/6	1 1/7	1 1/8	1 1/9	1 1/10
SHAFT ANGLE 135										HELIX ANGLE 10.0
17. 0.00	1.001	1.955	2.9	3.842	4.782	5.721	6.661	7.599	8.538	9.477
	-2.523	-3.441	-4.362	-5.288	-6.216	-7.146	-8.078	-9.011	-9.945	-10.880
0.05	0.994	1.941	2.878	3.813	4.746	5.680	6.613	7.546	8.479	9.411
	-2.514	-3.421	-4.333	-5.250	-6.170	-7.093	-8.018	-8.944	-9.871	-10.798
0.10	0.988	1.927	2.858	3.786	4.715	5.643	6.571	7.499	8.428	9.356
	-2.504	-3.398	-4.299	-5.206	-6.118	-7.032	-7.948	-8.866	-9.785	-10.705
0.15	0.982	1.914	2.842	3.763	4.687	5.612	6.536	7.461	0.000	0.000
	-2.492	-3.373	-4.024	-5.158	-6.059	-6.963	-7.869	-8.778	0.000	0.000
0.20	0.976	1.902	2.862	3.756	4.664	5.576	6.508	7.410	8.353	9.276
	-2.480	-3.345	-4.007	-4.922	-5.992	-6.743	-7.780	-8.559	-9.576	-10.476
0.25	0.970	1.891	2.883	3.777	4.684	5.597	6.513	7.431	8.350	9.271
	-2.466	-3.314	-3.988	-4.892	-5.791	-6.689	-7.586	-8.482	-9.377	-10.272
0.30	0.965	1.882	2.906	3.802	4.709	5.623	6.540	7.459	8.379	9.300
	-2.451	-3.280	-3.966	-4.858	-5.745	-6.631	-7.515	-8.398	-9.281	-10.163
0.35	0.960	1.874	2.931	3.829	4.739	5.654	6.573	7.494	8.416	9.339
	-2.435	-3.245	-3.942	-4.820	-5.694	-6.566	-7.436	-8.305	-9.174	-10.043
0.40	0.955	1.881	2.958	3.859	4.772	5.691	6.613	7.537	8.462	9.388
	-2.417	-3.233	-3.914	-4.778	-5.637	-6.494	-7.349	-8.203	-9.057	-9.910
0.45	0.951	1.890	2.986	3.892	4.810	5.733	6.659	7.587	8.517	9.447
	-2.398	-3.217	-3.884	-4.731	-5.574	-6.414	-7.253	-8.090	-8.927	-9.763
0.50	0.952	1.899	3.017	3.928	4.851	5.779	6.711	7.644	8.580	9.515
	-2.389	-3.198	-3.850	-4.680	-5.505	-6.326	-7.147	-7.966	-8.784	-9.601
18. 0.00	0.999	1.953	2.898	3.840	4.780	5.719	6.658	7.597	8.536	9.474
	-2.515	-3.433	-4.356	-5.282	-6.210	-7.141	-8.073	-9.006	-9.940	-10.875
0.05	0.992	1.939	2.876	3.811	4.744	5.678	6.611	7.544	8.477	9.410
	-2.506	-3.414	-4.326	-5.244	-6.165	-7.088	-8.013	-8.939	-9.867	-10.794
0.10	0.986	1.925	2.856	3.785	4.713	5.641	6.570	7.498	8.426	9.355
	-2.495	-3.391	-4.293	-5.201	-6.113	-7.028	-7.944	-8.862	-9.781	-10.701
0.15	0.980	1.912	2.839	3.762	4.686	5.610	6.535	0.000	0.000	0.000
	-2.484	-3.366	-4.026	-5.152	-6.054	-6.959	-7.865	0.000	0.000	0.000
0.20	0.974	1.900	2.857	3.753	4.663	5.574	6.507	7.430	8.352	9.275
	-2.471	-3.338	-4.009	-4.923	-5.988	-6.744	-7.777	-8.674	-9.573	-10.473
0.25	0.969	1.890	2.878	3.774	4.681	5.594	6.511	7.429	8.349	9.269
	-2.458	-3.307	-3.989	-4.893	-5.792	-6.690	-7.586	-8.482	-9.377	-10.272
0.30	0.964	1.880	2.901	3.798	4.706	5.620	6.537	7.456	8.377	9.298
	-2.443	-3.273	-3.967	-4.858	-5.746	-6.631	-7.515	-8.398	-9.281	-10.163
0.35	0.959	1.873	2.925	3.824	4.735	5.651	6.570	7.491	8.414	9.337
	-2.427	-3.240	-3.943	-4.820	-5.694	-6.566	-7.436	-8.305	-9.174	-10.043
0.40	0.954	1.880	2.952	3.854	4.768	5.687	6.610	7.534	8.459	9.386
	-2.409	-3.227	-3.915	-4.778	-5.637	-6.493	-7.348	-8.203	-9.056	-9.909
0.45	0.950	1.889	2.980	3.887	4.805	5.728	6.655	7.584	8.513	9.444
	-2.390	-3.211	-3.884	-4.731	-5.574	-6.414	-7.252	-8.089	-8.926	-9.762
0.50	0.951	1.898	3.010	3.922	4.846	5.774	6.706	7.640	8.576	9.512
	-2.382	-3.191	-3.850	-4.679	-5.504	-6.326	-7.146	-7.964	-8.783	-9.600

Let ϕ_{uk} be the solution of the equation (2.48). From equations (2.14) and (2.15), we get

$$\lambda_{uk} = \frac{1-i_{21}C\Sigma-ai_{21}C\Sigma S\phi_{uk}-i_{21}S\Sigma \tan\beta(S\phi_k-\theta^*_{k\epsilon}C\phi_k+a)}{i_{21}S\Sigma\, C\phi_k}$$

$$\theta_{uk} = \theta^*_k + \lambda_{uk}\tan\beta \pm \eta_1$$

and $\phi_{1uk} = \phi_{uk} - \theta_{uk}$.

The distance at which undercutting starts is given by

$$r_{2uk} = [R^2_{x2k} + R^2_{y2k}]^{1/2} \cos\alpha_{os} \qquad 2.50$$

$$z_{2uk} = R_{z2}\cos\alpha_{os}$$

and $$z_{1uk} = \lambda_{uk}\cos\alpha_{os}$$

where, $\underset{\sim}{R}_{2k} = [R_{x2k}(\theta_{uk},\phi_{1uk}),\ R_{y2k}(\theta_{uk},\phi_{1uk}),\ R_{z2k}(\theta_{uk},\phi_{1uk})]^T$

Here r_{uk}, z_{2uk} and z_{1uk} are non-dimensionalized with respective to nominal pitch radius of the cutter. This is done for the sake of convenience is use.

It can be observed that undercutting depends on Z_o, α_{os}, i_{20}, f_{os}, Σ, β and a. Some sample results for different set of these parameters are given in Table (2)[1]

2.10 Curvatures at the contact-point.

The normal curve on a surface is a curve obtained when a plane containing the normal, at that point of the surface, intersects it

---

[1] For more results see [22] .

The curvature of normal curve is called the normal curvature of the su... Out of the infinite positions of the plane, (the plane can rotate about the normal), at two positions normal curvatures, attain maximum and minimum values. These curvatures are called principal curvatures. Principal curvatures are used to find the contact zone, the contact stress, the surface durability ratings and for analysing the interference of the surface, if any.

The principal curvatures of the generating (pinion) surface are found easily because of its relatively simple geometry. Generally, the expressions for a generated (Gear) surface are more complex then those of the generating (pinion) surface. For this reason, defining the principal curvatures of a generated surface becomes more difficult.

Many investigators have found the principal curvatures of the gear tooth indirectly [8][15][16]. Litvin [17] related the princip... curvatures of generated surface with those of the generating surface and the parameters of motion[1]. In the subsequent development use will be made of the results of his investigations.

2.10.a Basic formulas

1° From the differential geometry [24], we know that the curvatures at any point of the surfaces on the normal plane containing the vector $\underset{\sim}{V}_r^1$ are given by

$$\chi^i = - \frac{\underset{\sim}{V}_r^i \cdot \dot{\underset{\sim}{e}}_r^i}{[\underset{\sim}{V}_r^i]^2} \quad ; \; i = 1,2 \qquad 2.51$$

---

[1] See appendix III.

where, $\underset{\sim}{V}^i_r$ is the velocity of the point in motion along the surface Σ_i and is given by

$$\underset{\sim}{V}^i_r = \frac{\partial \underset{\sim}{R}^i}{\partial \theta}\frac{d\theta}{dt} + \frac{\partial \underset{\sim}{R}^i}{\partial \lambda}\frac{d\lambda}{dt}, \qquad 2.52$$

$\dot{\underset{\sim}{e}}^i_r$ is the velocity of the tip of the unit normal when the contact point along with the normal is in motion on the surface and is given as

$$\dot{\underset{\sim}{e}}^i_r = \frac{\partial \underset{\sim}{e}_i}{\partial \theta}\frac{d\theta}{dt} + \frac{\partial \underset{\sim}{e}_i}{\partial \lambda}\frac{d\lambda}{dt}, \qquad 2.53$$

$\underset{\sim}{e}_i$ is the unit normal to the surface

and θ , λ are the parameters of the surface.

Positive sign of χ^i indicates that the normal vector points towards the center of curvature.

2° To find the principal curvatures, χ_I and χ_{II}, of surface Σ_1 at the contact point, Rodrigue's formula is used, according to which,

$$\dot{\underset{\sim}{e}}^1_r = -\chi_{I,II}\,\underset{\sim}{V}^1_r \qquad 2.54$$

where, I, II-indices of principal directions. Along the principal directions $\dot{\underset{\sim}{e}}^1_r$ and $\underset{\sim}{V}^1_r$ are collinear and the following relation holds good.

$$\dot{e}^1_{xr}/V^1_{xr} = \dot{e}^1_{yr}/V^1_{yr} = \dot{e}^1_{zr}/V^1_{zr} \qquad 2.55$$

To find the principal curvatures of generated surface, Σ_2 the following formulas are used [17] . These are more advantageous in practice than the use of Rodrigue's formula.

3° The principal curvatures, χ_{III} and χ_{IV} of the generated are given by [Appendix III] ,

$$\chi_{III} = [\chi_I + \chi_{II} + S + (\chi_I - \chi_{II} + G)/C2\sigma]/2$$
$$\chi_{IV} = [\chi_I + \chi_{II} + S - (\chi_I - \chi_{II} + G)/C2\sigma]/2 \qquad 2.56$$

where, $\tan(2\sigma) = 2F/[\chi_I - \chi_{II} + G]$, 2.57

$$F = a_{31}\, a_{32}/D^* \qquad 2.58$$

$$G = [a_{31}^2 - a_{32}^2]/D^*, \qquad 2.59$$
$$S = [a_{31}^2 + a_{32}^2]/D^*,$$

$$D^* = b_3 + \bar{V}_I^{12}\, a_{31} + \bar{V}_{II}^{12}\, a_{32} , \qquad 2.60$$

$$b_3 = \bar{e}_1 \cdot [\Omega_2 \times (\Omega_1 \times \bar{R}_1) - \Omega_1 \times (\Omega_2 \times \bar{R}_1 + A \times \Omega_2)], \qquad 2.61$$

$$a_{31} = (\bar{e}_1, \Omega_{12}, \bar{i}_I) - \chi_I \bar{V}_I^{12} , \qquad 2.62$$

$$a_{32} = (\bar{e}_1, \Omega_{12}, \bar{i}_{II}) - \chi_{II} \bar{V}_{II}^{12} , \qquad 2.63$$

$$\bar{V}_I^{12} = \bar{V}_1^{12} \cdot \bar{i}_I , \qquad 2.64$$

$$\bar{V}^{12}_{II} = \bar{\underset{\sim}{V}}^{12}_{1} \cdot \bar{\underset{\sim}{i}}_{II} \,, \qquad 2.65$$

σ - angle between the directions of χ_I and χ_{III},

$\bar{i}_I$, $\bar{i}_{II}$ - units vectors along the directions of χ_I and χ_{II} in the fixed co-ordinate system, $\bar{S}_1$,

$\bar{\underset{\sim}{V}}^{12}_{1}$ - relative velocity vector at the contact point in the fixed co-ordinate system, $\bar{S}_1$.

2.10.2 Principal curvatures in tapered gears

The principal curvatures in this case are found using the formulas given in the preceding section.

1° The principal curvatures of the generating surface, Σ_1, are found using equations (2.54) and (2.55). The vector

$$\underset{\sim}{V}^{1}_{r} = [\dot{\lambda} \tan \beta C\Theta_k + \Theta^* S\Theta_k \dot{\Theta}_k,\ \dot{\lambda} \tan \beta S\Theta_k - \Theta^* C\Theta_k \dot{\Theta}_k,\ \dot{\lambda}]^T \qquad 2.66$$

is obtained using equations (2.6) and (2.52). The vector $\dot{\underset{\sim}{e}}^{1}_{r}$ is given as [equations (2.9) and (2.53)]

$$\dot{\underset{\sim}{e}}^{1}_{r} = [S\Theta_k C\beta\ \dot{\Theta}_k,\ -C\Theta_k\ C\beta\ \dot{\Theta}_k, 0]^T \qquad 2.67$$

Using equation (2.55) one finds,

a. for principal direction I, $\dot{\Theta}_k = 0$

and b. for principal direction II, $\dot{\lambda} = 0$. 2.68

Now equations (2.68) and (2.54) yield,

$$\chi_I = 0 \text{ and } \chi_{II} = - C\beta/\theta_k^* \qquad 2.69$$

The involute helicoid is a ruled surface. For a ruled surface, one of its principal curvatures is zero which is also seen from equation (2.69). The unit vectors along the principal directions are found using the following expressions.

$$\underset{\sim}{i}_I = \left.\frac{\underset{\sim}{V}_r^1}{|\underset{\sim}{V}_r^1|}\right|_{\dot{\theta}_k=0} = [C\theta_k\ S\beta,\ S\theta_k\ S\beta,\ C\beta]^T \qquad 2.70$$

and

$$\underset{\sim}{i}_{II} = \left.\frac{\underset{\sim}{V}_r^1}{|\underset{\sim}{V}_r^1|}\right|_{\dot{\lambda}=0} = [S\theta_k,\ -C\theta_k,\ 0]^T \qquad 2.71$$

2° The principal curvatures of the generated surface Σ_2 are found using equations (2.56) to (2.65). Vectors $\underset{\sim}{e}_1$, $\underset{\sim}{i}_I$, $\underset{\sim}{i}_{II}$, $\underset{\sim}{R}_1$ and $\underset{\sim}{V}_1^{12}$ are expressed in the fixed coordinate system by the following

$$\bar{\underset{\sim}{e}}_1 = [-C\beta\ C\Phi_k,\ -C\beta\ S\Phi_k,\ S\beta]^T \qquad 2.72$$

$$\bar{\underset{\sim}{i}}_I = [S\beta\ C\Phi_k,\ S\beta\ S\Phi_k,\ C\beta]^T \qquad 2.73$$

$$\bar{\underset{\sim}{i}}_{II} = [S\Phi_k,\ -C\Phi_k,\ 0]^T \qquad 2.74$$

$$\bar{\underset{\sim}{R}}_1 = [\{S\Phi_k - \theta_k^* C\Phi_k\},\ -\{C\Phi_k + \theta_k^* S\Phi_k\},\ \lambda]^T \qquad 2.75$$

and

$$\bar{V}_{\sim 1}^{12} = \begin{Bmatrix} -[\bar{R}_{y1}(1-i_{21}C\Sigma) + \bar{R}_{z1}\, i_{21}\, S\Sigma] \\ [\bar{R}_{x1}(1-i_{21}C\Sigma) - a\, i_{21}\, C\Sigma] \\ [(\bar{R}_{x1} + a)\, i_{21}\, S\Sigma] \end{Bmatrix} \qquad 2.76$$

The vectors Ω_1, Ω_2, Ω_{12} and A are found, refering to Figure as follows [5] :

$$\Omega_1 = [0,0,1]^T \qquad 2.77$$

$$\Omega_2 = [0,\ i_{21}\, S\Sigma,\ i_{21}\, C\Sigma]^T \qquad 2.78$$

$$\Omega_{12} = [0,\ -i_{21}\, S\Sigma,\ 1 - i_{21}\, C\Sigma]^T \qquad 2.79$$

and $$A = [-a,\ 0,\ 0]^T \qquad 2.80$$

Now, using the preceding equations one can write,

$$b_3 = -(C\Phi_k + \Theta_k^* S\Phi_k) i_{21} S\Sigma S\beta + \lambda i_{21} S\Sigma S\Phi_k C\beta - a i_{21} C\Sigma C\Phi_k C\beta \qquad 2.81$$

$$\bar{V}_I^{12} = S\beta(1-i_{21}C\Sigma) - \lambda i_{21} S\Sigma C\Phi_k S\beta - a i_{21} C\Sigma S\Phi_k S\beta +$$

$$+ (S\Phi_k - \Theta_k^* C\Phi_k + a)\, i_{21}\, S\Sigma C\beta \qquad 2.82$$

$$\bar{V}_{II}^{12} = \Theta_k^*(1-i_{21}C\Sigma) - \lambda i_{21} S\Sigma S\Phi_k + a i_{21} C\Sigma C\Phi_k \qquad 2.83$$

$$a_{31} = i_{21}\, S\Sigma\, C\Phi_k$$

and $$a_{32} = [\Theta_k^* i_{21} S\Sigma S\Phi_k S\beta - \lambda i_{21} S\Sigma S\Phi_k C\beta + a i_{21} C\Sigma C\Phi_k C\beta]/\Theta_k^* \,. \qquad 2.84$$

The principal curvatures of the generated surface can be found using equations (2.56) to (2.60). The angle σ is calculated using equation (2.57).

CHAPTER 3

PRESSURE ANGLE

In this chapter, the method for calculating the pressure angles for higher kinematic pairs will be given. Using this analysis, a general formulation for the pressure angle of the tapered gears will be developed.

3.1 Pressure angle in higher kinematic pair.

The main function of the gears, or for that matter any machine element, is to transmit motion and/or power. The efficiency of power transmission is to be considered for judging the suitability of a machine element for any particular application. The mechanisms which will come in the purview of this chapter include plate cams, cylindrical cams, geneva wheels, gears etc.

The maximum stress which the surface can bear at a given contact point depends upon their material properties. The pressure angle provides us a measure of how efficiently force can be transmitted from one surface to the other contacting surface.

Let two surfaces Σ_1 and Σ_2, hinged at O_1 and O_2 respectively, be contacting at the point P at any instant [Figure 7]. We assume that $\underset{\sim}{V}_e^1$ and $\underset{\sim}{e}^1$ are the absolute velocity and unit normal vectors respectively in co-ordinate system S_1 which is fixed to surface Σ_1. Now $P_1 = |\underset{\sim}{V}_e^1 \cdot (F\underset{\sim}{e}^1)|$

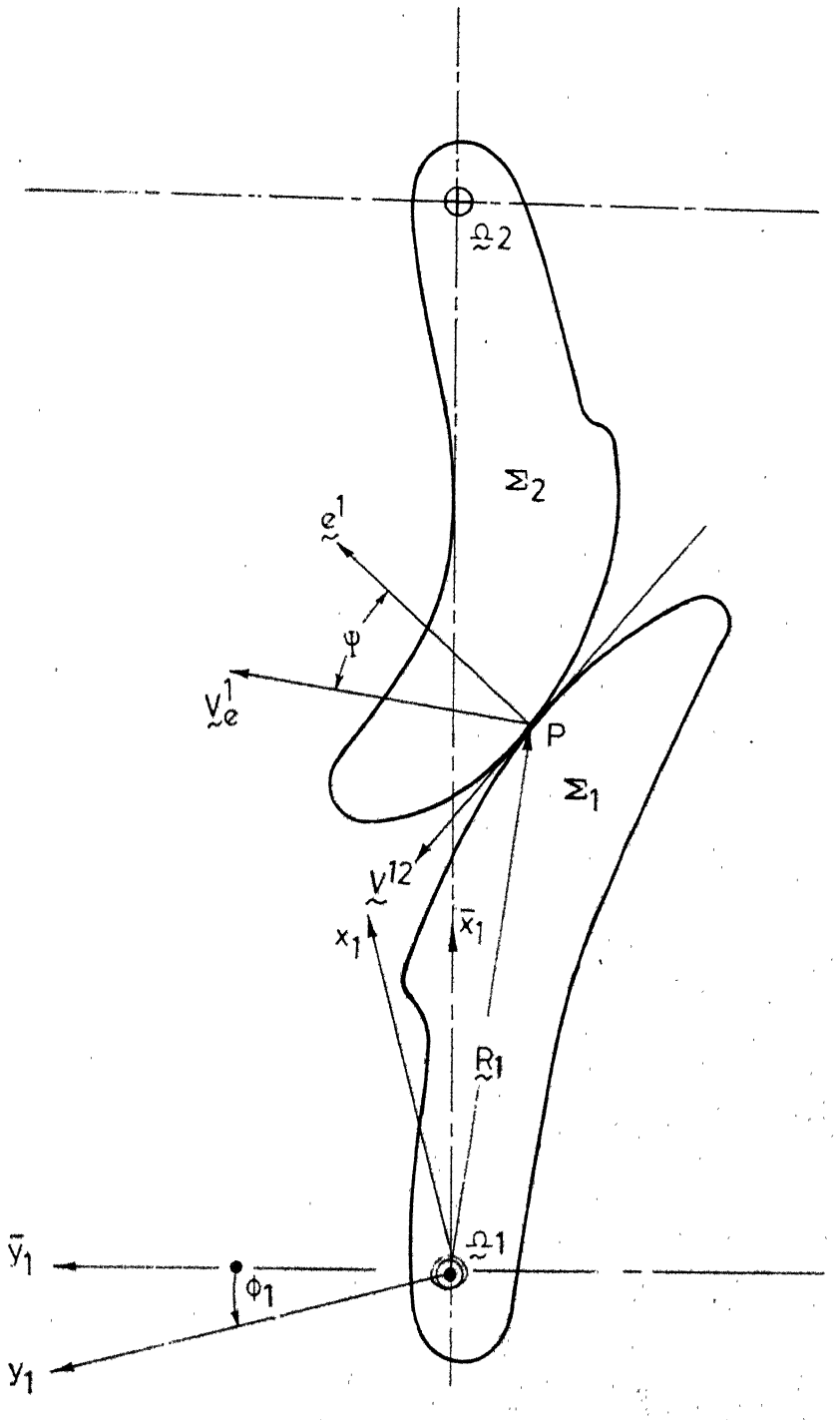

FIG. 7 PRESSURE ANGLE AT CONTACT POINTS

is the power transmitted at this instant. Here, the absolute sign is used to permit the arbitrary choice of the sign of the vector $\underset{\sim}{e}^1$. For a given force, F, the maximum power P_{max} which can be transmitted at this instant is $F|\underset{\sim}{V}_e^1|$. It can be seen that the ratio $|\underset{\sim}{V}_e^1 \cdot \underset{\sim}{e}^1| / F|\underset{\sim}{V}_e^1|$ is less than or equal to unity. Hence, we may write

$$\text{Cos } [\psi(\theta,\lambda)] = \frac{|\underset{\sim}{V}_e^1 \cdot \underset{\sim}{e}^1|}{|\underset{\sim}{V}_e^1|} \qquad 3.1$$

The vectors $\underset{\sim}{V}_e^1$ and $\underset{\sim}{e}^1$ can be evaluated from the following

$$\underset{\sim}{V}_e^1 = \underset{\sim}{\Omega}_1 \times \underset{\sim}{R}_1$$

and

$$\underset{\sim}{e}^1 = \frac{\partial \underset{\sim}{R}_1}{\partial \theta} \times \frac{\partial \underset{\sim}{R}_1}{\partial \lambda} \Big/ \left| \frac{\partial \underset{\sim}{R}_1}{\partial \theta} \times \frac{\partial \underset{\sim}{R}_1}{\partial \lambda} \right|$$

Here, θ and λ are parameters of surface Σ_1, $\underset{\sim}{\Omega}_1$ is the angular velocity vector of Σ_1 and $\underset{\sim}{R}_1$ is the position vector of point P [Figure 7] . These vectors have to be evaluated at the contact point. For conjugate surfaces it can be found using equation of contact.

It may be noted that the pressure angle does not depend upon the nature of surface Σ_2 as long as contact between Σ_1 and Σ_2 is at P. It may be also be observed from equation (3.1) that for high pressure angles the power transmitted will be less than the material would permit normally. In the following section, an application of the formula developed above is given.

3.2 Pressure angle in taperd gears

It was shown in Chapter 2 that the pitch surface of the pinion in mesh with the tapered gear is either conical or hyperboloidal

[see section 2.2] . Consequently, the pressure angle of the set changes along the face of the tooth. Also, it has been observed that if the point of contact and the surface Σ_1 of the pinion are known, the pressure angle of the gear combination can be easily found. The geometery of the pinion is simpler than that of a gear. Therefore, the expressions for the pressure angle will be derived considering the pinion geometery. The steps involved are given below.

3.2.1 The velocity vector $\underset{\sim}{V}^1_e$ is given by

$$\underset{\sim}{V}^1_e = \underset{\sim}{\Omega}_1 \times \underset{\sim}{R}_1 = \{- \omega_1 R_{y1} , \omega_1 R_{x1}, 0\}^T \qquad 3.2$$

where, R_{x1} and R_{y1} are the components of the vector $\underset{\sim}{R}_1$ along the respective co-ordinate axes [equation 2.6].

3.2.2 The unit normal can be written as

$$\underset{\sim}{e}^1 = [-C\theta_k \, C\beta, \, -C\theta_k \, C\beta, \, S\beta]^T \qquad 3.3$$

3.2.3 The pressure angle, ψ , is given as,

$$\psi = \cos^{-1} \left[\frac{C\beta}{(R_{x1}^2 + R_{y1}^2)^{1/2}} \right] \qquad 3.4$$

3.3 Pressure angle at points on pitch surface.

Equation (3.4) is valid for any point on the tooth surface. Generally, in gearing the designer is interested in the pressure angles at contact points on the pitch surface. Using equations (3.4) and (2.4), one can find

$$\alpha = \alpha(E^*,\lambda^*) = \text{Cos}^{-1}\left[\frac{1}{(E^{*2} + \lambda^{*2})^{1/2}}\right] \qquad 3.5$$

where

$$E^* = \frac{a(i_{21} - C\Sigma)\, i_{21}\, \text{Sec}\,\beta}{(1 - 2\, i_{21}\, C\Gamma + i_{21}^2)} \qquad 3.6$$

$$\lambda^* = \frac{i_{21}\, C\Sigma\, \lambda\, \text{Sec}\,\beta}{1 - i_{21}\, C\,\Sigma} \qquad 3.7$$

and α is the pressure angle at contact points on the pitch surface.

Figure 8 shows the variation of the pressure angle with E^* and λ^*.

For external and internal spur gears, $\Sigma = \pi$ and $\Sigma = 0$ respectively. For these cases the equations take following form

$$\alpha = \text{Cos}^{-1}\left[\frac{1 \pm i_{21}}{a\, i_{21}}\right] \qquad 3.8$$

Here, upper and lower sign are for external and internal spur gears respectively. Equation (3.8) is a familiar expression for the pressure angle in the aforementioned cases.

Similar expressions of pressure angles for spur tapered gears were derived earlier in the references [5][12] . For involute curve the pressure angle at any point on curve is given by

$\text{Cos}\,\psi = \frac{1}{r}$, where r is the radius of cylinder on which the point lies. This property of the curve was used to find the pressure angle. It is to be noted here that the equation (3.1) can be used for any surface.

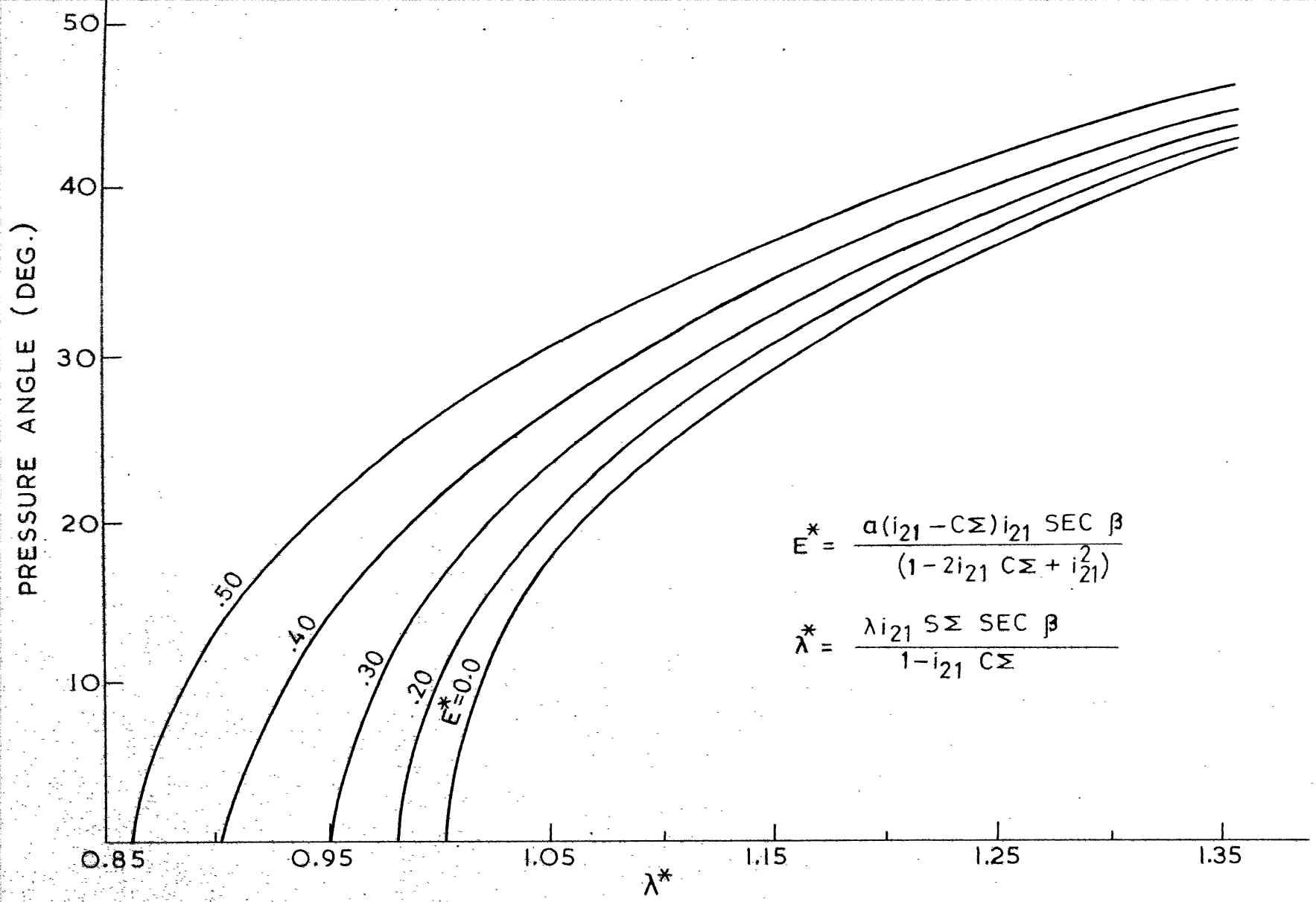

FIG. 8 PRESSURE ANGLE VARIATION IN TAPERED GEARS

CHAPTER 4

DURATION OF CONTACT

One of the important factors in the design of gears is the proportions of the tooth. These must be so chosen that the second pair of mating teeth is in contact before the first pair goes out of contact.

The boundaries of the tooth surfaces are established by the shape of the blank on which the teeth are formed. The volume common to the blanks of a pair of gears is the region of mesh. Only those portions of the surfaces of action lying with in the region of mesh are available for motion transmission. Furthermore the action limit curves [19] place an additional limit on tooth action. These restrictions establish the boundaries of effective surface of action [19] .

The extent of the effective surface of action determines the amount of rotation of the gear during which one pair of the tooth surfaces remains in contact. The ratio of this angle of rotation to the angular pitch is the contact ratio. The duration of contact is measured in terms of contact ratio. Contact ratio is sometimes reffered to as average number of tooth in contact or total contact ratio.

Here, for calculation of theoretical contact ratio it is assumed that no tip relief exists in the gears.

4.1 Contact ratio of gears having line contact.

The contact ratio of gears can be found using the concept of the field of contact [5] [12] [13][21] . In this method, it becomes necessary to draw the field of contact to have an idea of where the contact starts and ends. The concept of field of contact is extended here using the concept of sets, thereby eliminating the necessity of computing the boundaries of the field of contact, the lines of contact and subsequent plotting.

Let the set $\tilde{G}_1$ be the collection of points contained in the physical dimensions of the pinion.

$$\tilde{G}_1 = \{\underset{\sim}{x} | g_i(\underset{\sim}{x}) \leq 0,\ i = 1,n\} \qquad 4.1$$

Here g_i's are the n-surfaces which define boundaries of the blank. For on-center tapered gear these surfaces are: the face cone, the front cone and the back cone. In this case, n = 3 [Figure 5] . Similarly, a set $\tilde{G}_2$ is defined for the gear. The intersection of these two sets constitute the region of mesh. If $\tilde{R}$ is the set of the collection of points in the region of mesh, then

$$\tilde{R} = \tilde{G}_1 \cap \tilde{G}_2 \qquad 4.2$$

Consider the surface of action as mapping

$$\underset{\sim}{P}_c : E^2 \rightarrow E^3 \qquad 4.3$$

Here, E^2 and E^3 are the spaces of 2 and 3 dimensions respectively.

Let a set

$$\tilde{A} \equiv \{\theta | h_i(\theta) \leq 0,\ i = 1,2\}$$

where, $h_i = 0$ defines the action limit curve [19] on the contact surface. For an involute spur pinon,

$$h_1 = \theta_k + \phi_1 - \alpha = 0 \ , \ k = 0,1$$

with above definations, the condition for physical contact between the teeth surfaces is expressed mathematically as

$$\underset{\sim}{P}_c(\theta) \in \tilde{P} \ni \underset{\sim}{Q} \in \tilde{\Phi} \cap \tilde{A} \qquad 4.4$$

where, $\underset{\sim}{Q} = [\theta, \phi_1]^T$

θ - scalar parameter of tooth surface,

ϕ_1 - scalar parameter of motion that is angle of rotation of pinion

and $\tilde{\Phi}$ - set of a collection of ϕ_1 and θ .

The contact ratio is found by using the expression,

$$\epsilon_\gamma = \frac{\phi_{1\,max} - \phi_{1\,min}}{2\pi/Z_1} \qquad 4.5$$

where, $2\pi/Z_1$ is the angular pitch of the pinion teeth

$$\phi_{1\,max} = \underset{\underset{\sim}{Q} \in \tilde{\Phi} \cap \tilde{A}}{Max} \phi_1 \text{ , subject to } \underset{\sim}{P}_c(\underset{\sim}{Q}) \in \tilde{P} \qquad 4.6$$

and $\phi_{1\,max} = \underset{\underset{\sim}{Q} \in \tilde{\Phi} \cap \tilde{A}}{Min} \phi_1$, subject to $\underset{\sim}{P}_c(\underset{\sim}{Q}) \in \tilde{P}$ 4477

In finding the contact ratio from equation (4.5) the main problem is to evaluate the $\phi_1^{'s}$ given by the expressions (4.6) and (4.7). A procedure to evaluate these is described below.

Mostly, it is easier to estimate the set $\tilde{\Phi}$. Here it is assumed that the set $\tilde{\Phi}$ is given as

$$\tilde{\Phi} \equiv [\underset{\sim}{\Theta} | \Theta \in I_\Theta,\ \phi_1 \varepsilon I_\phi]$$

where, $I_\Theta \equiv [\theta | \theta^1 \leq \theta \leq \theta^2]$

$$I_\phi \equiv [\phi_1 | \phi^1 \leq \phi_1 \leq \phi^2]$$

here, ϕ^1 and ϕ^2 are so chosen that,

$$\underset{\sim}{P}_c(\theta,\phi^1) \notin \tilde{P}\ \forall\ \theta \in I_\theta \text{ and } [\theta,\phi^1] \in \tilde{A} \qquad 4.8$$

and $\underset{\sim}{P}_c(\theta,\phi^2) \notin \tilde{R}\ \forall\ \theta \in I_\theta$ and $[\theta,\phi^2] \in \tilde{A}$

The intervals I_Θ and I_ϕ are problem dependent. In case of the involute spur pinion the parameter θ corresponds to the angle of development of the involute curve [Figure 2]. The contact point in this case can not go beyound the base cylinder and the external cylinder of the pinion. Thus, $I_\Theta \equiv [0,\theta_e]$. Here, θ_e is the angle of development corresponding to the external cylinder. The interval I_ϕ is dependent on the type of gear set and the coordinate system. For the spur face gear set and for the coordinate system used, it can be taken as $I_\phi \equiv [-\delta_1(2\pi/Z_1), \delta_1(2\pi/Z_1)]$. Here δ_1 is the arbitrary constant such that, $\delta_1 > 1$. The efficiency of this procedure depends to a certain extent on the choice of I_ϕ and I_Θ.

In cases where the set $\tilde{\phi} = I_\theta \otimes I_\phi$ is known it is possible to evaluate ϕ_{1min} and ϕ_{1max} by adopting a systematic search. Let, $\Delta\theta$ and $\Delta\phi$ be the increments in θ and ϕ_1 respectively and

$$\ell = \text{integer } [(\theta^2 - \theta^1)/\Delta\theta] + 1 \qquad 4.9$$

The method then consists of the following steps.

Step 1 Set, $\theta = \theta^1, \Delta\phi_1 = \Delta\phi$ and $\phi_1 = \phi^1$

Step 2 Find R_{ci} , $\underset{\sim}{R}_{ci} = \underset{\sim}{R}_c\ (\theta + i\Delta\theta,\ \phi_1 + \Delta\phi_1)$, $i = 1,\ell$

Step 3 If any R_{ci} satisfies equation (4.4) then go to step 5; if not, next step follows.

Step 4 ϕ_1 is incremented by $\Delta\phi_1$. Step 2 is repeated

Step 5 If $\Delta\phi_1 \leq e$ where e is a specified accuracy; the procedure terminates and $\phi_{1min} = \phi_1 + \Delta\phi_1$. Otherwise, $\Delta\phi_1$ is halved and the procedure is repeated starting with step 2.

Similarly, using the preceding steps, and setting $\phi_1 = \phi^2$ and $\Delta\phi_1 = -\phi_1$, ϕ_{1max} is estimated.

This procedure may be easily adopted for computer programming. The use of the method is illustrated by an example in the last chapter.

4.2 Contact ratio of gears having point contact.

In this case the contact point is defined by the given parameter of motion, ϕ_1 . The procedure described in the

previous section is modified to suit this condition. The modified procedure is as follows.

Step 1 Set, $\phi_1 = \phi^1$ and $\Delta\phi_1 = \Delta\phi$

Step 2 Find $\underset{\sim}{P}_c = \underset{\sim}{P}_c(\phi_1 + \Delta\phi_1)$

Step 3 If $\underset{\sim}{P}_c$ satisfies the following condition,

$$\underset{\sim}{P}_c(\phi_1) \subset \tilde{P},\ \phi_1 \in \tilde{\Phi} \cap \tilde{\Lambda}$$

where, $\tilde{\Phi}$ set of collection of ϕ_1 then go to step 5, if not, next step follows

Step 4 ϕ_1 is incremented by $\Delta\phi_1$. The procedure is repeated starting with step 2

Step 5 If $\Delta\phi_1 \leq e$, the procedure terminates and $\phi_{1min} = \phi + \Delta\phi_1$. Otherwise, $\Delta\phi_1$ is halved and once again start with step 2.

Similarly, setting $\phi_1 = \phi^2$ and $\Delta\phi_1 = -\Delta\phi$, ϕ_{1max} is estimated following the preceding procedure.

CHAPTER 5

ANALYSIS OF FACE GEARS

The face gear is a particular case of the tapered gear. A tapered gear is termed as a face gear when the gear and pinion shafts are at right angle. Here face gears in mesh with the cylindrical pinions will be considered. The pinion considered have the teeth of either involute spur or involute helicoid form. The gear with spur pinion is termed as the spur face gear. The gear in mesh with helical pinion is termed as spiral face gear. The face gear is generated by a cutter substantially of the same size and form of the pinion. The gears may have either intersecting axes, forming the on-center gear or non-intersecting axes, forming an off-set arrangement. The on-center face gear set is functionally identical with a bevel gear set. In both these cases, pitch surfaces are conical.

Face gears have the same types of limitations on face width as discussed earlier in chapter 2. Here the limiting inside (minimum) diameter is governed by the undercutting of the tooth. This diameter is always larger than the diameter where pressure angle on the pitch surface is zero [2] . The maximum usable out side diameter is the diameter at which the teeth become pointed. This constraint may be relaxed in some case for practical reasons [2] . Equations for tooth profile and curvatures and the conditions of undercutting and pointing are developed in the first few sections of this chapter.

The problems of localization of the contact, finding the contact spot and the contact zone, evaluation of contact stress and the surface durability rating are discussed in the remaining sections.

5.1 Spiral face gears

The contents of Chapter 2 will be used for finding the equations applicable to this case. As mentioned earlier, for face gears the shaft angle is 90 degrees.

5.1.1. Contact line, surface of action and conjugate tooth surface

Substituting in equations (2.14),(2.15),(2.16) and (2.17) $\Sigma = \pi/2$, we get the following :

a. the equation of contact,

$$\lambda = \lambda(\theta_k, \phi_1) = \frac{(1 - i_{21}\tan\beta(S\Phi_k - (\theta_k \mp \eta)C\Phi_k + a))}{i_{21}\, C\, \Phi_k\, \mathrm{Sec}^2\, \beta} \qquad 5.1$$

b. the equation of contact line;

$$\underset{\sim}{R}_{\ell c}(\theta_k, \phi_1) = \begin{Bmatrix} [S\ \theta_k - C_k^*\ C\ \theta_k] \\ -[C\ \theta_k + \theta_k^*\ S\ \theta_k] \\ \lambda \end{Bmatrix} \qquad 5.2$$

c. the equation of contact surface ;

$$\underset{\sim}{R}_c\ (\theta_k, \phi_1) = \begin{Bmatrix} [S\ \Phi_k - \theta_k^*\ C\ \Phi_k] \\ -[C\ \Phi_k + \theta_k^*\ S\ \Phi_k] \\ \lambda \end{Bmatrix} \qquad 5.3$$

and d. the equation of gear tooth profile,

$$\underset{\sim}{R}_{2k} = \left\{ \begin{array}{l} [(S\Phi_k - \theta_k^* \, C \, \Phi_k) \, C \, \phi_2 - \lambda S \, \phi_2 + a \, C \, \phi_2] \\ -[(S\Phi_k - \theta_k^* C\Phi_k) S\phi_2 + \lambda C \, \phi_2 + a \, S \, \phi_2] \\ -[C \, \Phi_k + \theta^* \, S \, \Phi_k] \end{array} \right\} ; \; k = U, L \qquad 5.4$$

Here, λ is given by equation (5.1)

$$\theta_k^* = \theta_k - \lambda \tan \beta \mp \eta_1$$

$$\Phi_k = \theta_k + \phi_1$$

and $$\phi_2 = i_{21} \, \phi_1$$

5.1.2. Addendum surface of the face gear

The addendum surface of the face gear is a plane [Section 2.7.1] ,

$$r_f + z_2 = 0 \qquad 2.26$$

where, $r_f = [1 - 2 \, f_{os} \, / z_1]/\cos \alpha_{os}$

Here, cutter or pinion is assumed to be standard, that is, $\xi_{on} = \xi_{1n} = 0$

5.1.3. Pointing of the gear teeth

The condition of pointing, equations (2.39) and (2.40), assumes a simple form,

$$r_f + R_{z2k} = 0 \; , \; k = U, \; L$$

$$R_{x2U} - R_{x2L} = 0$$

and

$$R_{y2U} - R_{y2L} = 0 \qquad 5.5$$

where, R_{x2k}, R_{y2k} and R_{z2k} are the respective components of vector defined by equation (5.4).

Parameters, obtained from the solution of equations (5.5), are substituted in equation (2.42) to get the radius at which the pointing starts on the gear tooth.

5.1.4 Undercutting of gear teeth

The condition of undercutting is obtained when $\pi/2$ is substituted for Σ in equation (2.48). The form of the condition becomes

$$(i_{21} \tan\beta(S\,\Phi_k + a)\,S\,\Phi_k - C\,\Phi_k)[S\,\Phi_k - i_{21}\tan\beta \cdot S\,\Phi_k(R_{cx} + a)] + i_{21}\,C^3\,\Phi_k\,\Theta^*_{ke}\tan\beta - i_{21}^2\,C^3\,\Phi_k \cdot \Theta^*_{ke}\sec^2\beta\,(R_{cx} + a) = 0 \qquad 5.6$$

It can be written in the general form as

$$F_u(\Phi_k) = 0 \qquad 5.7$$

5.1.5 Curvatures

The principal curvatures of the pinion tooth surface Σ_1 can be obtained from equations (2.69). The principal curvatures of the gear tooth surface Σ_2 is found using equations developed in Section 2.10.2. The expressions for the gear under consideration are given below :

$$a_{31} = i_{21}\,C\,\Phi_1 \qquad 5.8$$

$$a_{32} = \frac{i_{21}\,S\,\Phi_k}{\Theta^*_k}\,[\Theta^*_k\,S\beta - \lambda\,C\,\beta] \qquad 5.9$$

$$D^* = \frac{i_{21}^2}{\Theta_k^*}\left[\Theta_k^* C \beta C \Phi_k(a + S \Phi_k) - C \beta(\Theta^* C^2 \phi_k - \right.$$

$$\left. - \lambda^2 S^2 \Phi_k) - \Theta^* S\beta\lambda\right] \qquad 5.10$$

$$X_{III} = \frac{1}{2}\left[X_I + X_{II} + \frac{X_I - X_{II} + G}{\cos \sigma} + S\right]$$

$$X_{IV} = \frac{1}{2}\left[X_I + X_{II} - \frac{X_I - X_{II} + G}{\cos \sigma} + S\right] \qquad 2.56$$

$$\tan 2\sigma = 2F/(X_I - X_{II} + G) \qquad 2.57$$

$$F = a_{31}\, a_{32}/D^* \qquad 2.58$$

$$G = (a_{31}^2 - a_{32}^2)/D^*$$

and $$S = (a_{31}^2 + a_{32}^2)/D^* \qquad 2.59$$

5.2 Face gears in mesh with spur pinion [surface gear]

The spur face gear is a particular case of the spiral face gear. For this case helix angle, β, is equal to zero. The equations applicable are obtained using the contents of the previous sections.

5.2.1 Equation of contact, contact line, surface of action and conjugate tooth profile

Substituting $\beta = 0$ in equation (5.1) we get,

$$\lambda - 1/C\, \Phi_k = 0 \qquad 5.11$$

Similarly, equation of the line of contact, the surface of action and the conjugate tooth profile are obtained. These are as given below :

$$\underset{\sim}{R}_{\ell c} = \begin{Bmatrix} [S\ \Theta_k - \Theta_k^*\ C\ \Theta_k] \\ -[C\ \Theta_k + \Theta_k^*\ S\ \Theta_k] \\ \lambda \end{Bmatrix} \qquad 5.12$$

$$\underset{\sim}{R}_{c} = \begin{Bmatrix} [S\ \Phi_k - \Theta_k^*\ C\ \Phi_k] \\ -[C\ \Phi_k + \Theta_k^*\ S\ \Phi_k] \\ \lambda \end{Bmatrix} \qquad 5.13$$

and

$$\underset{\sim}{R}_{2k} = \begin{Bmatrix} [R_{cx}\ C\ \phi_2 - \lambda\ S\ \phi_2 + a\ C\ \phi_2] \\ -[R_{cx}\ S\ \phi_2 + \lambda\ C\ \phi_2 + a\ S\ \phi_2] \\ -[R_{cy}] \end{Bmatrix} \qquad 5.14$$

where, $\underset{\sim}{R}_c = [R_{cx}, R_{cy}, R_{cz}]^T$, $\Theta_k^* = \Theta_k \mp \eta_1$ 5.15

$\Phi_k = \Theta_k + \phi_1$ and $k = U, L$

Slightly transformed versions of these equations have been derived earlier [5] [11] [12] .

5.2.2 Pointing of gear tooth

The addendum surface of the gear is given by the equation (2.26). The condition of pointing for the case of spur face gear is written as

$$r_f + R_{z2k} = 0 \ , \ k = U, L$$

$$R_{x2U} - R_{x2L} = 0 \qquad 5.5$$

and $$R_{y2U} - R_{y2L} = 0$$

where, $\underset{\sim}{R}_{2k} = [R_{x2k}, R_{y2k}, R_{z2k}]^T$; is given by equation (5.14)

and $$r_f = (1 - 2/Z_1)/\cos\ \alpha_o \qquad 5.17$$

Equation (5.5), in general, is represented as

$$F_p\ (\underset{\sim}{\Theta}) = \underset{\sim}{0}\ , \text{ where, } \underset{\sim}{\Theta} = [\Theta_U,\ \phi_{1U},\ \Theta_L,\ \phi_{1L}]^T \qquad 5.18$$

The limiting radius can be evaluated using equations (2.42).

There are four equations in the set of equations (5.18) or (5.5) and there are four unknowns. The first two of these equations have simpler forms and can be used to eliminate two of the unknown from the last two equations. It will then be a set of two equations in two unknown. The conditions of pointing in this form have been derived earlier [5] [11] [12] .

5.2.3. Undercutting of gear tooth

The condition of undercutting for spur face gear is obtained from equation (5.6) considering $\beta = 0$. As a result, the condition becomes

$$S^2\ \Phi_k + i_{21}^2\ \Theta_{ke}^*(a + S\ \Phi_k - \Theta_{ke}^*\ C\ \Phi_k)\ C^3\ \Phi_k = 0 \qquad 5.19$$

Let ψ_k be the solution of this equation. The radius at which undercutting occurs is obtained considering,

$$r_{2uk} = [(R_{cx} + a)^2 + R_{cy}^2]^{1/2} \cos\ \alpha_o \quad , \text{ or}$$

$$r_{2uk} = [(S\psi_k - \Theta_{ke}^*\ C\ \phi_k + a)^2 + (1/i_{21}\ C\ \psi_k)^2]^{1/2} \cos\ \alpha_o, [k = U,L] \qquad 5.20$$

The limiting inner radius will be the larger of the two obtained from the preceding equation.

5.2.4. Curvatures

The principal curvatures of the gear tooth surface Σ_2 of the spur face gear is obtained by substituting $\beta = 0$ in equations (5.8), (5.9) and (5.10). The curvatures are found from the following equations

$$a_{31} = i_{21}\, C\, \Phi_k \qquad 5.21$$

$$a_{32} = -i_{21}\, \lambda\, S\, \Phi_k/\Theta_k^* \qquad 5.22$$

$$D^* = i_{21}^2[\Theta_k^*(S\Phi_k - \Theta_k^* C\Phi_k + a)C\Phi_k + \lambda^2 S^2 \Phi_k]/\Theta_k^* \qquad 5.23$$

$$\chi_{III} = [\chi_I + \chi_{II} + S + (\chi_I - \chi_{II} + G)/C\ 2\sigma]/2 \qquad 2.48$$

$$\chi_{IV} = [\chi_I + \chi_{II} + S - (\chi_I - \chi_{II} + G)/C\ 2\sigma]/2$$

$$\tan 2\sigma = -2\lambda\, S\, \Phi_k/(S\, \Phi_k + a) \qquad 5.24$$

$$G = i_{21}^2\, (\Theta_k^{*2}\, C^2\, \Phi_k - \lambda^2\, S^2\, \Phi_k)/\Theta_k^{*2}\, D^*$$

$$\text{and } S = i_{21}^2(\Theta_k^{*2}\, C^2\, \Phi_k + \lambda^2\, S^2\, \Phi_k)/\Theta_k^{*2}\, D^* \qquad 5.25$$

5.3 Contact localization in hypoid spur face gears

The need to localize contact in gear teeth arose from the fact that a localized contact makes the gear less sensitive to assembly and manufacturing errors [2] . The contact conditions can be appreciably improved by suitable localization [25] . Coniflex bevel gears have better performance characteristics than the conventional octoidal bevel gears. In these gears, the localization is achieved

by crowning the teeth. Face gears are given the effect of crowning by the selection of cutter having one or more teeth than the mating pinion [23].

In this section, the contact localization for the spur face gears in mesh with the cylindrical involute spur pinion is considered. The contact is localized at the midpoint of the tooth width. The formulas to calculate the main geometric propotions of the pinion and assembly distances are developed here.

In face gear transmission, if the number of teeth of the pinion and the cutter are equal than the contact of teeth surfaces is along a line. The contact may be localized by taking a different number of teeth of the cutter than in the pinion ($Z_1 \leq Z_0$) [2][25] .

Consider that the surface F of the cutter generates the surface Σ_2 of the gear and Σ_1 of the pinion simultaneously. Surfaces Σ_1 and Σ_2 have the same relative motion as that when they mesh with each other. Surfaces F and Σ_1 have internal meshing. Let the line of contact between F and Σ_1 be D_1 and the line of contact between F and Σ_2 be D_2. These two lines lie on the surface F. In general, these two lines will not be coinciding with each other but will have a common point M (point of intersection of D_1 and D_2). Since the point M belongs to both the lines of contact, surfaces Σ_1 and Σ_2 will be in point contact at M and will be having the desired relative motion. From this inspection it is seen that, if the cutter geometry is different from that of the pinion, there will be a point contact.

5.3.1. Line of action

The line of action between the gear and pinion is the curve of intersection of the two surfaces of action. These two surfaces are, the surface of action between cutter and gear and that between cutter and pinion.

The pitch point P of the cutter and pinion is the point of intersection of the common tangent to their respective base circles, r_{bo} and r_{b1} [Figure 9] , with the line of centers joining O_1 and O. In the fixed coordinate system, $\bar{S}_1$, the line of contact D_1 passes through the point of contact M lying on one side, say U, of the cutter surface F. The point M has an angle of development of involute curve, $\theta^*_{OU} = \theta_{OU} - \eta_o$ [Figure 9] . From Figure 9 it is seen that

$$\phi_U = \theta_{OU} + \phi_o = \alpha = \text{constant} \qquad 5.26$$

where, α is the pressure angle between the pinion and the cutter. Similarly, for the pinion

$$\phi_U = \theta_{1U} + \phi_1 = \theta_{1U} + \phi_o/i_{o1} = \alpha$$

Following expressions are obtained considering the cases when the contact point M lie on sides, U and L, of the cutter and the pinion surface,

$$\phi_k = \theta_{ok} + \phi_o = \theta_{1k} + \phi_o/i_{o1} = \alpha$$

$$\theta^*_{ok} = \theta_k \mp \eta_o$$

and $$\theta^*_{1k} = \theta_k \mp \eta_1, \; k = U,L.$$

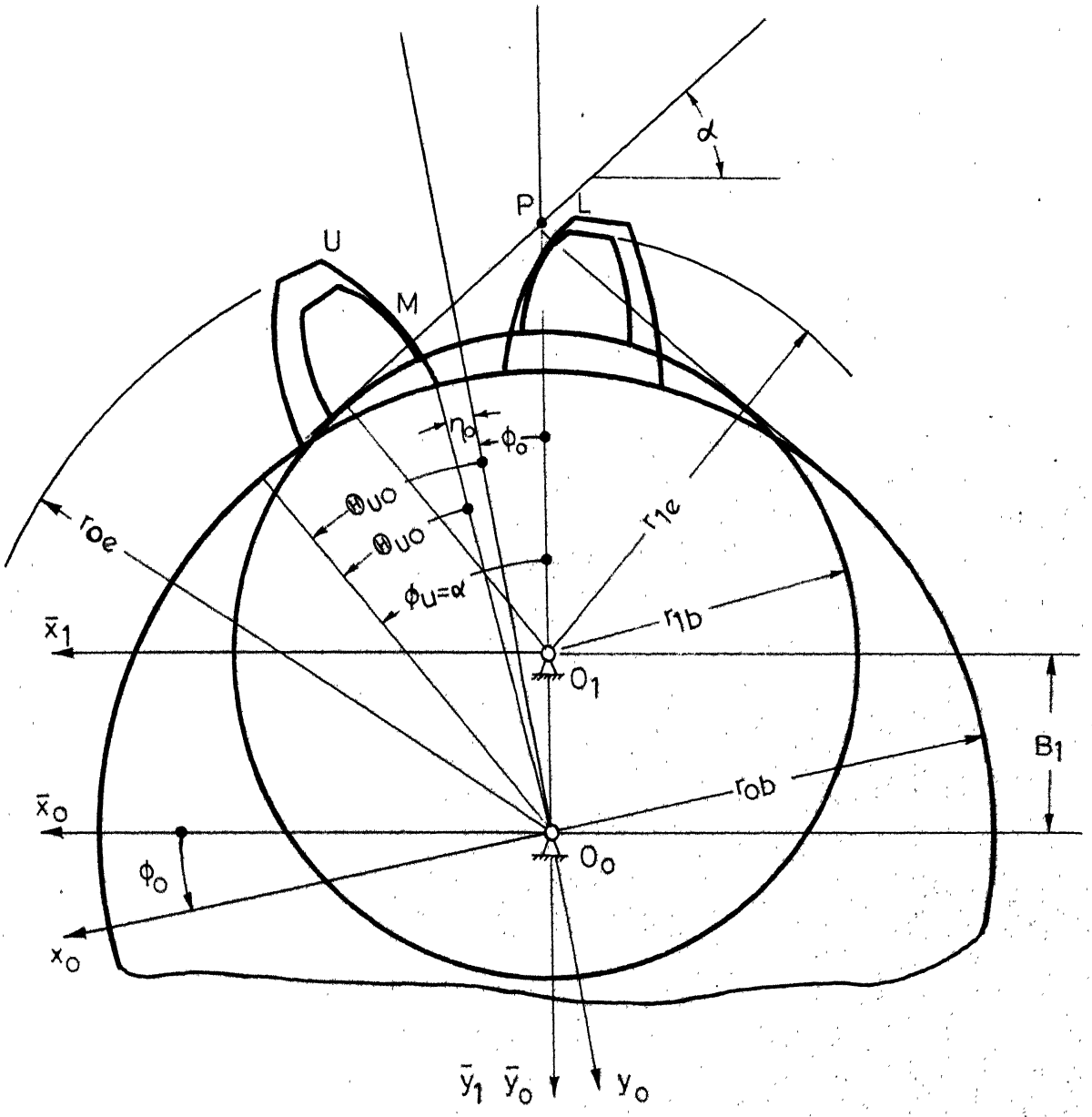

FIG. 9 MESHING OF CUTTER AND PINION

Again, from Figure 9, it is seen that

$$\phi_k = \alpha = \cos^{-1} [(r_{bo} - r_{b1})/B_1] \qquad 5.27$$

where, B_1 - center distance.

To find the line of action, between surface Σ_1 and Σ_2, it is sufficient to simultaneously consider equations (5.27) and (5.13). This consideration reveals that the line of action is tangent to the base circles of radii r_{b_o} and r_{b_1} and lies on the plane

$$z_1 = 1/(i_{20} C \alpha) \qquad 5.28$$

By choosing the correction factor, ξ_1, suitably, the contact is localized at the middle of the tooth width. The procedure to choose the correction factor is given in the next section.

5.3.2 Geometrical calculations

It is assumed that the following are given

a. parameters of the cutter (Z_o, m, ξ_o, f_o, c_o, and α_o)

b. transmission ratios, $i_{2o} = Z_o/Z_2$ and $i_{o1} = Z_1/Z_o$.

and c. non-dimensionalized off-set 'a'.

The calculation of correction factor, ξ_1, and assembly distances consists of the following steps.

1° The internal and external radii, r_{2i} and r_{2e} are chosen to avoid the undercutting and pointing of the teeth. The limiting dimensions can be determined using the contents of sections 5.2.3 and 5.2.2.

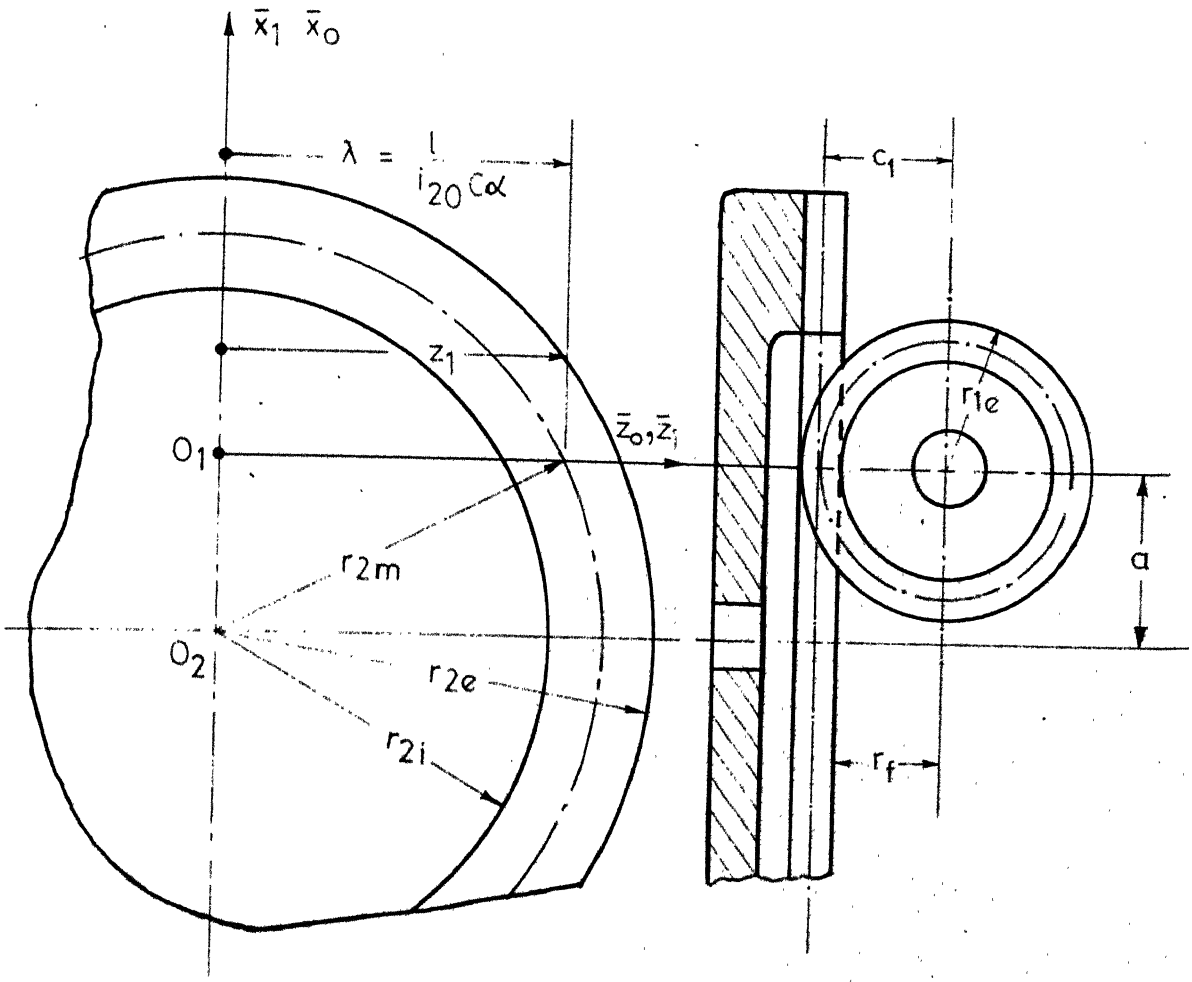

FIG.10 NOTATION FOR HYPOID FACE GEAR MESHING

2° The pressure angle of pinion and cutter is found using the following equations. [Figure 10]

$$r_{2m} = (r_{2i} + r_{2e})/2 \qquad 5.31$$

$$\text{and } z_{\cdot} = (r_{2m}^2 - a^2)^{1/2} = 1/(i_{20}\ C\ \alpha) \qquad 5.32$$

Here, r_{2m} is the mean radius of gear. r_1 gives the position of the plane containing the line of action of surfaces Σ_1 and Σ_2. For direct calculations of the pressure angle the following expression is used.

$$\cos \alpha = 1/[i_{21}\{((r_{2i} + r_{2e})/2)^2 - a^2\}^{1/2}] \qquad 5.33$$

3° Correction factor, ξ_1, is now calculated [8].

$$\text{inv } \alpha = 2\,\frac{\xi_o - \xi_1}{Z_o - Z_1}\,\tan \alpha_o - \text{inv } \alpha_o$$

$$\text{or } \xi_1 = (Z_o - Z_1)\ [\text{inv } \alpha_o - \text{inv } \alpha]/(2 \tan \alpha_o) \qquad 5.34$$

Here it is assumed that $\xi_o = 0$.

4° The distance, C_1 from the axis of pinion to the median axis of gear is given by [Figure 10]

$$C_1 = m/2\ [Z_o - (Z_o - Z_1) \cos \alpha_o/\cos \alpha] \qquad 5.35$$

5° The external radius of the pinion is found using

$$r_{1e} = m[Z_o/2 - B_1 + f_o] \qquad 5.36$$

Referring to Figure 9, the distance, B_1, between the axes of cutter and pinion is found from

$$B_1 = m(Z_o - Z_1) \cos \alpha_o/(2 \cos \alpha) \qquad 5.37$$

where f_o - addendum factor; generally, $f_o = 1$.

5.4 Contact spot and contact zone on the tooth surface

In this section, discussions are confined to the surfaces having point contact.

Surfaces of the gear teeth undergo an elastic deformation under load and at any instant they contact each other on an area around the point of contact. This area of contact is known as a contact spot. As the gears rotate, these spots move on the gear teeth along with the theoretical point of contact. The total area swept by by contact spots on a tooth surface is called the contact zone [Figure 11].

The form of a contact zone, to a great extent, is influenced by the direction of the line of action. The dimension of the contact zone is determined by the size of contact spot.

If the contact zone has some general inclination with respect to the median line of the tooth width then, it is said to have a diagonal character. In such a case, when gear rotate, the change of the distance of the point of application of the normal force between the tooth and the supports of the gears give rise to variations of the support reaction. This is not a desirable situation. In case of the spur face gear, the contact zone has a favourable form, since contact zone does not have a diagonal character. [Figure 11].

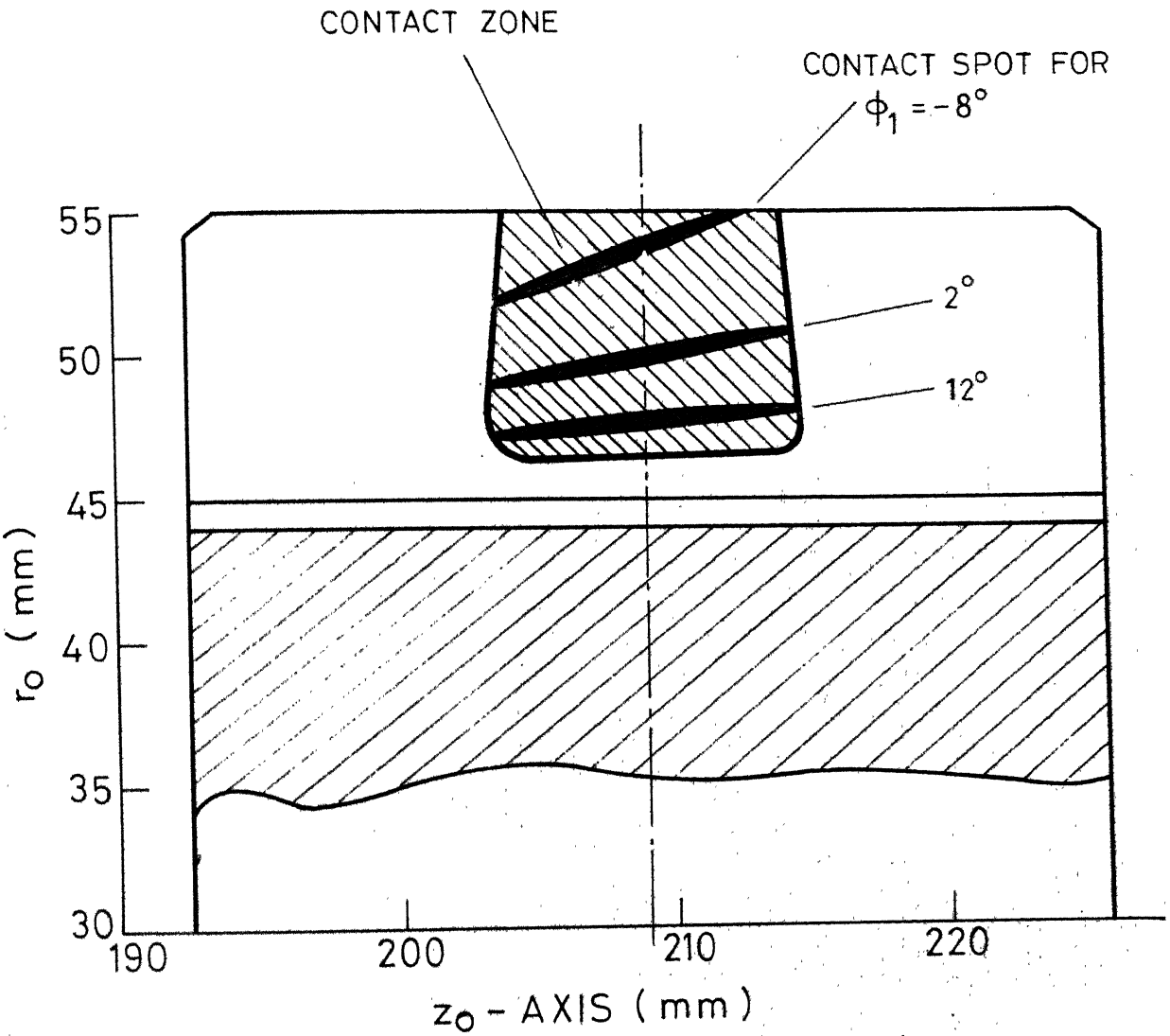

FIG.11 CONTACT ZONE AND CONTACT SPOT ON PINION TOOTH.

ON-CENTER FACE GEAR : $\Sigma = \pi/2$, $\beta = 0$, $\alpha = 0$, $Z_1 = 18$, $Z_o = 20$, $i_{21} = .25$, $m = 5$ mm, $P = 100$ Kg AND $\alpha_o = 20°$

In this section, a method is described to find the contact zone on spur face gear teeth. It is assumed that following are known :

a. the principal curvatures at points of contact

b. the location of points of contact

and c. the angle between the two sets of the directions of the curvatures [Section 2.10.1]

5.4.1 Condition of intersection of two surfaces in the neighbourhood of a contact point.

From differential geometry it can be shown that the normal deviation ℓ at point P in the neighbourhood of M [Figure 12a] is given by [24]

$$\ell = 1/2\ \chi(\eta^2 + \zeta^2) = 1/2\ \chi\rho^2 \qquad 5.38$$

where, $\rho = \bar{MP}$, η and ζ axes lie on the tangent plane at point M. η and ζ are the co-ordinates of point P. ℓ is positive along the direction of the normal $\underset{\sim}{e}$ and χ is the normal curvature of the surface on the plane containing $\underset{\sim}{e}$ and $\overline{MM}^1$ [Figure 12a]. Let MN gives the direction of the normal plane corresponding to one of the principal curvatures of the surface at point M, Figure 12a. Euler's formula for curvature of the surface in normal plane passing through MM' gives [24]

$$\chi = \chi_I\ C^2\ q + \chi_{II}\ S^2\ q \qquad 5.39$$

where, $q = \nu - \sigma$ [Figure 12a]

χ_I - principal curvature in the direction MN

χ_{II} - second principal curvature.

Equations (5.38) and (5.39) may be used to find ℓ. These two equations also define the surface in the neighbourhood of point M provided χ_I and χ_{II} are known. The value ℓ is called normal deviation of the surface at point M'.

At the point of contact of two surfaces, one has to make sure that in the neighbourhood of that point two surfaces do not intersect. To achieve this, values of $\ell^{(i)}$; i = 1,2; have to be compared.

Let σ_1 and σ_2 be the angles corresponding to the directions of the principal curvatures χ_I and χ_{III} in the coordinate system, η, ζ and ℓ [Figure 12b]. Now, using from (5.39) we may write,

$$2\ell^{(1)} = \rho^2 [\chi_I C^2(\nu-\sigma_1) + \chi_{II} S^2(\nu-\sigma_1)]$$
$$2\ell^{(2)} = \rho^2 (\chi_{III} C^2 (\nu-\sigma_2) + \chi_{IV} S^2(\nu-\sigma_1)] \qquad 5.40$$

The clearence between the surfaces at a distance ρ from point M is found from,

$$C_\ell = |\ell^{(1)} - \ell^{(2)}|. \qquad 5.41$$

It is seen from equations (5.40) and (5.41) that C_ℓ will change with the angle ν. If the sign of C_ℓ, for constant value of ρ, be same for all values of ν, it means that in the neighbourhood of M surfaces Σ_1 and Σ_2 do not intersect. For visual inspection, $\ell^{(i)}(\nu)$, should be preferably given in polar coordinate system. $\ell^{(i)}$ may have the negative sign [Figure 12c]. The curves, $\ell_1(\nu)$ and $\ell_2(\nu)$, are drawn using the following equation.

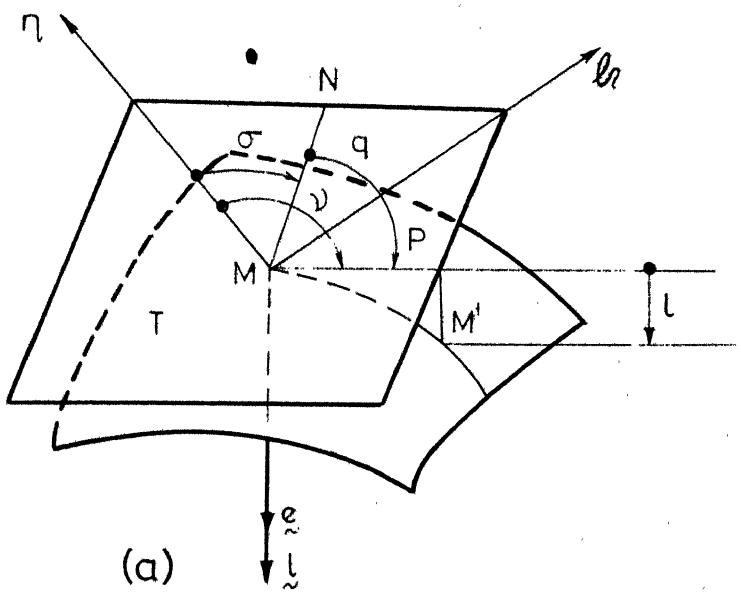

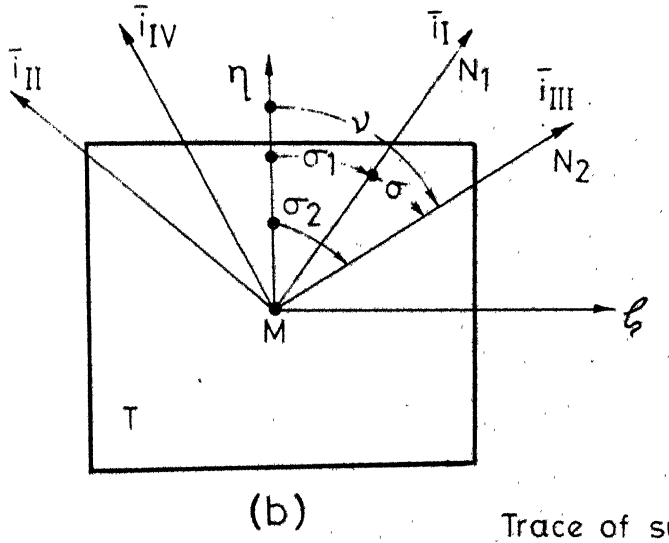

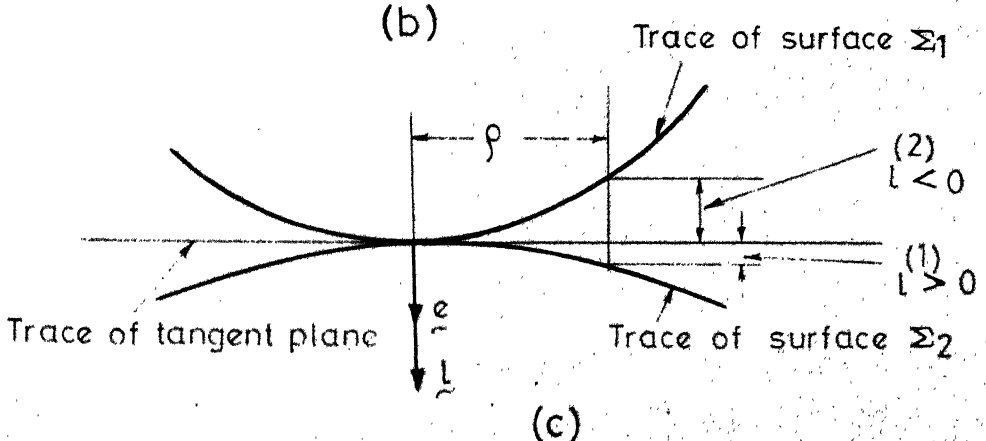

FIG. 12 COORDINATE SYSTEM FOR NORMAL DEVIATION OF TWO SURFACES IN CONTACT

$$\ell_i = \ell^{(i)} + d \qquad 5.42$$

The value of d is arbitrarily chosen, such that $\ell_i > 0$ for $0 \leq \nu \leq 2\pi$. A circle with radius d, in the diagram is considered as a line of zero curvature . Figure 13 shows a typical plot of these curves.

As $\ell^{(1)} - \ell^{(2)} = \ell_1 - \ell_2$, the condition of non-intersection of the curves, $\ell_1(\nu)$ and $\ell_2(\nu)$, is considered as a criteria for non-intersection of the surfaces in the neighbourhood.

5.4.2 Dimensions of contact spot.

The solution of the contact problem between two elastic bodies contacting at a point is achieved with the following assumptions [26] .

a The principal curvatures of both the surfaces Σ_1 and Σ_2 are known. The angle, σ, between the first principal directions of the contacting surfaces is also known.

b The magnitude of the load and the elastic constants of the materia are known. It is assumed that the contact force is normed to the surface, deformation is elastic, Hook's law is obeyed and the material are homogeneous and isotropic.

c It is assumed that surfaces in the neighbourhood of the theoretical point of contact do not intersect and the contact spot is small in comparison with the contacting surfaces.

Here, the expression for C_ℓ is expressed in a form such that Hertz's general solution for the contact problem can be used.

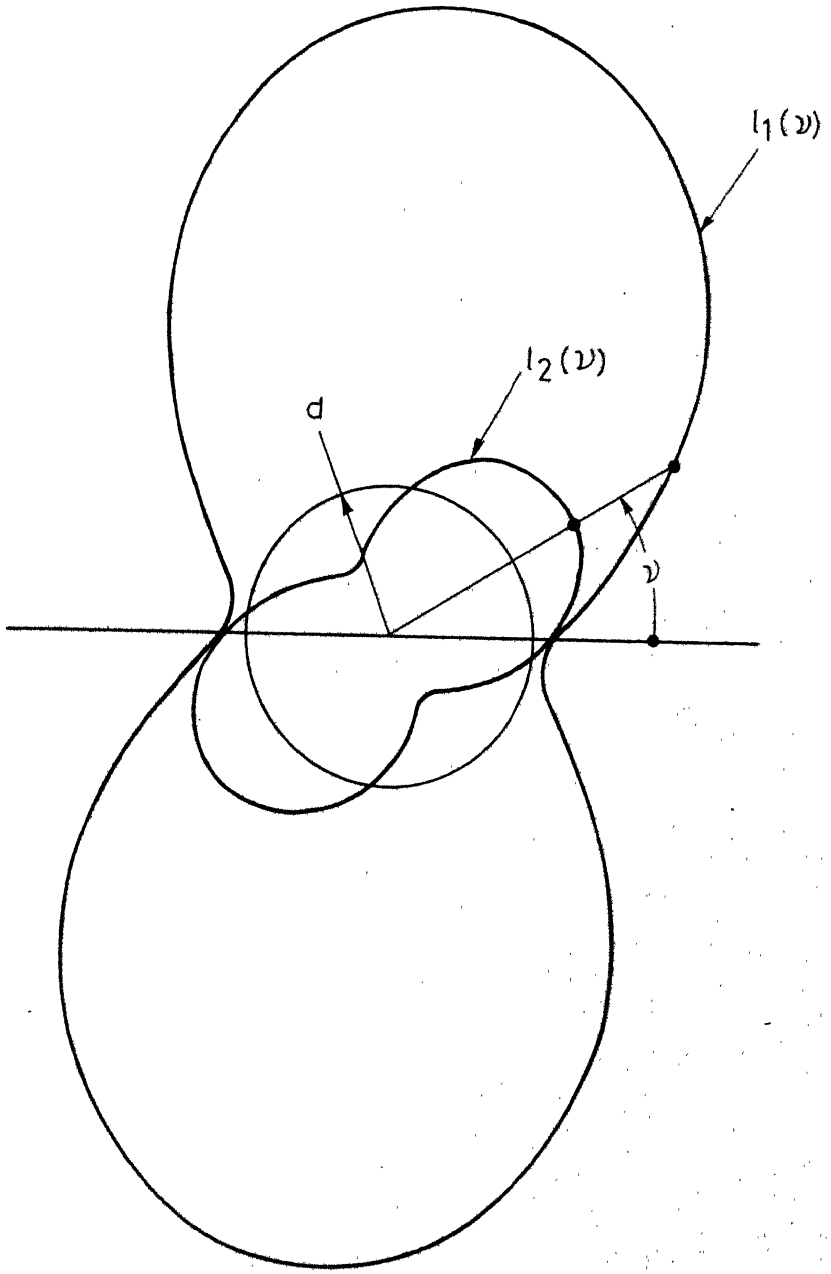

FIG. 13 NORMAL DEVIATION OF THE SURFACES

[26] [27] [28] . This will lead to the following results : displacement of the surfaces as a result of deformation, magnitude and distribution of the pressure in the contact spot, form and dimensions of the contact spot.

Equations (5.40) and (5.41) give the following expression

$$\text{Abs.}\left|\chi_{I}\, C^2(\nu-\sigma_1) + \chi_{II}\, S^2(\nu-\sigma_1) - \chi_{III} C^2(\nu-\sigma_2) - \chi_{IV} S^2(\nu-\sigma_2)\right| \rho^2 = 2\, C_{\ell} \qquad 5.43$$

Using transformations,

$$\rho^2 = \eta^2 + \zeta^2 \text{ , } \cos\nu = \eta/\rho \text{ and } \sin\nu = \zeta/\rho \text{ ,}$$

equation (5.43) is written as

$$\text{Abs.}\left|\eta^2(\chi_I\, C^2\,\sigma_1 + \chi_{II}\, S^2\,\sigma_1 - \chi_{III}\, C^2\,\sigma_2 - \chi_{IV}\, S^2\,\sigma_2) + \right.$$

$$+\zeta^2(\chi_I\, S^2\,\sigma_1 + \chi_{II}\, C^2\,\sigma_1 - \chi_{III}\, S^2\,\sigma_2 - \chi_{IV}\, C^2\,\sigma_2) +$$

$$\left.\eta\zeta(g_1\, S2\,\sigma_1 - g_2\, S2\,\sigma_2)\right| = 2\, C_{\ell} \qquad 5.44$$

where, $g_1 = \chi_I - \chi_{II}$ and $g_2 = \chi_{III} - \chi_{IV}$ 5.45

Now σ_1 may be so chosen that the coefficient of the product term $\eta\zeta$ in equation (5.44) is zero. In other words

$$g_1\, S2\sigma_1 - g_2\, S2\,\sigma_2 = 0 \qquad 5.46$$

From equation (5.46) it follows that

$$\tan(2\sigma_1) = \frac{g_2\, S2\sigma}{g_1 - g_2\, C2\sigma} \qquad 5.47$$

Finally the following equation is obtained using equations (5.44), (5.46) and (5.47)

$$B\,\eta^2 + A\,\zeta^2 = \pm C_\ell \qquad 5.48$$

where

$$A = \tfrac{1}{4}[\,\chi_{s1} - \chi_{s2} - (g_1^2 - 2g_1g_2\,C2\sigma + g_2^2)^{1/2}]$$
$$B = \tfrac{1}{4}[\,\chi_{s1} - \chi_{s2} + (g_1^2 - 2g_1g_2\,C2\sigma + g_2^2)^{1/2}] \qquad 5.49$$

and $\chi_{s1} = \chi_I + \chi_{II}$ and $\chi_{s2} = \chi_{III} + \chi_{IV}$. 5.50

It can be seen from equation (5.48) that A and B must have the same sign if the surfaces are not intersecting in the neighbourhood of contact points.

The solution of the contact problem follows from Hertz's solution [26] and one gets the following results

$$\cos\tau = |(A-B)/(A+B)| \qquad 5.51$$

$$k^* = \left[\frac{3}{4|A+B|}\left\{\frac{1-\nu_1^2}{E_1} + \frac{1-\nu_2^2}{E_2}\right\}\right]^{1/3} \qquad 5.52$$

$$a = a^* k^* p^{1/3} \qquad 5.53$$

$$b = b^* k^* p^{1/3} \qquad 5.54$$

$$\delta = \delta^* k^{*2} p^{2/3} |A+B| \qquad 5.55$$

$$S(\eta,\zeta) = \frac{3P}{2\pi ab}\left[1 - (\eta/a)^2 - (\zeta/b)^2\right] \qquad 5.56$$

and $$S_{max} = 3P/(2\pi ab) \qquad 5.57$$

where, A and B are given by equations(5.49),

a,b - the semimajor and minor axes of the contact spot,

δ - the relative approach of remote points in the contacting bodies,

a^*,b^*,c^* - coefficients depending on the parameter $\cos\tau$; Table 4 [28],

ν_1, ν_2 - Poisson's ratios of bodies 1 and 2 respectively,

E_1, E_2 - Young's modulii in kg/mm^2 of bodies 1 and 2 respectively,

P - normal compressure load in kg,

S - Compressive stress at the point (η,ζ) in kg/mm^2,

and S_{max} - maximum compressive stress at the contact point in kg/mm^2.

It is noted from equation (5.48) that for a given value of C_ℓ the dimensions of the contact spot are given by

$$a = \left|C_\ell/A\right|^{1/2} \text{ and } b = \left|C_\ell/B\right|^{1/2} \qquad 5.58$$

It is advantageous to compaire the relative dimensions of contact spots of different types of gears. For this purpose, equation (5.58) can be used. This is independent of the solution

TABLE 4 *STRESS CONSTANTS*

TAC	ASTR	BSTR	DSTR
1.0000	INFNITY	0.00000	0.00000
0.99950	23.95000	0.16300	0.17100
0.99900	18.53000	0.18500	0.20700
0.99850	15.77000	0.20100	0.23000
0.99800	14.25000	0.21200	0.24900
0.99750	13.15000	0.22000	0.26600
0.99700	12.26000	0.22800	0.27900
0.99650	11.58000	0.23500	0.29100
0.99600	11.02000	0.24100	0.30200
0.99550	10.53000	0.24600	0.31100
0.99500	10.15000	0.25100	0.32000
0.99450	9.77000	0.25600	0.32800
0.99400	9.46000	0.26000	0.33600
0.99350	9.17000	0.26400	0.34300
0.99300	9.92000	0.26800	0.35000
0.99250	8.68000	0.27100	0.35600
0.99200	8.47000	0.27500	0.36200
0.99150	8.27000	0.27800	0.36800
0.99100	8.10000	0.28100	0.37300
0.99090	8.06200	0.28140	0.37450
0.99050	7.93000	0.28400	0.37900
0.99000	7.76000	0.28700	0.38400
0.98950	7.62000	0.28900	0.38800
0.98900	7.49000	0.29200	0.39300
0.98850	7.37000	0.29400	0.39800
0.98800	7.25000	0.29700	0.40200
0.98750	7.13000	0.29900	0.40700
0.98700	7.02000	0.30100	0.41100
0.98650	6.93000	0.30300	0.41600
0.98600	6.84000	0.30500	0.42000
0.98550	6.74000	0.30700	0.42300
0.98500	6.64000	0.31000	0.42700

discussed earlier. The value of C_ℓ may be arbitrarily given. The area of an ellipse of contact, πab, is considered as the measure for comparison.

In the following sub-section, the procedure to find the contact zone, in the spur face gear set with localized contact, is discussed.

5.4.3 Contact zone in the spur face gears

1° Using the results obtained in section 5.3.2, the pressure angle α is found from

$$\cos \alpha = 1/i_{21}[\{(r_{2i} + r_{2e})/2\}^2 - a^2]^{1/2} \qquad 5.33$$

where, $$\alpha = \phi_k = \theta_{ok} + \phi_o = \theta_{1k} + \phi_o/i_{o1} \qquad 5.60$$

and $$\lambda = 1/(i_{21}\ C\ \alpha) \qquad 5.61$$

Semi space width angle, η_1, for corrected involute gear is given by

$$\eta_1 = \pi/2Z_1 - \text{inv}\ \alpha_o - 2\xi_1 \tan \alpha_o/Z_1 \qquad 5.62$$

Here, ξ_1 is given by equation (5.34), while η_o is evaluated from

$$\eta_o = \pi/2Z_1 - \text{inv}\ \alpha_o \text{ for } \xi_o = 0. \qquad 5.63$$

2° The line of action,

$$\underset{\sim}{R}_c(\phi_1) = [S\alpha - \theta^*_{ok}\ C\alpha\ , -(C\alpha + \theta^*_{ok}\ S\alpha), 1/i_{20}\ C\alpha]^T \qquad 5.64$$

is found using equations (5.60) and (5.13). Here,

$$\theta^*_{ok} = \alpha - \phi_o \mp \eta_o \qquad 5.65$$

$$\theta^*_{1k} = \alpha - \phi_o/i_{o1} \mp \eta_1 \qquad 5.66$$

and $$\phi_o = i_{o1} \cdot \phi_1 \qquad 5.67$$

3° The duration of contact and the limits of ϕ_1; ϕ_{1max} and ϕ_{1min}; can be found using the contents of Chapter 4.

4° The contact point on a pinion is found considering [Section 5.3.1]

$$z_o = \lambda \qquad 5.68$$

$$r_o = (R^2_{cx}+R^2_{cy})^{1/2} = (1 + \theta^*_{ok})^{1/2} \qquad 5.69$$

5° The principal curvatures of pinion and cutter are given by the following equations [equation (2.63)].

$$\chi_{Io} = 0 \ , \ \chi_{IIo} = -1/\theta^*_{ok} \qquad 5.70$$

and $$\chi_{I1} = 0 \ , \ \chi_{III} = -1/\theta^*_{1k} \qquad 5.71$$

6° The principal curvatures at the contact point of the gear tooth are found using the following expressions.

$$\chi_{III} = [\chi_{Io} + \chi_{IIo}+S+(\chi_{Io} - \chi_{IIo}+G)/C2\sigma] /2$$

$$\chi_{IV} = 1/2 [\chi_{Io} + \chi_{IIo}+S-(\chi_{Io}- \chi_{IIo}+G)/C2\sigma] /2 \qquad 5.72$$

$$\tan(2\sigma) = -2\lambda S\alpha/(S\alpha+a) \qquad 5.73$$

$$D^* = i_{20}^2[\Theta^*_{ok}(S\alpha - \Theta^*_{ok}C\alpha+a)\ C\alpha + \lambda^2\ S^2\alpha]$$

$$C = i_{20}^2(\Theta^{*2}_{ok}\ C\alpha - \lambda^2\ S^2\alpha)/\Theta^{*2}_{ok}\ D^* \qquad 5.74$$

$$S = i_{20}^2(\Theta^*_{ok}\ C\alpha + \lambda^2\ S^2\alpha)/\Theta^{*2}_{ok}\ D^* \qquad 5.75$$

It may be noted that these curvatures are non-dimensionalized with respect to the base radius, $r_{ob} = mZ_oC\alpha_o/2$, of the cutter.

7° The values of A and B are found using equation (5.49). Here,

$$\chi_{s1} = (\chi_{I1} + \chi_{III})/r_{ob}$$

$$\chi_{s2} = (\chi_{III} + \chi_{IV})/r_{ob} \qquad 5.76$$

$$r_1 = (\chi_{I1} - \chi_{III})/r_{ob}$$

and

$$r_2 = (\chi_{III} - \chi_{IV})/r_{ob} \qquad 5.77$$

8° The maximum stress, major and minor axes of contact spot and the displacement δ are found using equations (5.57), (5.53), (5.54) and (5.55).

9° The angle between the major axis of contact spot and the direction of χ_I is evaluated from

$$\tan(2\sigma_1) = g_2\ S2\sigma/(g_1 - g_2C2\sigma) \qquad 5.47$$

10° The position of the contact spot on the pinion tooth can be varied by giving different values to ϕ_1 in the range $[\phi_{1min}, \phi_{1max}]$. The area swept by the spot on tooth surface is the contact zone.

Figure 11 shows typical contact zone on pinion tooth.

5.5 Surface durability ratings of spur face gears with localized contacts

Spur face gear with point contacts are considered here. In gears with point contacts, comparatively small loads develop high compressive stress. The beam strength of the gear teeth is seldom a limiting factor in designing these gears [6]. This may not be true for a gear having vary small tooth width or for a case hardered gear. Mostly, the surface wear is the deciding factor in rating these gears. The wear is largely dependent on the maximum pressure between the two surfaces [14].

Analysis of the limiting wear loads of the gears is approximate to a certain exent. Point contact is assumed but plastic deformation and wear may develop a definite width of contact [6]. This, in turn, will reduce the predicted value of the contact stress. Therefore, the theoretically predicted values must be checked against service data and experience.

5.5.1 Design point in the contact cycle

The contact stress is used as a measure of the surface wear in gears [6]. The contact stress is constantly changing during

contact cycle. Therefore, some critical point on gear tooth profile has to be selected for the basis of computation of limiting load.

The pitch point may be considered as the critical point or design point [6] [29]. One of the reasons for this choice is the fact that in many cases wear on gear teeth first becomes prominent at or near the pitch point. Possibly, one of the contributing factors for this effect is the fact that one pair of teeth is usually carrying the entire load when contact exists on this part of the tooth. For contacts near the top or the bottom of the active profile, two pairs of the mating teeth are usually sharing the load.

Here it is assumed that the worst condition will be in that part of contact cycle when only one pair of teeth is in contact. The design point is a point where a minimum load, in this range (when one pair of teeth is in contact), will induce the given allowable stress.

The range, ϕ'_{1min} to ϕ'_{1max}, of angle of rotation, when one pair of teeth is in contact is found considering the following expressions.

$$\phi'_{1min} = \phi_{1min} + 2\pi/Z_1$$

and

$$\phi'_{1max} = \phi_{1max} - 2\pi/Z_1 \qquad 5.78$$

5.5.2 Rating formula

The problem of how to find the induced stress for a given load was discussed in Section 5.4. In the present section, a reversed problem is considered. The problem here is to find the permissible load

C_H - hardness ratio factor

C_T - temperature factor

C_R - factor of reliability.

The tangential load at the contact point is found from

$$P_t = P_n \cos\psi \qquad 5.82$$

where ψ is the pressure angle at the contact point. In case of a spur face gear, ψ is given by

$$\cos\psi = \frac{1}{[1 + 0^*_{1k}]^{1/2}} \qquad 5.83$$

And the rated tangential load at contact point is given by

$$P_{rt} = [\frac{2}{3} \pi k^{*2} a^* b^* S_{ac} \frac{C_L C_H}{C_T C_R}]^3 \frac{\cos\psi \; C_V}{C_s C_f C_o}$$

where[1],

C_V - dynamic load factor

C_f - surface condition factor

C_o - over load factor

C_s - size factor.

The Horse Power can be calculated considering

$$hp = \frac{2\pi N P_{rt} r}{1.5 \times 10^6} \qquad 5.84$$

where, N - speed of pinion in rpm,

r - radius of point of contact in mm.

---

[1] See reference [14] .

It has been shown in Section 5.4.3 that in case of spur face gears, r is found from (use the equation (5.69) for pinion)

$$r = (1 + \theta^*_{1k})^{1/2} \, r_{1b} \qquad 5.85$$

where, $r_{1b} = \frac{m Z_1}{2} \cos \alpha_o$.

The rated capacity is found using the following expression

$$hp_{rated} = \min_{\phi_1 \in [\phi'_{1min}, \phi'_{1max}]} \left[\frac{2\pi N}{4.5\times10^6} \left(\frac{2}{3} \pi k^{*2} a^* b^* S_{ac} \frac{C_L \, C_H}{C_T \, C_R}\right) 3 \frac{r \cos\psi \, C_V}{C_s \, C_f \, C_o}\right] \qquad 5.86$$

k^*, a^* and b^* are found using equations (5.52), (5.49), (5.50), (5.51) and Table 4. For the case of face gears they are found using the material given in Section (5.4.3). The minimisation involved in expression (5.86) is performed through iteration by assigning different values to ϕ_1 in the specified range.

For Tables 5 and 6 following values of the factors are taken.

$$C_L = C_H = C_T = C_R = C_f = C_o = C_s = 1 \qquad 5.87$$

and $C_V = 50/[50 + \sqrt{V_T}]$, V_T is the pitch line velocity in fpm. 5.88

This corresponds to the dynamic load factor for hobbed or shaped involute gears [14] . The value of S_{ac} is taken to be 95 kg/mm^2 for commercially used steel gears having the minimum hardness as 300 BHN. [14] . In designs for non-standard conditions the tabulated values may be modified according to the following equation

TABLE 5 SURFACE DURABILITY RATINGS OF SPUR FACE GEAR

I12	D1 MM	M MM	Z1	ASTAR	RATINGS IN PS AT DIFFERANT RPM 100	720	1750	3600
1.5	25.0	1.25	20.0	0.00	0.017	0.105	0.227	0.413
				0.10	0.019	0.121	0.262	0.477
				0.20	0.022	0.134	0.292	0.531
				0.30	0.024	0.148	0.321	0.584
				0.40	0.026	0.159	0.346	0.629
				0.50	0.027	0.168	0.365	0.664
	33.0	1.5	22.0	0.00	0.041	0.252	0.540	0.972
				0.10	0.048	0.293	0.629	1.132
				0.20	0.054	0.329	0.706	1.271
				0.30	0.059	0.361	0.774	1.393
				0.40	0.064	0.391	0.838	1.509
				0.50	0.068	0.417	0.894	1.610
	48.0	2.0	24.0	0.00	0.133	0.791	1.666	2.953
				0.10	0.155	0.927	1.954	3.463
				0.20	0.175	1.042	2.197	3.893
				0.30	0.192	1.143	2.410	4.270
				0.40	0.208	1.238	2.608	4.622
				0.50	0.222	1.326	2.794	4.952
	75.0	2.5	30.0	0.00	0.580	3.337	6.879	11.951
				0.10	0.682	3.925	8.091	14.057
				0.20	0.771	4.436	9.142	15.884
				0.30	0.855	4.916	10.133	17.604
				0.40	0.931	5.353	11.033	19.169
				0.50	1.002	5.764	11.881	20.641
	108.0	3.0	36.0	0.00	1.842	10.253	20.731	35.432
				0.10	2.221	12.363	24.996	42.722
				0.20	2.529	14.077	28.463	48.647
				0.30	2.832	15.766	31.878	54.484
				0.40	3.084	17.170	34.716	59.335
				0.50	3.325	18.509	37.425	63.964
	144.0	4.0	36.0	0.00	4.251	23.016	45.816	77.304
				0.10	5.126	27.752	55.243	93.211
				0.20	5.836	31.601	62.905	106.138
				0.30	6.537	35.392	70.453	118.874
				0.40	7.119	38.543	76.725	129.457
				0.50	7.674	41.550	82.711	139.557

FOR THIS TABLE DZO=1

TABLE 5 SURFACE DURABILITY RATINGS OF SPUR FACE GEAR

I12	D1 MM	M MM	Z1	ASTAR	RATINGS IN PS AT DIFFERANT RPM 100	720	1750	3600
2.0	25.0	1.25	20.0	0.00	0.022	0.140	0.303	0.552
				0.10	0.026	0.159	0.345	0.629
				0.20	0.028	0.176	0.382	0.695
				0.30	0.031	0.191	0.414	0.755
				0.40	0.033	0.204	0.444	0.808
				0.50	0.035	0.217	0.470	0.856
	33.0	1.5	22.0	0.00	0.056	0.341	0.730	1.315
				0.10	0.064	0.390	0.837	1.507
				0.20	0.071	0.433	0.929	1.673
				0.30	0.077	0.471	1.010	1.818
				0.40	0.082	0.505	1.082	1.949
				0.50	0.088	0.536	1.149	2.070
	48.0	2.0	24.0	0.00	0.181	1.079	2.273	4.028
				0.10	0.208	1.241	2.615	4.633
				0.20	0.231	1.379	2.906	5.150
				0.30	0.252	1.501	3.163	5.605
				0.40	0.270	1.612	3.397	6.020
				0.50	0.288	1.715	3.614	6.404
	75.0	2.5	30.0	0.00	0.792	4.556	9.391	16.315
				0.10	0.917	5.276	10.874	18.893
				0.20	1.025	5.899	12.158	21.123
				0.30	1.123	6.459	13.314	23.131
				0.40	1.210	6.960	14.345	24.922
				0.50	1.292	7.431	15.316	26.609
	108.0	3.0	36.0	0.00	2.549	14.190	28.691	49.036
				0.10	2.972	16.544	33.451	57.173
				0.20	3.342	18.607	37.622	64.301
				0.30	3.680	20.486	41.422	70.796
				0.40	3.987	22.199	44.884	76.713
				0.50	4.289	23.875	48.274	82.507
	144.0	4.0	36.0	0.00	5.883	31.853	63.408	106.987
				0.10	6.859	37.139	73.930	124.739
				0.20	7.714	41.769	83.147	140.292
				0.30	8.494	45.988	91.545	154.461
				0.40	9.204	49.832	99.197	167.373
				0.50	9.899	53.596	106.689	180.014

TABLE 5 SURFACE DURABILITY RATINGS OF SPUR FACE GEAR

I12	D1 MM	M MM	Z1	ASTAR	RATINGS IN PS AT DIFFERANT RPM 100	720	1750	3600
4.0	25.0	1.25	20.0	0.00	0.047	0.293	0.637	1.160
				0.10	0.052	0.321	0.697	1.269
				0.20	0.055	0.344	0.747	1.361
				0.30	0.059	0.365	0.792	1.443
				0.40	0.062	0.384	0.833	1.517
				0.50	0.065	0.402	0.873	1.590
	33.0	1.5	22.0	0.00	0.117	0.716	1.536	2.766
				0.10	0.128	0.783	1.680	3.025
				0.20	0.138	0.842	1.806	3.253
				0.30	0.147	0.897	1.925	3.466
				0.40	0.155	0.947	2.031	3.657
				0.50	0.162	0.992	2.128	3.831
	48.0	2.0	24.0	0.00	0.381	2.272	4.789	8.486
				0.10	0.418	2.491	5.251	9.304
				0.20	0.451	2.688	5.666	10.041
				0.30	0.480	2.863	6.033	10.692
				0.40	0.506	3.017	6.359	11.268
				0.50	0.531	3.164	6.669	11.818
	75.0	2.5	30.0	0.00	1.687	9.705	20.004	34.754
				0.10	1.855	10.668	21.988	38.201
				0.20	2.006	11.541	23.789	41.330
				0.30	2.141	12.317	25.388	44.109
				0.40	2.267	13.041	26.880	46.700
				0.50	2.383	13.707	28.252	49.085
	108.0	3.0	36.0	0.00	5.551	30.902	62.482	106.791
				0.10	6.129	34.121	68.991	117.915
				0.20	6.635	36.937	74.684	127.646
				0.30	7.097	39.511	79.889	136.541
				0.40	7.527	41.904	84.727	144.810
				0.50	7.921	44.099	89.165	152.396
	144.0	4.0	36.0	0.00	12.812	69.370	138.090	232.996
				0.10	14.147	76.597	152.475	257.268
				0.20	15.314	82.917	165.057	278.497
				0.30	16.381	88.696	176.560	297.906
				0.40	17.373	94.067	187.252	315.946
				0.50	18.284	98.995	197.061	332.496

$$hp_{service} = hp_{rated} \left[\frac{C_L C_H S_{ac}}{C_T C_R 95} \right]^3 \frac{C_V}{50/(50 + \sqrt{V_T}) C_s C_f C_o} \qquad 5.89$$

where,

$hp_{service}$ - service capacity of the gear.

In Table 5, the maximum permissible face width is assumed. The face widths taken in Table 6 are from Table 13 - 9 of [14] . This has been done to facilitate the comparison of the results.

TABLE 6 SURFACE DURABILITY RATINGS OF ON-CENTER FACE GEARS

DZO=1

I12	D1 INCH	D2 INCH	Z1	FACE INCH	ASTAR	HORSE POWER AT DIFFERENT RPM 100	720	1750	3600
1.5	1.0	1.5	20.0	0.085	0.000	0.018	0.109	0.237	0.432
	1.4	2.1	22.0	0.125	0.000	0.053	0.320	0.684	1.227
	2.0	3.0	24.0	0.172	0.000	0.161	0.954	2.005	3.544
	3.0	4.5	30.0	0.250	0.000	0.632	3.628	7.471	12.970
	4.0	6.0	36.0	0.359	0.000	1.698	9.506	19.284	33.050
	6.0	9.0	36.0	0.547	0.000	5.547	29.861	59.259	99.734
2.0	1.0	2.0	20.0	0.141	0.000	0.022	0.135	0.293	0.533
	1.4	2.8	22.0	0.203	0.000	0.065	0.398	0.850	1.526
	2.0	4.0	24.0	0.297	0.000	0.202	1.198	2.519	4.452
	3.0	6.0	30.0	0.438	0.000	0.804	4.616	9.508	16.506
	4.0	8.0	36.0	0.578	0.000	2.128	11.917	24.174	41.431
	6.0	12.0	36.0	0.859	0.000	6.888	37.085	73.593	123.859
4.0	1.0	4.0	20.0	0.375	0.000	0.045	0.281	0.609	1.109
	1.4	5.6	22.0	0.516	0.000	0.134	0.818	1.748	3.138
	2.0	8.0	24.0	0.719	0.000	0.416	2.467	5.185	9.165
	3.0	12.0	30.0	1.031	0.000	1.656	9.510	19.585	34.002
	4.0	16.0	36.0	1.250	0.000	4.271	23.915	48.512	83.142
	6.0	24.0	36.0	1.500	0.000	12.248	65.941	130.857	220.235

CHAPTER VI

RESULTS, DISCUSSIONS AND CONCLUSIONS

In this chapter, some illustrative example problems are solved and their results are discussed. At the end of the chapter, general discussions on tapered and face gears are presented. Based on these discussions, conclusions are drawn.

The computer programs for executing the necessary computation have been developed. The results of the computation are presented in this chapter. The description of these programs and more numerical results obtained are given in the report [22] .

6.1 Intersection curves for face gears

The intersection of the two surfaces, U and L with the tip plane of the face gear gives two intersection curves. The study of these curves presents a clear picture of the pointing phenomenon, as will be clear from the following example.

To find the intersection curves for a face gear, given the following :

$\Sigma = \pi/2$, $\beta = 0$, $\Delta^* = 0$, $Z_1 = 20$, $i_{21} = 0.2$, $\alpha_o = 20°$, $\xi_o = 0$, $f_o = 1$ and $c_o = 0.25$.

The results obtained are given in Table 7. For any λ , the first and second rows give the co-ordinates of intersection curves for surfaces U and L respectively. In this table, co-ordinates are

TABLE 7 CO-ORDINATES OF INTERSECTION CURVES

* LAMDA	X-COOR	Y-COOR	Z-COOR
5.2500	0.0450	-0.9000	4.9406 U
	-0.0450	-0.9000	4.9406 L
5.3500	0.0406	-0.9000	5.0348
	-0.0406	-0.9000	5.0348
5.4500	0.0361	-0.9000	5.1292
	-0.0361	-0.9000	5.1292
5.5500	0.0314	-0.9000	5.2236
	-0.0314	-0.9000	5.2236
5.6500	0.0265	-0.9000	5.3181
	-0.0265	-0.9000	5.3181
5.7500	0.0214	-0.9000	5.4125
	-0.0214	-0.9000	5.4125
5.8500	0.0161	-0.9000	5.5070
	-0.0161	-0.9000	5.5070
5.9500	0.0107	-0.9000	5.6014
	-0.0107	-0.9000	5.6014
6.0500	0.0051	-0.9000	5.6958
	-0.0051	-0.9000	5.6958
6.1500	-0.0007	-0.9000	5.7901
	0.0007	-0.9000	5.7901
6.2500	-0.0066	-0.9000	5.8845
	0.0066	-0.9000	5.8845
6.3500	-0.0127	-0.9000	5.9788
	0.0127	-0.9000	5.9788
6.4500	-0.0189	-0.9000	6.0731
	0.0189	-0.9000	6.0731
6.5500	-0.0252	-0.9000	6.1674
	0.0252	-0.9000	6.1674
6.6500	-0.0316	-0.9000	6.2616
	0.0316	-0.9000	6.2616

non-dimensionalized with respect to the nominal pitch radius of the pinion. The intersection curves are shown in figure 6. Pointing of the tooth starts at the point P.

6.2 Optimum helix angle

It is observed from Figure 14 that the face width of the spiral face gear changes with helix angle of the pinion. It is seen that for a given eccentricity the face width attains a maximum value for a particular helix angle, which may be termed as optimal helix angle. The following example illustrates this.

Example 2

To study the face width variation in spur face gear having the following parameters :

$\Sigma = \pi/2$, $\beta = 0\text{-}20°$, $\Lambda^* = 0$, 0.2 and 0.4, $Z_1 = 20$, $i_{21} = 25$, $\alpha_{on} = 20°$, $\xi_{on} = 0$, $f_{on} = 1$ and $c_{on} = 0.25$.

The maximum and minimum radii are found using the material of sections 5.13 and 5.14. The difference of these two radii are given in Table 8. The values of optimal helix angle obtained are given in Table 9. The radii in Tables 8 and 9 are non-dimensionalized with respect to the radius of the base cylinder of the pinion.

6.3 Contact ratio in Tapered gears

The contact ratio is found using the method described in section 4.1. The set, $\tilde{R}$, is defined by following expressions. The expressions are on-center spur tapered and face gears ($a = 0$) and

TABLE 8 VARIATION OF FACE WIDTH OF FACE GEARS WITH HELIX ANGLE

I21=0.25 Z1=20

BETA	W	R2P	R2U	BETA	W	R2P	R2U	ASTAR
0.0	0.86	4.922	4.063					0.00
1.0	0.85	4.922	4.074	11.0	0.76	4.945	4.183	
2.0	0.84	4.922	4.086	12.0	0.76	4.950	4.193	
3.0	0.83	4.923	4.097	13.0	0.75	4.955	4.204	
4.0	0.82	4.925	4.108	14.0	0.75	4.961	4.214	
5.0	0.81	4.926	4.119	15.0	0.74	4.967	4.224	
6.0	0.80	4.929	4.130	16.0	0.74	4.973	4.234	
7.0	0.79	4.931	4.141	17.0	0.74	4.980	4.245	
8.0	0.78	4.934	4.151	18.0	0.73	4.987	4.255	
9.0	0.78	4.937	4.162	19.0	0.73	4.995	4.265	
10.0	0.76	4.950	4.193	20.0	0.43	5.003	4.569	
0.0	0.73	4.986	4.257					0.20
1.0	0.74	4.969	4.234	11.0	0.82	4.822	3.999	
2.0	0.74	4.953	4.212	12.0	0.83	4.808	3.982	
3.0	0.75	4.937	4.189	13.0	0.82	4.795	3.980	
4.0	0.76	4.922	4.165	14.0	0.81	4.783	3.977	
5.0	0.76	4.907	4.142	15.0	0.80	4.770	3.974	
6.0	0.77	4.877	4.095	17.0	0.78	4.746	3.967	
8.0	0.79	4.863	4.072	18.0	0.77	4.734	3.964	
9.0	0.80	4.849	4.048	19.0	0.76	4.722	3.960	
10.0	0.81	4.835	4.024	20.0	0.75	4.710	3.956	
0.0	0.61	5.174	4.568					0.40
1.0	0.61	5.142	4.535	11.0	0.63	4.836	4.204	
2.0	0.61	5.110	4.502	12.0	0.64	4.806	4.171	
3.0	0.61	5.079	4.469	13.0	0.64	4.747	4.103	
5.0	0.61	5.077	4.403	1 .0	0.65	4.718	4.069	
6.0	0.61	4.986	4.375	16.0	0.65	4.688	4.034	
7.0	0.62	4.956	4.337	17.0	0.66	4.659	3.999	
8.0	0.62	4.926	4.304	18.0	0.67	4.629	3.964	
9.0	0.62	4.896	4.271	19.0	0.67	4.600	3.929	
10.0	0.63	4.866	4.238	20.0	0.68	4.570	3.894	

TABLE 9 OPTIMUM HELIX ANGLES FOR FACE GEARS

Z1	ASTAR	R2P/R2U/WIDTH/BETA I21 = 1	I21 = 1/4	I21 = 1/7	
17.0	0.00	1.263	4.969	8.689	R2P
		1.099	4.071	7.048	R2U
		0.164	0.898	1.641	WIDTH
		0.0	0.0	0.0	BETA
	0.05	1.261	4.961	8.676	
		1.098	4.066	7.039	
		0.162	0.887	1.622	
		5.1	5.7	5.8	
	0.10	1.256	4.938	8.634	
		1.094	4.051	7.013	
		0.162	0.887	1.622	
	0.15	1.248	4.899	8.565	
		1.088	4.026	6.967	
		0.160	0.874	1.598	
		7.7	8.6	8.7	
	0.20	1.236	4.842	8.464	
		1.079	3.989	6.901	
		0.157	0.854	1.563	
		10.4	11.7	11.8	
	0.25	1.221	4.765	8.328	
		1.068	3.939	6.812	
		0.153	0.827	1.517	
		13.2	14.8	15.0	

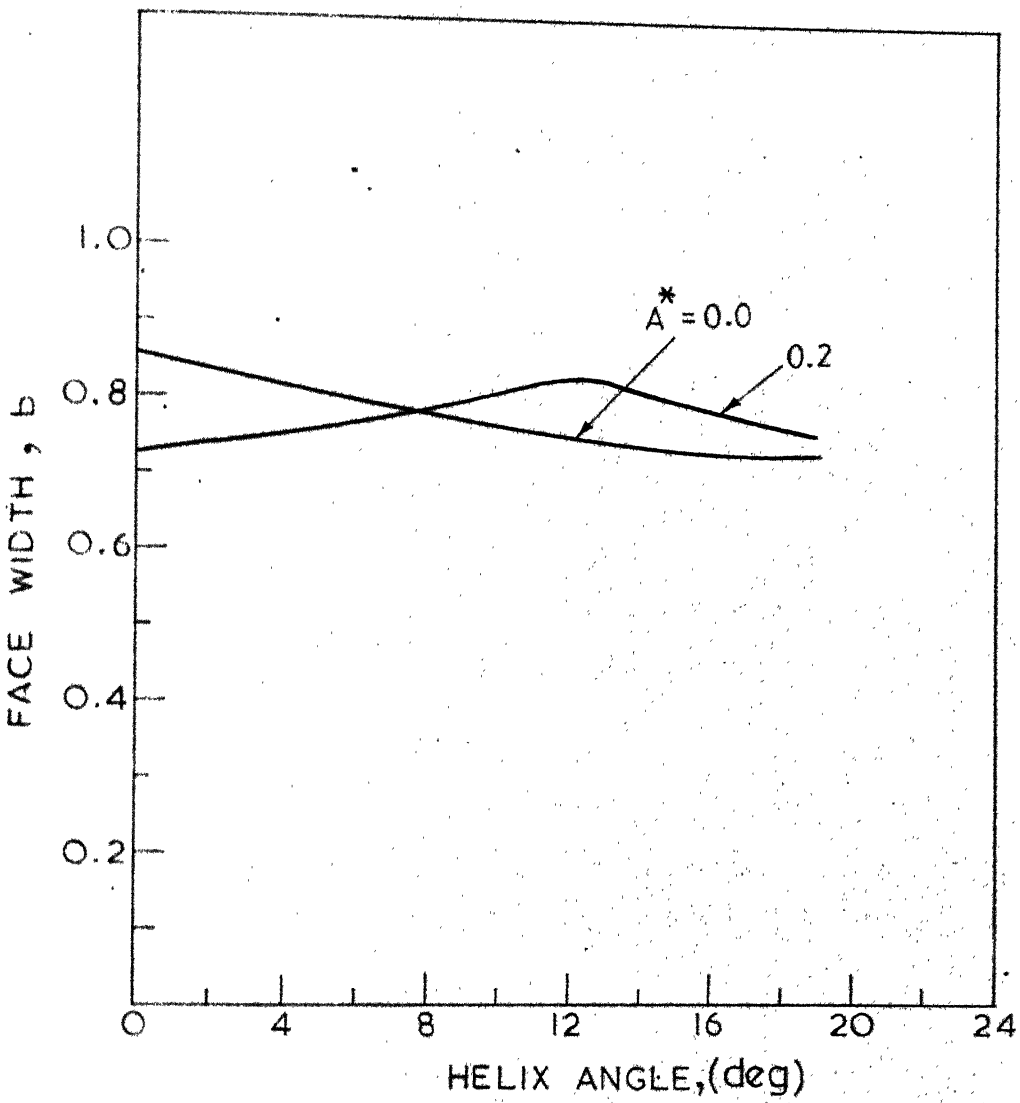

FIG. 14 VARIATION OF FACE WIDTH WITH HELIX ANGLE.

(FACE GEAR: $\Sigma = \pi/2$, $Z_1 = 20$, $i_{21} = .25$ AND $\alpha_0 = 20^\circ$)

off-set spur face gears ($a \neq 0$) [Figure 5].

$$g_1 = [\cot \Sigma\{z_2+r_f/S\Sigma-r_{2F} \text{ cor } \Sigma\} - r_{2F}]^2 - x_2^2-y_2^2 \leq 0 \qquad 6.1$$

$$g_2 = x_2^2+y_2^2 -[\cot \Sigma\{z_2+r_f/S\Sigma-r_{2B} \cot \Sigma\}-r_{2B}]^2 \leq 0 \qquad 6.2$$

$$g_3 = r_f/S\Sigma + z_2-(x_2^2+y_2^2)^{1/2} \cot \Sigma \leq 0$$

where,

$$[x_2,y_2,z_2]^T = [R_{cx} + a,\ R_{cy}\ C\Sigma - R_{cz}\ S\Sigma,\ R_{cy}\ S\Sigma + R_{cz}\ C\Sigma]^T$$

and $\underset{\sim}{R}_c = [R_{cx}, R_{cy}, R_{cz}]^T$

$$g_4 = R_{cx}^2 + R_{cy}^2 - r_{1c}^2 \leq 0 \qquad 6.4$$

$$g_5 = \lambda_F - R_{cz} \leq 0 \qquad 6.5$$

$$g_6 = R_{cz} - \lambda_B \leq 0 \qquad 6.6$$

g_1, g_2 and g_3 correspond to the front cone, the back cone and the face cone of the gear blank. The expressions g_4, g_5 and g_6 are related to the pinion blank. [Figure 5].

Sets I_θ and I_ϕ may be defined by the following expressions.

$$I_\theta \equiv [\theta_k \mid 0 \leq \theta_k \leq \pm 35°]^1,\ k = U,L \qquad 6.7$$

$$I_\phi = [\phi_1 \mid -30° \leq \phi_1 \leq 30°] \qquad 6.8$$

The set $\underset{\sim}{A}$ may be defined as

---

[1] Upper and lower signs are for surfaces U and L respectively.

$$\tilde{A} \equiv [\Phi_k \mid \pm \Phi_k \geq 0],\ k = U,L \qquad 6.9$$

where $\Phi_k = \phi_1 + \theta_k$

The method is illustrated by the following example problem.

Example 3

To find the contact ratio of the face gear set given the following parameters.

$\Sigma = \pi/2$, $\beta = 0$, $\Lambda^* = 0$, $i_{21} = 0.25$, $Z_1 = 18$, $\alpha_o = 20°$, $\xi_o = 0$, $f_o = 1$, $c_o = 0.25$, $\lambda_i = 4.1$ $\lambda_e = 4.4$ [Figure 3], $r_{2i} = 4.1$ and $r_{2e} = 4.4$.

The results of the computation are given in Table 10.

6.4 Normal deviation of tooth surface in contact

The method to find the normal deviation of surfaces in contact is described in section 5.4.1. The following example is solved using this method.

Example 4

For $\Sigma = \pi/2$, $\beta = 0$, $\Lambda^* = 0$, $i_{21} = 0.25$. $Z = 18$, $Z_o = 19$, $m = 5$mm, $\alpha_o = 20°$, $\xi_o = 0$, $f_o = 1$, $c_o = .25$, $\frac{1}{2}\rho^2 = 0.5$ and $d = 20$, find the polar graph of the normal deviation of surfaces in contact at a point where $\phi_1 = 0°$.

The results are given in Table 11. The polar graph is shown in Figure 13.

TABLE 10 CONTACT RATIO IN TAPERED GEARS

ITER.	FAI1	THT.	FAIK	G(1)	G(2)	G(3)	G(4)	G(5)	G(6)
1	-20.0	28.7	12.8	-0.087	-2.463	-0.140	-0.148	-0.002	-0.298
2	-22.5	31.2	12.8	-0.114	-2.436	-0.150	-0.102	-0.002	-0.298
3	-23.7	32.6	13.0	-0.153	-2.397	-0.157	-0.074	-0.005	-0.295
4	-24.4	33.0	12.7	-0.125	-2.425	-0.156	-0.067	-0.001	-0.299
5	-24.7	33.3	12.8	-0.135	-2.415	-0.158	-0.060	-0.002	-0.298
6	-24.8	33.7	13.0	-0.163	-2.387	-0.161	-0.052	-0.005	-0.295
1	15.0	3.1	22.2	-1. 73	-0.577	-0.000	-0.3 5	-0.221	-0.079
2	15.0	3.1	22.2	-1. 73	-0.577	-0.000	-0.3 5	-0.221	-0.079
3	15.0	3.1	22.2	-1. 73	-0.577	-0.000	-0.3 5	-0.221	-0.079
4	15.0	3.1	22.2	-1. 73	-0.577	-0.000	-0.3 5	-0.221	-0.079
5	15.0	3.1	22.2	-1. 73	-0.577	-0.000	-0.3 5	-0.221	-0.079
6	15.2	4.2	23.5	-2.318	-0.232	-0.000	-0.393	-0.261	-0.039

START OF CONTACT -24.8 DEG
END OF CONTACT 15.2 DEG
CONTACT RATIO 2.000

START OF CONTACT -24.8 DEG
END OF CONTACT 15.2 DEG
CONTACT RATIO 2.0

TABLE 11 NORMAL DEVIATION OF TEETH SURFACES OF ON-CENTER SPUR FACE GEAR SET

NU DEG	L1	L2	L1-L2
.000	21.680	21.560	.120
10.000	26.910	24.810	2.100
20.000	35.050	27.240	7.810
30.000	45.130	28.580	16.550
40.000	55.930	28.660	27.270
50.000	66.140	27.470	38.670
60.000	74.550	25.150	49.400
70.000	80.120	21.990	58.130
80.000	82.200	18.360	63.840
90.000	80.520	14.700	65.820
100.000	75.300	11.460	63.840
110.000	67.150	9.020	58.130
120.000	57.080	7.680	49.400
130.000	46.280	7.600	38.680
140.000	36.060	8.790	27.270
150.000	27.660	11.110	16.550
160.000	22.080	14.280	7.800
170.000	20.010	17.910	2.100
180.000	21.680	21.560	.120
190.000	26.910	24.810	2.100
200.000	35.050	27.240	7.810
210.000	45.130	28.580	16.550
220.000	55.930	28.660	27.270
230.000	66.140	27.470	38.670
240.000	74.550	25.150	49.400
250.000	80.120	21.990	58.130
260.000	82.200	18.360	63.840
270.000	80.520	14.700	65.820
280.000	75.300	11.460	63.840
290.000	67.150	9.020	58.130
300.000	57.080	7.680	49.400
310.000	46.280	7.600	38.680
320.000	36.060	8.790	27.270
330.000	27.660	11.110	16.550
340.000	22.080	14.280	7.800
350.000	20.010	17.910	2.100
360.000	21.680	21.560	.120

6.5 Variation of contact stress

Variation of contact stress for one cycle of contact is studied for a case given in example 5.

Example 5

To find the variation of contact stress as the contact point moves, for the following case :

$\Sigma = \pi/2$, $\beta = 0$, $\Delta^* = 0$, $i_{21} = 0.25$, $Z_1 = 18$, $Z_o = 19$, $m = 5$mm, $\alpha_o = 20°$, $\xi_o = 0$, $f_o = 1$, $c_o = 0.25$ and $P = 100$ kg. Contact is localized at the mid-point of the tooth width.

The method used is described in Section 5.4.2. The stress constants, used in equations (5.5.3) and (5.5.4), are given in Table 4. The results are given in Table 12. The variation is shown in Figure 15. The curves in Figure 15 are drawn assuming the contact of one pair of teeth. Actually, a portion of these curves is used when one pair of teeth are in contact. This portion is shown by continuous lines. Beyond these portions, shown by dashed lines in Figure 15, two pairs will be in contact. As in these portions load is being shared, actual contact stress on any particular pair of teeth will be substantially less than that shown in Figure 15.

6.6 Effect of number of teeth in cutter on contact stress and on contact zone

The difference between numbers of teeth in cutter and pinion has an effect on contact stress. This effect is illustrated in the following example.

TABLE 12A VARIATION OF CONTACT STRESS WITH THE ANGLE OF ROTATION OF PINION

NO OF TEETH ON CUTTER	19.0	
NO OF TEETH ON PINION	18.0	
TRANSMISSION RATIO BETWEEN CUTTER AND GEAR	0.2500	
PRESSURE ANGLE OF CUTTER	20.0	DEG
MODULE OF CUTTER AND GEAR SET	5.0	MM
INNER RADIUS OF FACE GEAR SET	183.005	MM
OUTER RADIUS OF FACE GEAR SET	214.250	MM

CORRECTION PARAMETERS

CUTTER SHIFT FACTOR	0.000	
PINION SHIFT FACTOR	-0.026	
CUTTER TOOTH SPACE ANGLE	3.9	DEG
PINION TOOTH SPACE ANGLE	4.2	DEG
PRESSURE ANGLE OF GEAR SET	26.0	DEG

GEOMETRIC DISTENCES

B	2.614	MM
C	44.886	MM
RE1	49.886	MM
RT	42.500	MM

TABLE 12B CURVETURES

FAI1	KAI1	KAI2	SIG	KAI3	KAI4	BCAP	ACAP	SIG1
-16.0	0.00000	-0.03586	-41.8	C.01261	-0.00865	0.00006	0.01985	-16.1
-14.0	0.00000	-0.03787	-41.8	C.01238	-0.00876	0.00006	0.02069	-15.3
-12.0	0.00000	-0.04011	-41.8	C.01216	-0.00888	0.00006	0.02164	-14.5
-10.0	0.00000	-0.04263	-41.8	0.01194	-0.00900	0.00006	0.02273	-13.7
-8.0	0.00000	-0.04549	-41.8	0.01174	-0.00912	0.00006	0.02400	-12.8
-6.0	0.00000	-0.04877	-41.8	C.01154	-0.00924	0.00006	0.02547	-12.0
-4.0	0.00000	-0.05255	-41.8	0.01134	-0.00937	0.00006	0.02721	-11.1
-2.0	0.00000	-0.05697	-41.8	0.01116	-0.00950	0.00006	0.02926	-10.3
-0.0	0.00000	-0.06220	-41.8	C.01098	-0.00964	0.00006	0.03171	-9.4
2.0	0.00000	-0.06849	-41.8	C.01080	-0.00977	0.00006	0.03470	-8.6
4.0	0.00000	-0.07619	-41.8	C.01063	-0.00992	0.00006	0.03839	-7.7
6.0	0.00000	-0.08585	-41.8	0.01047	-0.01007	0.00006	0.04307	-6.9
8.0	0.00000	-0.09831	-41.8	0.01031	-0.01022	0.00006	0.04914	-6.0
10.0	0.00000	-0.11499	-41.8	C.01015	-0.01037	0.00006	0.05733	-5.1
12.0	0.00000	-0.13850	-41.8	C.01000	-0.01053	0.00006	0.06893	-4.3
14.0	0.00000	-0.17410	-41.8	C.00986	-0.01070	0.00006	0.08657	-3.4
16.0	0.00000	-0.23431	-41.8	C.00972	-0.01087	0.00006	0.11652	-2.5

TABLE 12C DIMENSION OF CONTACT SPOT AND STRESS

FAI1	ABS	TAO	DEL	ASMAL	BSMAL	AREA	S
-16.0	0.039822	0.9943	0.00312	6.65565	0.17719	3.70499	40.49
-14.0	0.041484	0.9945	0.00314	6.64479	0.17377	3.62748	41.35
-12.0	0.043389	0.9947	0.00315	6.64860	0.16984	3.54749	42.28
-10.0	0.045581	0.9949	0.00317	6.64957	0.16564	3.46016	43.35
-8.0	0.048116	0.9952	0.00318	6.63885	0.16106	3.35911	44.65
-6.0	0.051066	0.9954	0.00320	6.63444	0.15638	3.25939	46.02
-4.0	0.054528	0.9957	0.00322	6.64337	0.15137	3.15928	47.48
-2.0	0.058630	0.9960	0.00325	6.65077	0.14606	3.05185	49.15
-0.0	0.063545	0.9963	0.00327	6.66555	0.14016	2.93503	51.11
2.0	0.069519	0.9966	0.00329	6.67385	0.13385	2.80637	53.45
4.0	0.076910	0.9969	0.00331	6.69131	0.12696	2.66893	56.20
6.0	0.086254	0.9972	0.00333	6.72267	0.11954	2.52463	59.41
8.0	0.098400	0.9975	0.00337	6.75075	0.11166	2.36811	63.34
10.0	0.114776	0.9979	0.00339	6.77934	0.10341	2.20245	68.11
12.0	0.137975	0.9982	0.00343	6.82911	0.09377	2.01182	74.56
14.0	0.173256	0.9986	0.00347	6.86951	0.08351	1.80232	83.23
16.0	0.233156	0.9990	0.00355	6.96916	0.07131	1.56133	96.07

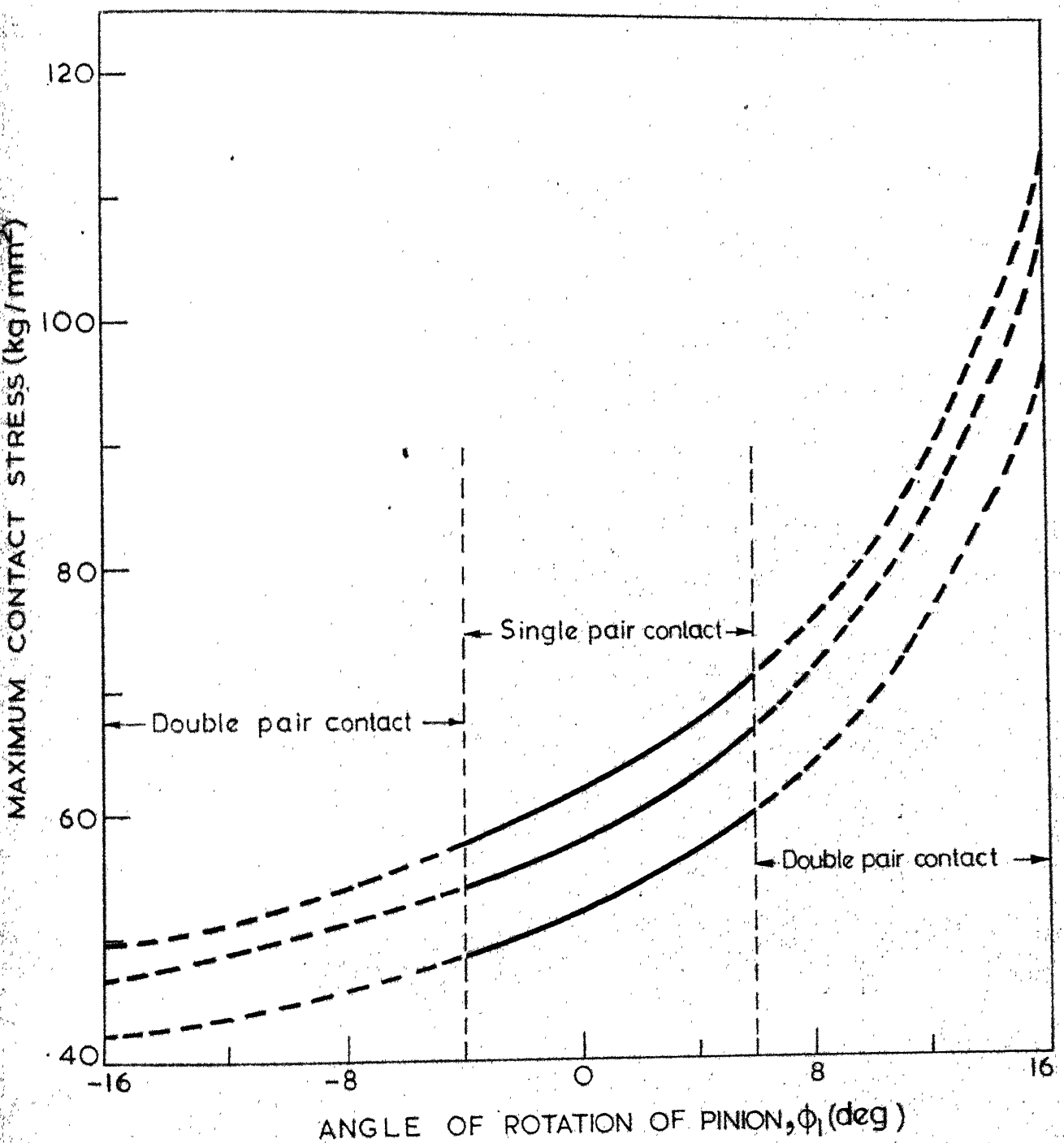

FIG.15. VARIATION OF CONTACT STRESS WITH NUMBER OF TEETH IN CUTTER.

(ON CENTER FACE GEAR: $\Sigma = \pi/2$, $\beta = 0$, $a = 0$, $Z_1 = 18$, $i_{21} = .25$, $m = 5$ mm, $P = 100$ kg. AND $\alpha_0 = 20^\circ$).

Example 6

To study the effect of number of teeth in cutter on contact stress and on contact zone. Following parameters are given.

$\Sigma = \pi/2$, $\beta = 0$, $\Delta^* = 0$, $i_{21} = 0.25$, $Z_1 = 18$, $DZO = Z_o - Z_1 = 1,2,3$ $m = 5mm$, $\alpha_o = 20°$, $\xi_o = 0$, $f_o = 1$, $c_o = 0.25$ and $P = 100$ kg. Contact is localized at the mid-point of the tooth width. The method used is described in Section 5.4.2. The results obtained are listed in Table 13. The effects are shown in Figures 15 and 16.

6.7 Effect of number of teeth in cutter on surface durability rating

It is seen in the previous example that the number of teeth in cutter affects the contact stress. Consequently, the surface durability rating is also affected. This effect can be observed in the following example.

Example 7

To find the effect of number of teeth of the cutter on the surface durability rating of face gears. Following parameters are specified.

$\Sigma = \pi/2$, $\beta = 0$, $\Delta^* = 0$, $Z_1 = 20$, 25, 30 and 35, $i_{21} = 0.25$, $m = 2.5$ mm, $DZO = 1$ to 5, $S_{ac} = 95$ kg/mm^2 and $C_V = 50/(50 + \sqrt{V_T})$.- Where V_T is in fpm. Standard cutters are assumed.

The inner and outer radii of the face gear are found from the considerations of undercutting and pointing of teeth. The method to find the surface durability rating is given in Section 5.5. The results

TABLE 13 EFFECT OF THE NUMBER OF TEETH IN CUTTER ON CONTACT STRESS

DZO * FAIL	1 STRESS KG/MM^2	1 AREA MM^2	2 STRESS KG/MM^2	2 AREA MM^2	3 STRESS KG/MM^2	3 AREA MM^2
-16	41.8	3.587	46.8	3.207	49.6	3.023
-14	42.6	3.520	47.7	3.147	50.7	2.960
-12	43.5	3.455	48.7	3.078	51.7	2.899
-10	44.6	3.360	49.8	3.009	52.9	2.838
- 8	45.8	3.274	51.1	2.932	54.3	2.761
- 6	47.1	3.186	52.6	2.854	55.9	2.684
- 4	48.5	3.094	54.3	2.761	57.7	2.599
- 2	50.1	2.9 3	56.0	2.67	59.6	2.517
0	52.1	2.880	57.7	2.599	61.9	2.423
2	54.3	2.760	60.8	2.467	64.6	2.323
4	57.1	2.627	63.7	2.353	67.9	2.214
6	60.2	2.491	67.4	2.225	71.5	2.098
8	64.0	2.342	71.7	2.091	76.1	1.971
10	68.8	2.179	77.0	1.947	81.8	1.833
12	75.2	1.995	89.2	1.780	89.5	1.677
14	83.7	1.791	94.0	1.595	99.8	1.503
16	96.6	1.553	108.2	1.386	115.4	1.300

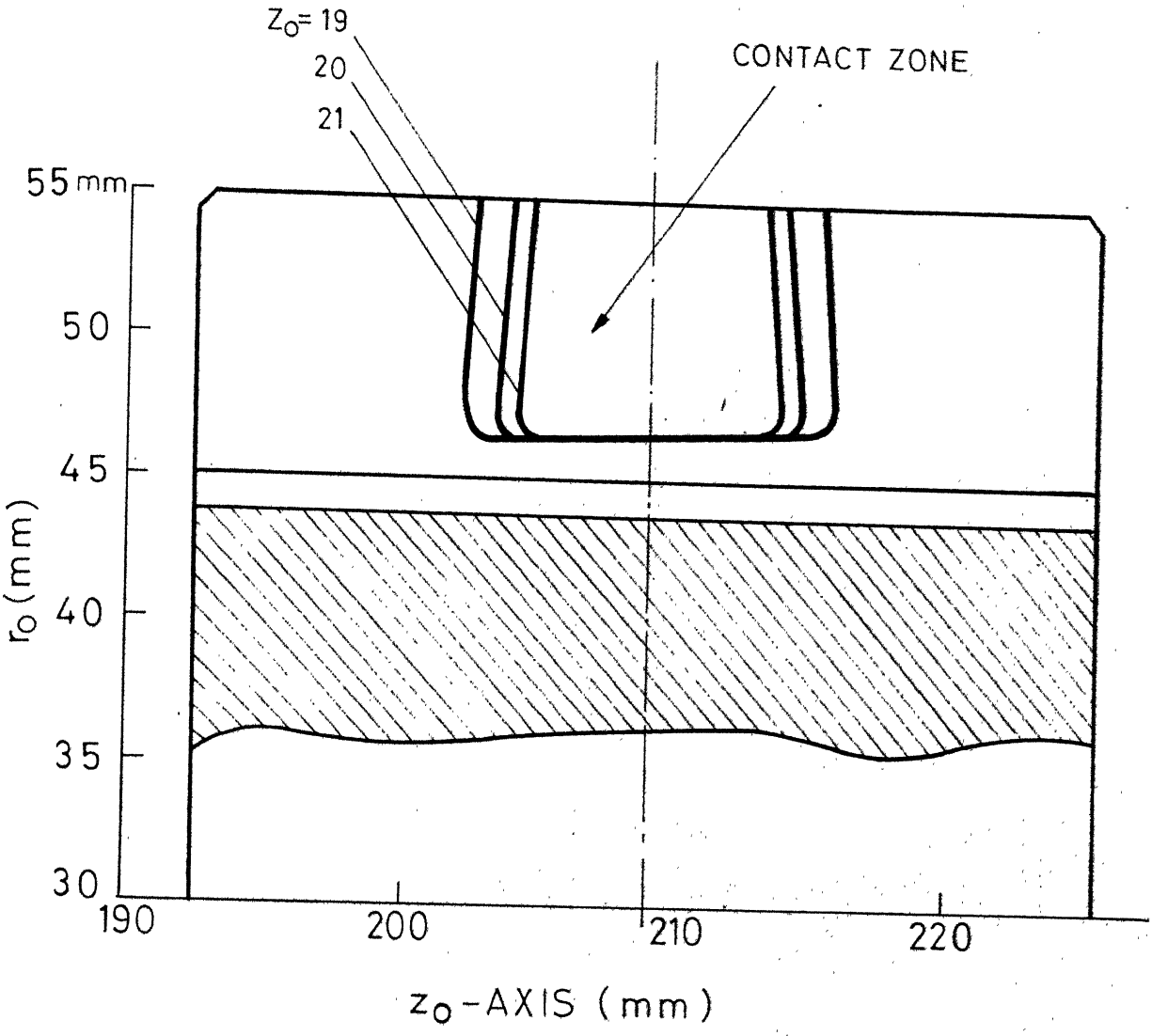

FIG.16 EFFECT OF NUMBER OF TEETH IN CUTTER ON CONTACT ZONE ON PINION TOOTH.

(ON-CENTER FACE GEAR: $\Sigma = \pi/2, \beta = 0, a = 0, Z_1 = 18, i_{21} = .25,$ $m = 5$ mm, $P = 100$ Kg AND $\alpha_o = 20°$).

TABLE 14 EFFECT OF THE NUMBER CF TEETH IN CUTTER ON SURFACE DURABILITY RATINGS

I12	Z1/DZC	M	ASTAR	HP AT 100 RPM	CONTACT RATIO	ALFA DEG
4.0	20/1	2.5	0.00	.363	1.73	20.8
	2			.272		
	3			.239		
	4			.222		
	5			.214		
4.0	25/1	2.5	0.00	.858	1.74	21.1
	2			.632		
	3			.544		
	4			.496		
	5			.474		
4.0	30/1	2.5	0.00	1.687	1.76	21.2
	2			1.224		
	3			1.049		
	4			.952		
	5			.891		
4.0	35/1	2.5	0.00	2.978	1.78	21.2
	2			2.138		
	3			1.805		
	4			1.620		
	5			1.502		

obtained are given in Table 14. The variation of surface durability rating with DZO is shown in Figure 17.

6.8 Variation of surface durability rating with other independent design parameters.

The surface durability ratings of spur face gears with localized contacts also depend upon the following

1. eccentricity, a
2. pressure angle, α
3. number of teeth in the pinion, Z_1
4. module, m.

The variations of surface durability ratings with these parameters are given in Tables 15, 16, 17 and 18. The variations are shown in Figures 18, 19, 20 and 21. Unless specified, the inner and outer radii are taken to be limiting radii and contact is localized at mean radius of the blanks.

6.9 Discussions and Conclusions

The discussions and conclusions are based on the results given in this dissertation. Detailed results are published in reference [22]. The ranges of parameters covered in the report [22] are given in Appendix IV.

An examination of Tables 1 and 2 reveals that the face width of a gear tooth is sensitive to angle Σ between the shaft axes, the transmission ratio i_{21}, the non-dimensionalized eccentricity A* and helix angle β. For the same number of teeth in pinion, and for

TABLE 15 VARIATION OF SURFACE DURABILITY RATING WITH ECCENTRICITY

I12	Z1	M	ASTAR	HP AT 100 RPM	CONTACT RATIO	ALFA DEG
1.5	30	2.5	0.00	.580	1.64	23.8
			0.10	.682	1.59	24.9
			0.20	.771	1.55	25.7
			0.30	.855	1.52	26.4
			0.40	.931	1.54	26.9
			0.50	1.002	1.48	27.1
2.0	30	2.5	0.00	.792	1.69	22.7
			0.10	.917	1.64	23.9
			0.20	1.025	1.59	24.8
			0.30	1.123	1.56	25.6
			0.40	1.210	1.53	26.1
			0.50	1.292	1.51	26.6
4.0	30	2.5	0.00	1.687	1.76	21.2
			0.10	1.855	1.72	22.2
			0.20	2.006	1.68	22.9
			0.30	2.141	1.65	23.5
			0.40	2.267	1.63	24.1
			0.50	2.300	1.60	24.6

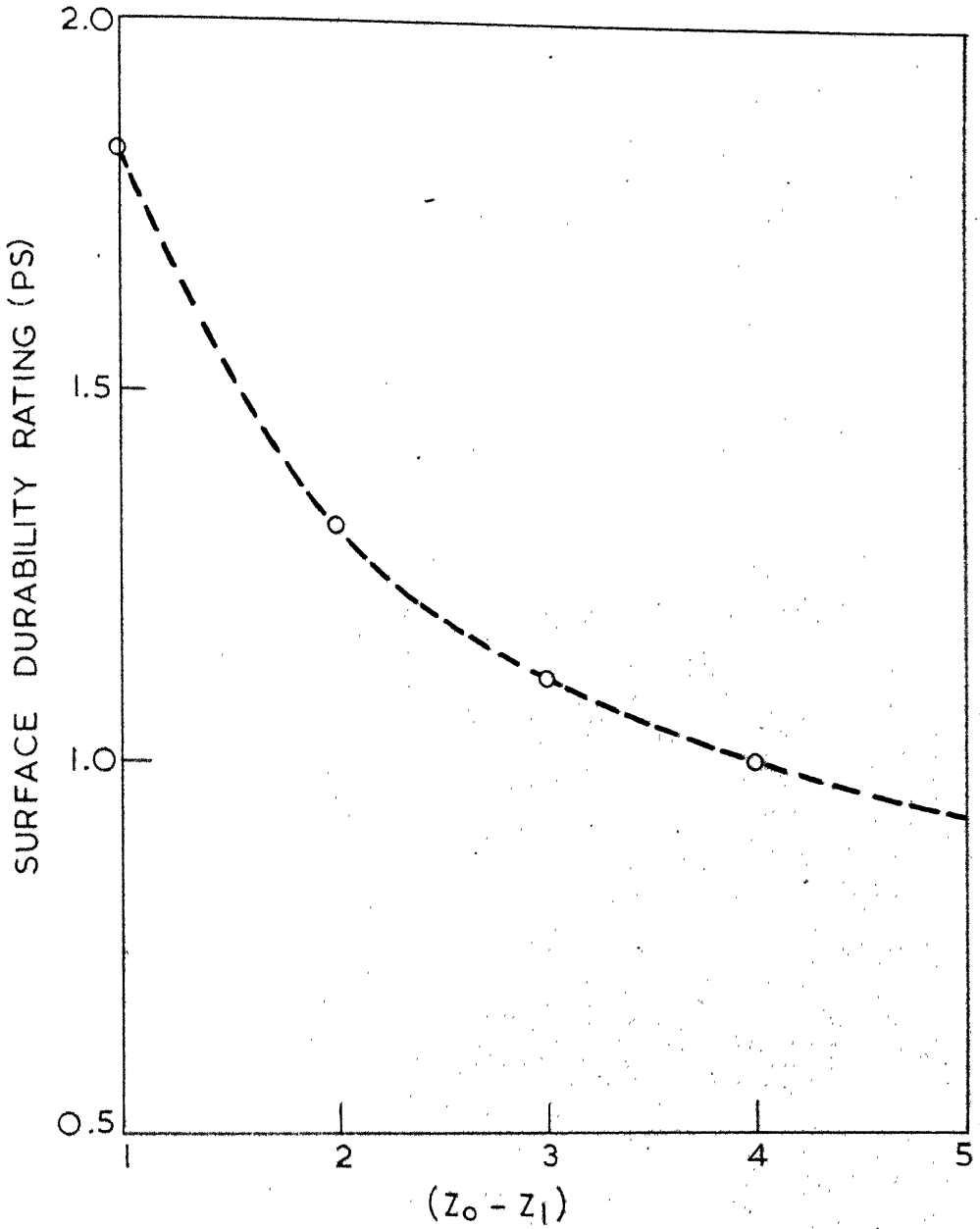

FIG. 17 VARIATION OF SURFACE DURABILITY RATING WITH NUMBER OF TEETH IN CUTTER.

(ON CENTER FACE GEAR: $\Sigma = \pi/2$, $\beta = 0^\circ$, $a = 0$, $Z_1 = 30$, $i_{21} = .25$, $m = 2.5$ mm, $\alpha_o = 20^\circ$ AND rpm = 100).

TABLE 16 VARIATION OF SURFACE DURABILITY RATING WITH PRESSURE ANGLE

I12	Z1	M	ASTAR	HP AT 100 RPM	CONTACT RATIO	ALFA DEG
4.0	30	2.5	0.00	1.610	1.82	20.0
				1.748	1.72	22.0
				1.890	1.63	24.0
				2.018	1.54	26.0
4.0	30	2.5	0.10	1.734	1.82	20.0
				1.846	1.72	22.0
				1.984	1.63	24.0
				2.100	1.54	26.0
4.0	30	2.5	0.20	1.856	1.82	20.0
				1.960	1.72	22.0
				2.078	1.63	24.0
				2.181	1.54	26.0
4.0	30	2.5	0.30	1.990	1.82	20.0
				2.072	1.72	22.0
				2.171	1.63	24.0
				2.269	1.54	26.0
4.0	30	2.5	0.40	2.127	1.82	20.0
				2.185	1.72	22.0
				2.262	1.63	24.0
				2.356	1.54	26.0
4.0	30	2.5	0.50	2.264	1.82	20.0
				2.296	1.72	22.0
				2.353	1.63	24.0
				2.444	1.54	26.0

TABLE 17 VARIATION OF SURFACE DURABILITY RATING WITH THE NUMBER OF TEETH IN PINION

I12	Z1	M	ASTAR	HP AT 100 RPM	CONTACT RATIO	ALFA DEG
4.0	20	2.5	0.00	.363	1.73	20.8
	22			.526	1.74	20.9
	24			.734	1.74	21.1
	30			1.687	1.76	21.2
	36			3.262	1.79	20.9
4.0	20	2.5	0.10	.397	1.69	21.8
	22			.575	1.69	21.9
	24			.804	1.70	22.0
	30			1.855	1.72	22.1
	36			3.602	1.75	21.8
4.0	20	2.5	0.20	.426	1.65	22.7
	22			.618	1.66	22.8
	24			.868	1.66	22.8
	30			2.006	1.68	22.9
	36			3.899	1.72	22.5
4.0	20	2.5	0.30	.451	1.62	23.4
	22			.658	1.62	23.5
	24			.924	1.63	23.6
	30			2.141	1.65	23.5
	36			4.171	1.69	23.1
4.0	20	2.5	0.40	.474	1.59	24.1
	22			.695	1.60	24.1
	24			.974	1.60	24.1
	30			2.267	1.63	24.1
	36			4.423	1.66	23.7
4.0	20	2.5	0.50	.497	1.57	24.7
	22			.728	1.57	24.7
	24			1.022	1.58	24.7
	30			2.383	1.60	24.6
	36			4.655	1.63	24.2

TABLE 18 VARIATION OF SURFACE DURABILITY RATING WITH MODULE

I12	Z1	M	ASTAR	HP AT 100 RPM	CONTACT RATIO	ALFA DEG
4.0	20	1.25	0.00	.047	1.73	20.8
		1.5		.081		
		2.0		.188		
		2.5		.363		
		3.0		.620		
		4.0		1.438		
4.0	20	1.25	0.10	.052	1.69	21.8
		1.5		.088		
		2.0		.206		
		2.5		.397		
		3.0		.678		
		4.0		1.573		
4.0	20	1.25	0.20	.055	1.65	22.7
		1.5		.095		
		2.0		.221		
		2.5		.426		
		3.0		.727		
		4.0		1.688		
4.0	20	1.25	0.30	.059	1.62	23.4
		1.5		.100		
		2.0		.234		
		2.5		.451		
		3.0		.770		
		4.0		1.789		
4.0	20	1.25	0.40	.062	1.59	24.1
		1.5		.105		
		2.0		.246		
		2.5		.474		
		3.0		.810		
		4.0		1.881		
4.0	20	1.25	0.50	.065	1.57	24.7
		1.5		.111		
		2.0		.258		
		2.5		.477		
		3.0		.849		
		4.0		1.971		

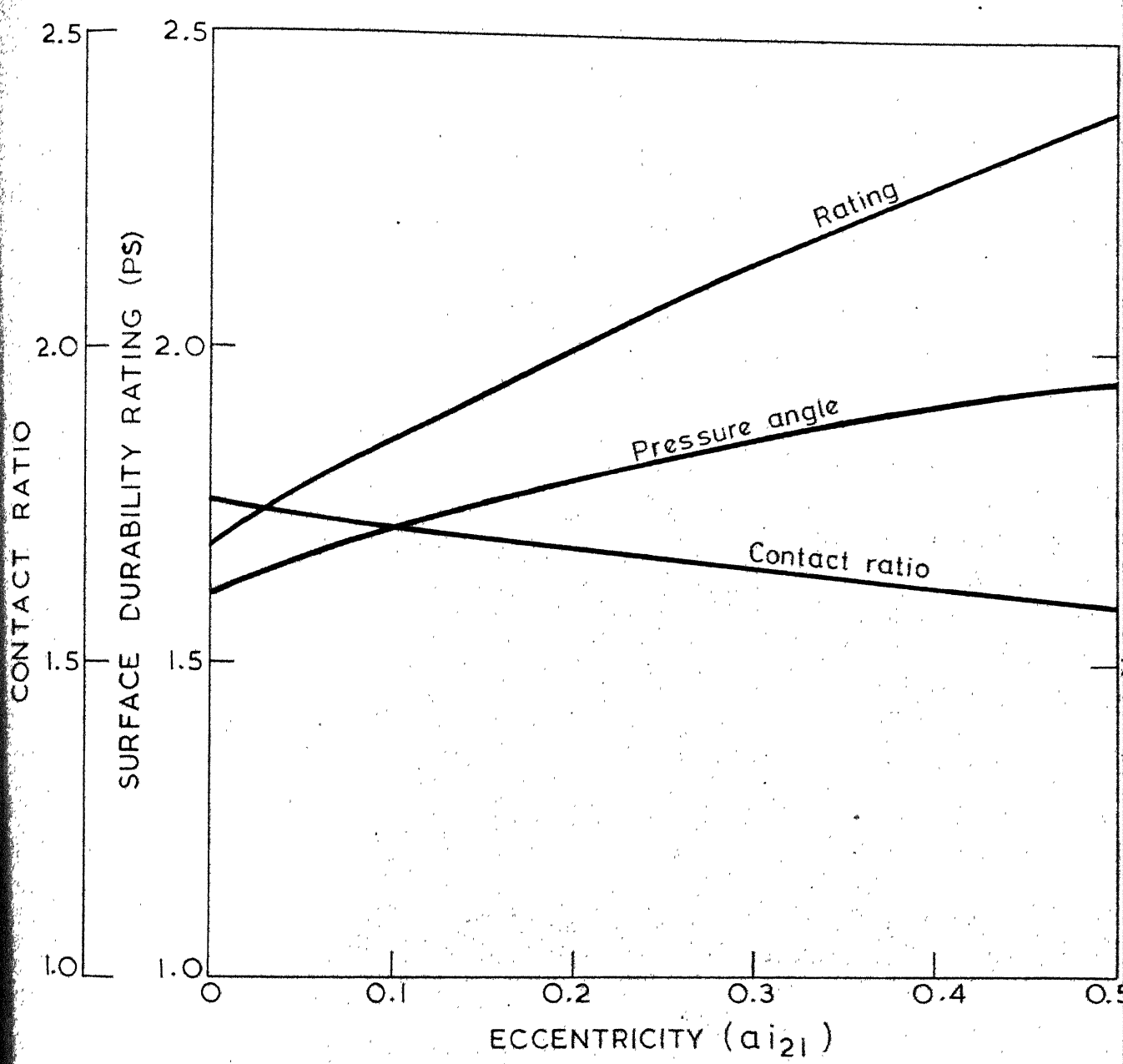

FIG.18 VARIATION OF SURFACE DURABILITY RATING, CONTACT RATIO AND PRESSURE ANGLE WITH ECCENTRICITY.

(OFF-SET FACE GEAR : $\Sigma = \pi/2$, $\beta = 0^\circ$, $Z_1 = 30$, $i_{21} = .25$, DZO=1, m = 2.5 mm, $\alpha_o = 20^\circ$ AND rpm = 100).

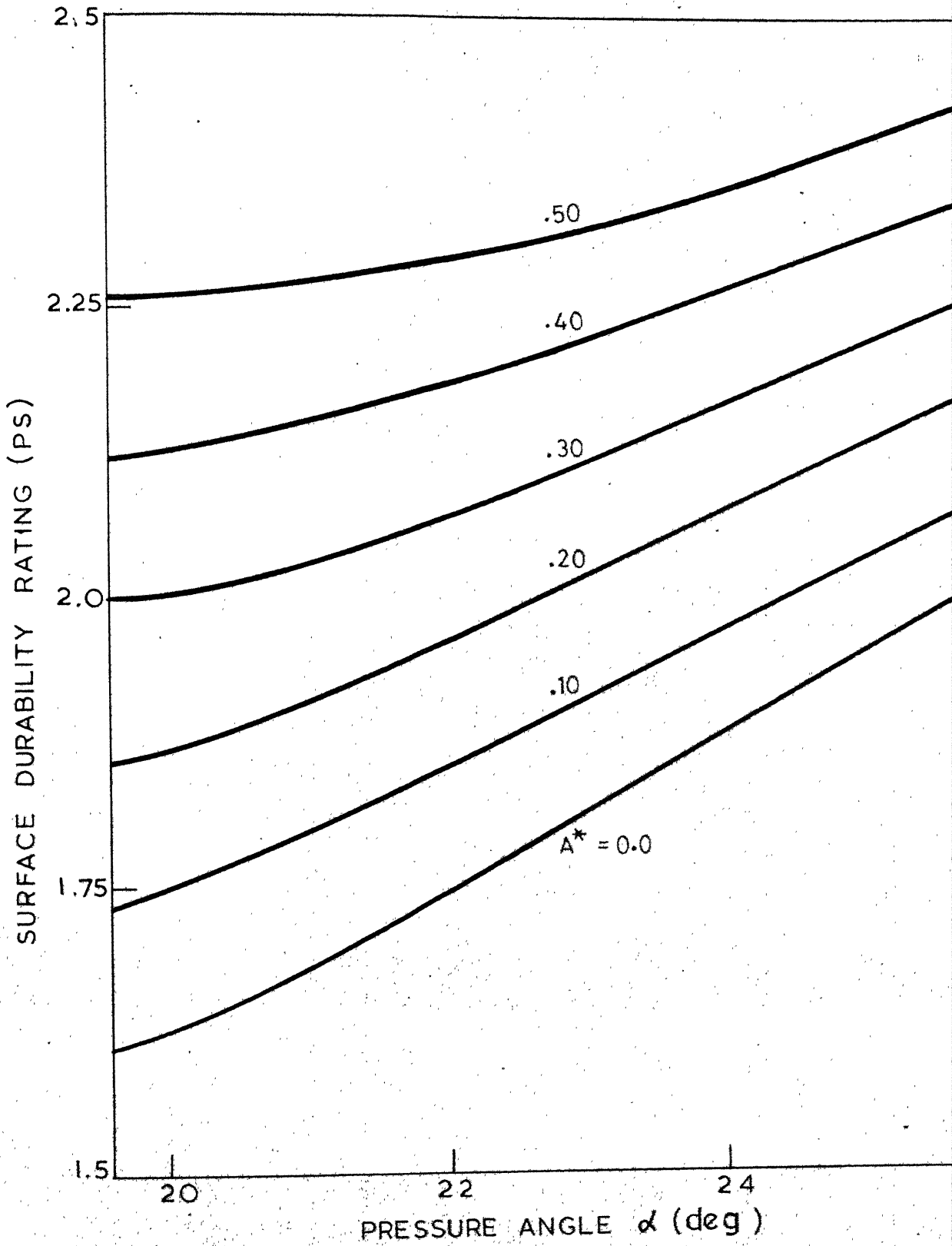

FIG.19. VARIATION OF SURFACE DURABILITY RATING WIT
PRESSURE ANGLE.

(OFF-SET FACE GEAR: $\Sigma = \pi/2$, $\beta = 0^\circ$, $Z_1 = 30$, $i_{21} = .2$

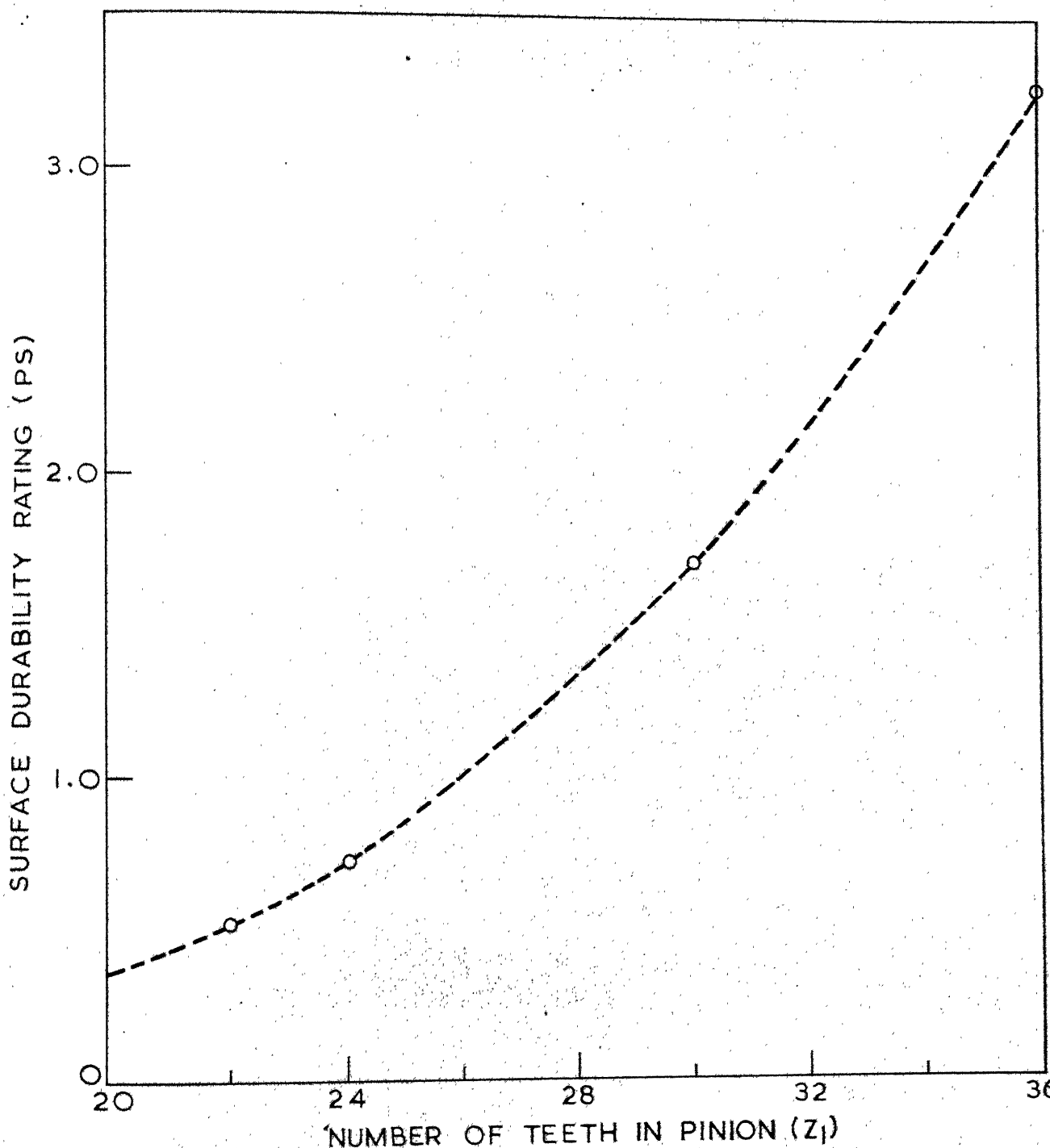

FIG.20 VARIATION OF SURFACE DURABILITY RATING WITH NUMBER OF TEETH IN PINION

(ON-CENTER FACE GEAR: $\Sigma = \pi/2$, $\beta = 0°$, $a = 0$, $i_{21} = .25$, $m = 2.5$ mm, $D20 = 1$, $\alpha_0 = 20°$ AND rpm = 100).

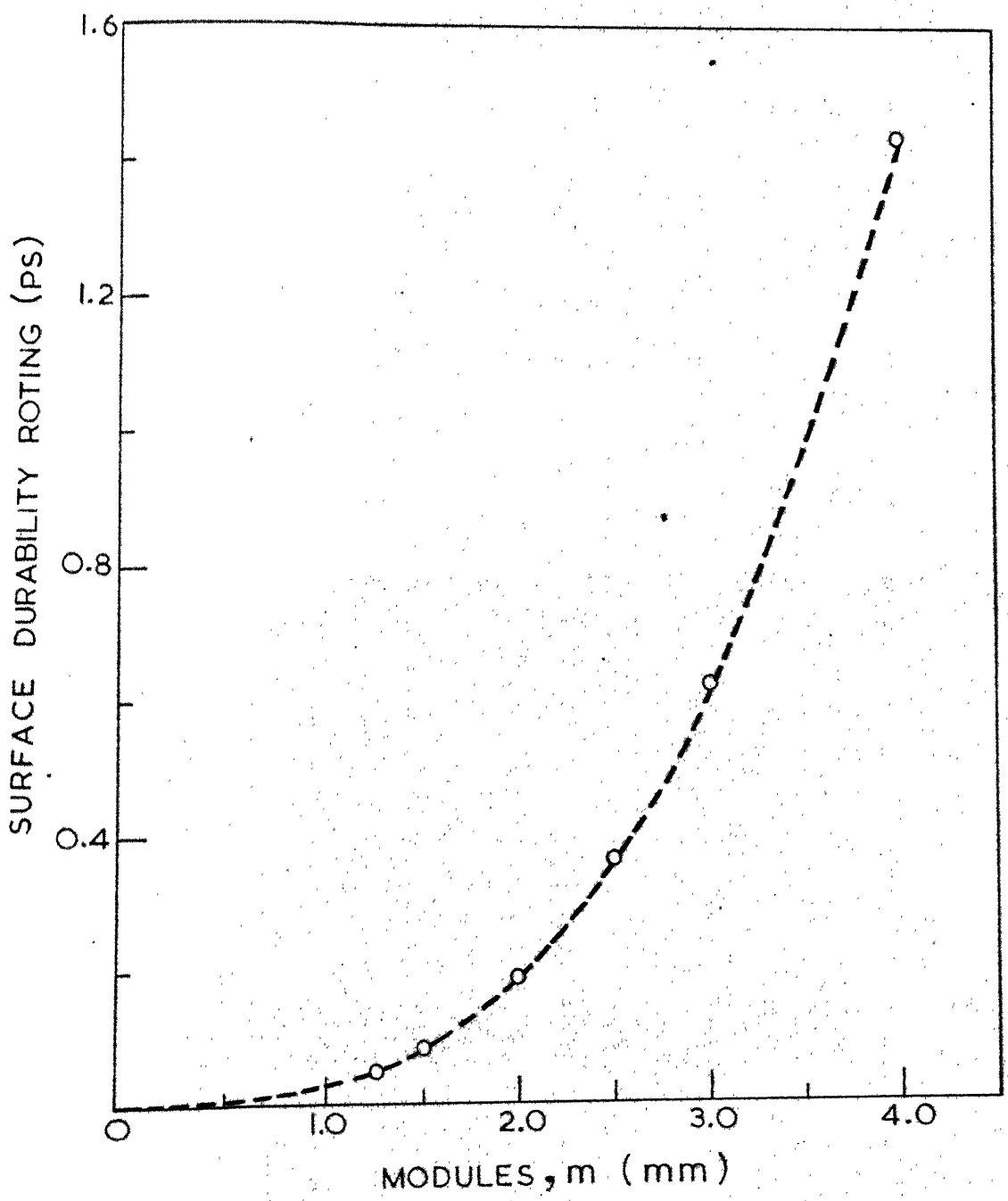

FIG. 21 VARIATION OF SURFACE DURABILITY RATING WITH MODULE.

(ON-CENTER FACE GEAR: $\Sigma = \pi/2$, $\beta = 0°$, $Z_1 = 20$, $i_{21} = .25$, $DZ_o = 1$, $\alpha_o = 20°$ AND rpm = 100).

the same transmission ratio and module, the face width is minimum when $\Sigma = 90$ degrees, that is, for face gears. The face width increases when Σ deviates from 90 degrees. It becomes infinite at values $\Sigma = 180$ degrees or $\Sigma = 0$ degree. These two cases correspond to the external and internal spur gears respectively. The face width decreases with an increase in the transmission ratio. This decrease is less prominent at higher transmission ratios. With an increase of the off-set, the face width decreases. An interesting result is that for a particular transmission ratio and module, the face width does not change appreciably when the number of teeth in a pinion are changed. For on-center face gears, the face width of gears, measured radially decreases with an increase of the helix angle.

In hypoid tapered gears, the blank shape for maximum utilization of surface of action is a curved surface. Face width and other characteristics depend upon the size and shape of the gear blank. In the present dissertation a method is given to find a suitable conical surface for a gear blank [Section 2.7] . In the absence of any accepted standard, choice is made of blank shape which is easy to manufacture and control. A need for further studies in this direction is felt to have a standardized practice for the selection of the shape of a gear blank.

The pressure angle on the pitch surface of tapered gears varies along the face. It is minimum at the small end of the blank cone and is maximum at the large end. In face gears, if the computed face width is large and has to be reduced, it is suggested that most

increase in the difference (DZO) the area of contact zone decreases. This results in lower surface durability rating with higher values of DZO [Figure 17] . The effect of DZO on gear tooth may be considered to be some sort of 'crowning' of the tooth. For an optimum load capacity, incorporating some crowning effect, DZO should be one. Similar result was also suggested by Francis and Silvagi [2] .

In the present work, it is found that the pressure angle (α), the difference in numbers of teeth in cutter and pinion (DZO) are the two additional convenient parameters to specify a face gear. The knowledge of α and DZO give the location of contact and the amount of correction to be applied while generating the pinion. Once these two are specified, the contact ratio, curvature and surface durability rating can be computed. For the specification of spur face gears, the following information should be available

i) Number of teeth of the involute pinion (Z_1)

ii) Transmission ratio (i_{21})

iii) Off-set (a)

iv) Pressure angle of the cutter (α_o)

v) Pressure angle (α)

vi) Difference in number of teeth of cutter and pinion (DZO).

The effect of contact localization on the contact ratio is shown in Figure 22. The contact ratio is determined by the blank sizes of pinion and gear and the line of action. These change with the contact localization. Consequently, the contact ratio is affected. It is observed that when contact is localized so as to have more

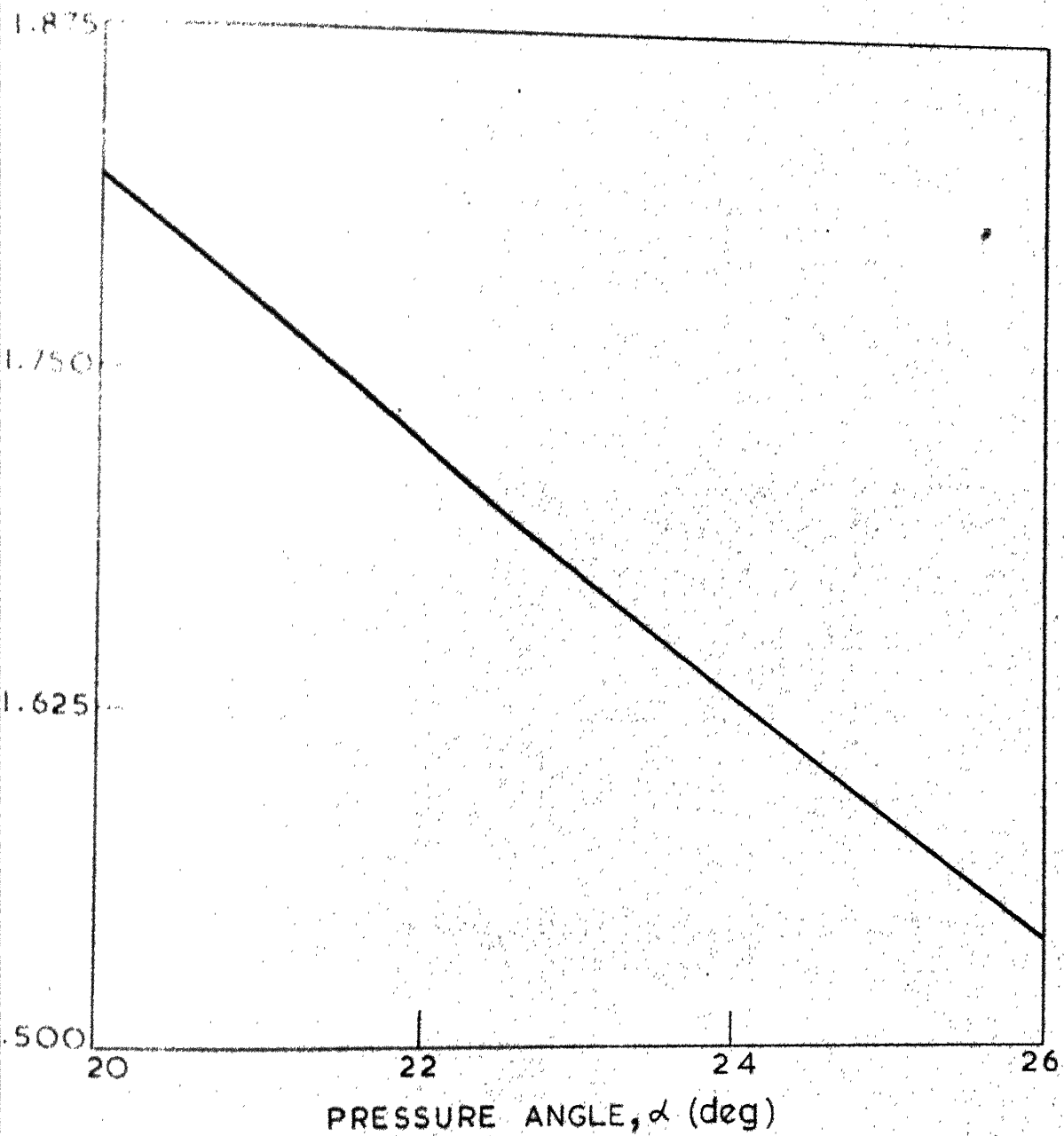

FIG. 22. VARIATION OF CONTACT RATIO WITH PRESSURE ANGLE.

(ON-CENTER FACE GEAR: $\Sigma = \pi/2$, $\beta = 0^\circ$, $a = 0$, $Z_1 = 30$, $i_{21} = .25$, $DZO_1 = 1$, $m = 2.5$ mm AND $\alpha_o = 20^\circ$).

favourable contact conditions, the contact ratio decreases; but the net effect is an increase in the surface durability rating.

To find the surface durability ratings of the face gears, in most of the cases the conditions are considered to be critical on the pitch surface [6] [29] . This forms the basis for evaluation of surface durability ratings. The critical contact conditions are considered to correspond to the contact point where the contact stress for single pair contact is maximum. It is observed that this point generally lies near the pitch surface. For some contact localization, this critical point may also lie on the pitch surface.

The dynamic loads on face gears can,theoretically,be evaluated by solving the differential equation of motion, considering varying system stiffness and damping factors. It is an involved task. In the present dissertation, the dynamic load factors for a face gear set is taken to be equal to that of hobbed or shaped spur gears [14] . Table 6 has been prepared based on the above assumption and presented in the similar form as Table 13-9 in reference [14] . It is seen from these two tables that the surface durability ratings are not exactly the same. In Table 6, the dynamic load factor is taken as mentioned earlier, S_{ac} = 135000 lb/in^2 and all other factors in equation (5.86) are assumed to be unity. As the table in reference [14] does not specify all these factors, so, strictly speaking, these two tables can not be compared.

It is seen from Figure 18 that the amount of off-set affects the surface durability ratings. The same conclusion was drawn in

reference [30] from a different point of view. These results have been contradicted by Coleman [29] . He has reported that an increase in pinion off-set leads to a decrease in load carrying capacity. Coleman arrived at this conclusion considering the effect of off-set on scoring. In the present work, load capacity is found considering resistance of the surface to pitting.

APPENDIX I

TRANSFORMATION MATRICES

The vector[1], R_α , given in S_α co-ordinate system is transformed to S_β co-ordinate system using the expression of the following type.

$$\begin{Bmatrix} R_\beta \\ 1 \end{Bmatrix} = [Q_{\beta\alpha}] \begin{Bmatrix} R_\alpha \\ 1 \end{Bmatrix} \qquad \text{I.1}$$

where, α , β are indices of co-ordinate systems and $Q_{\beta\alpha}[4 \times 4]$ is the transformation matrix for the co-ordinate systems.

The following are the transformation matrices for the co-ordinate system used in this work [Figure 1] .

$$Q_{\bar{1}1} = \begin{bmatrix} C\phi_1 & -S\phi_1 & 0 & 0 \\ S\phi_1 & C\phi_1 & 0 & 0 \\ 0 & 0 & 0 & 0 \\ 0 & 0 & 0 & 0 \end{bmatrix} \qquad \text{I.2}$$

$$Q_{1\bar{1}} = Q^T_{\bar{1}1} \qquad \text{I.3}$$

$$Q_{\bar{2}\bar{1}} = \begin{bmatrix} 1 & 0 & 0 & a \\ 0 & C\Sigma & -S\Sigma & 0 \\ 0 & S\Sigma & C\Sigma & 0 \\ 0 & 0 & 0 & 1 \end{bmatrix} \qquad \text{I.4}$$

---

1 Here, the vectors are $[3 \times 1]$ matrices.

$$Q_{22}^{-} = \begin{bmatrix} C\phi_2 & S\phi_2 & 0 & 0 \\ -S\phi_2 & C\phi_2 & 0 & 0 \\ 0 & 0 & 1 & 0 \\ 0 & 0 & 0 & 1 \end{bmatrix} \qquad \text{I.5}$$

and

$$Q_{21} = \begin{bmatrix} (C\phi_1 C\phi_2 + C\Sigma S\phi_1 S\phi_2), (-S\phi_1 C\phi_2 + C\Sigma C\phi_1 S\phi_2), (-S\Sigma S\phi_2), (aC\phi_2) \\ (-C\phi_1 S\phi_2 + C\Sigma S\phi_1 C\phi_2), (S\phi_1 S\phi_2 + C\Sigma C\phi_1 C\phi_2), (-S\Sigma C\phi_2), (-aS\phi_2) \\ (S\Sigma S\phi_1), (S\Sigma C\phi_1), (C\Sigma), 0 \\ 0, 0, 0, 1 \end{bmatrix}$$

APPENDIX II

CONDITION OF UNDERCUTTING OF GEAR TOOTH

Undercutting of the space mesh is due to the appearance of singular (cuspoidal) points on the surface of tooth during its generation. The fact that the surface generated by the cutting edge at the tip of the cutter cuts off some working portion of the tooth surface Σ_2 explains the undercutting of the space mesh. Undercutting leads to weaker teeth and the curvatures of the surfaces near the singular points have the values unfavorable from the point of view of contact stress. Therefore, the surfaces Σ_1 and Σ_2 should be limited so that the singular points are excluded.

The condition for undercutting of tooth generated by single parametric generation is given by Litvin [8] . The brief description of the development of condition for undercutting is given here for our direct reference.

It has been found in Litvin's work that for cuspoidal points the following condition holds good.

$$\underset{\sim}{V}_{ri} = 0, \; i = 1,2 \qquad \text{II.1}$$

where, $\underset{\sim}{V}_{ri}$ is the velocity of the contact point when it is moving on surface Σ_1 . This condition was used to locate cuspoidal points on the tooth surface. Direct use of the criterion $\underset{\sim}{V}_{r2} = 0$

for eliminating the cuspoidal points of contact of the surface Σ_2 is not always advantageous because surface Σ_2 is expressed in a complex form. The velocities of motion, $\underset{\sim}{V}_{r1}$ and $\underset{\sim}{V}_{r2}$ of the contact point along surfaces Σ_1 and Σ_2, respectively, are related by the following

$$\underset{\sim}{V}_{r2} = \underset{\sim}{V}_{r1} + \underset{\sim}{V}_1^{12} \qquad \text{II.2}$$

where $$\underset{\sim}{V}_{r1} = \frac{\partial \underset{\sim}{R}_1}{\partial \theta_k} \frac{d\theta_k}{dt} + \frac{\partial \underset{\sim}{R}_1}{\partial \lambda} \frac{d\lambda}{dt} \qquad \text{II.3}$$

It is assumed that these vectors are expressed in the co-ordinate system S_1. Equation (II.2) gives three scalar equations:

$$\frac{V_{x1}^{12}}{V_{xr1}} = \frac{V_{y1}^{12}}{V_{yr1}} = \frac{V_{z1}^{12}}{V_{zr1}} = -1 \qquad \text{II.4}$$

Out of these equations, only two are independent, as

$$\underset{\sim}{V}_{r1} \cdot \underset{\sim}{N}_1 = \underset{\sim}{V}_1^{12} \cdot \underset{\sim}{N}_1 = 0 \text{ (velocity vectors } \underset{\sim}{V}_{r1} \text{ and } \underset{\sim}{V}_1^{12} \text{ lie on the tangent plane)}$$

The equation of contact,

$$f(\theta_k, \lambda, \phi_1) = 0 , \qquad \text{II.5}$$

is an identity for all values of ϕ_1. By differentiating one gets,

$$\frac{\partial f}{\partial \theta_k} \cdot \frac{d\theta_k}{dt} + \frac{\partial f}{\partial \lambda} \frac{d\lambda}{dt} + \frac{\partial f}{\partial \phi_1} \frac{d\phi_1}{dt} = 0. \qquad \text{II.6}$$

Equations (II.4) and (II.6) contain the following three independent equations.

$$\frac{\partial f}{\partial \theta_k}\frac{d\theta_k}{dt} + \frac{\partial f}{\partial \lambda}\frac{d\lambda}{dt} = -\frac{\partial f}{\partial \phi_1}\frac{d\phi_1}{dt}$$

$$\frac{\partial R_{x1}}{\partial \theta_n}\frac{d\theta_k}{dt} + \frac{\partial R_{x1}}{\partial \lambda}\frac{d\lambda}{dt} = -V_{x1}^{12} \qquad \text{II.7}$$

$$\frac{\partial R_{z1}}{\partial \theta_k}\frac{d\theta_k}{dt} + \frac{\partial R_{z1}}{\partial \lambda}\frac{d\lambda}{dt} = -V_{z1}^{12}$$

As the system of equations is consistent the following condition must hold good.

$$\det \begin{vmatrix} \frac{\partial f}{\partial \theta_k} & \frac{\partial f}{\partial \lambda} & \frac{\partial f}{\partial \phi_1}\cdot\frac{d\phi_1}{dt} \\ \frac{\partial R_{x1}}{\partial \theta_k} & \frac{\partial R_{x1}}{\partial \lambda} & V_{x1}^{12} \\ \frac{\partial R_{z1}}{\partial \theta_k} & \frac{\partial R_{z1}}{\partial \lambda} & V_{z1}^{12} \end{vmatrix} = 0$$

The above equation is called the condition of undercutting. It can also be written as

$$V(\theta_k, \lambda, \phi_1) = 0 \qquad \text{II.9}$$

Equations (II.5) and (II.9) define the relation between the parameters of the surface, θ_k and λ, at the cuspoidal points of contact on the surface Σ_2.

APPENDIX III

PRINCIPAL CURVATURES AND DIRECTION ON THE GENERATED SURFACE

Spatial gearing with intersecting and offset axes are considered in this appendix. It is assumed that the first derivative of the velocity ratio (transmission ratio) is equal to zero, in the contact point locality. The equations, connecting principal curvatures and principal directions of the teeth surfaces are obtained. These equations have been derived earlier by Litvin [17] .

Consider two surfaces Σ_1 and Σ_2 in contact at a point. Let $\bar{i}_I$ and $\bar{i}_{II}$ be the unit vectors along principal directions and χ_I and χ_{II} be the principal curvatures of the surface Σ_1 at the contact point. The $\bar{i}_{III}$ and $\bar{i}_{IV}$ are the unit vectors along the principal directions and χ_{III} and χ_{IV} are the principal curvatures of the surface Σ_2.σ is the angle between the vectors $\bar{i}_I$ and $\bar{i}_{III}$ [Figure 12b] .

It can be proved that the following equations hold good at the contact point [17] .

$$\bar{R}_{\sim 1} = \bar{R}_{\sim 2},\ \bar{e}_{\sim 1} = \bar{e}_{\sim 2},\ \bar{e}_{\sim i} \cdot \bar{V}^{12}_{\sim 1} = 0;\ i = 1,2 \qquad \text{III.1}$$

$$\dot{\bar{R}}_{\sim 1} = \dot{\bar{R}}_{\sim 2},\ \dot{\bar{e}}^{1}_{\sim} = \dot{\bar{e}}^{2}_{\sim},\ \frac{d}{dt}(\bar{e}_{\sim i} \cdot \bar{V}^{12}_{\sim 1}) = 0 \qquad \text{III.2}$$

$$\bar{V}^{2}_{\sim r} = \bar{V}^{1}_{\sim r} + \bar{V}^{12}_{\sim} \qquad \text{III.3}$$

$$\dot{\underset{\sim}{e}}^2_r = \dot{\underset{\sim}{e}}^1_r + \underset{\sim}{\Omega}_{12} \times \underset{\sim}{e}_1 \qquad \text{III.4}$$

and

$$\dot{\underset{\sim}{e}}^1_r \cdot \underset{\sim}{V}^{12}_1 + (\underset{\sim}{\Omega}_1, \underset{\sim}{e}_1, \underset{\sim}{V}^{12}_1) + (\underset{\sim}{e}_1, \underset{\sim}{\Omega}_{12}, \dot{\underset{\sim}{R}}_1) = 0 \qquad \text{III.5}$$

Here, all vectors are assumed to be in fixed co-ordinate system $\bar{S}_1$. The vectors in equations (III.3) and (III.4), when resolved along the directions $\bar{i}_I$ and $\bar{i}_{II}$, give rise to following expressions [Figure 12b].

$$\bar{V}^2_{rI} = \bar{V}^2_{rIII}\, C\sigma - \bar{V}^2_{rIV}\, S\sigma$$

$$\bar{V}^2_{rII} = \bar{V}^2_{rIII}\, S\sigma + \bar{V}^2_{rIV}\, C\sigma$$

$$\dot{\bar{e}}^2_{rI} = \dot{\bar{e}}^2_{rIII}\, C\sigma - \dot{\bar{e}}^2_{rIV}\, S\sigma$$

$$\dot{\bar{e}}^2_{rII} = \dot{\bar{e}}^2_{rIV}\, S\sigma + \dot{\bar{e}}^2_{rIV}\, C\sigma$$

Along the principal directions the following equations hold good (Rodrigue's formula) [24].

$$\dot{\underset{\sim}{e}}^m_{ri} = -\chi_i \underset{\sim}{V}^m_{ri} \qquad m = 1 \ (i = I, II),\ m = 2 \ (i = III, IV) \qquad \text{III.6}$$

After transformation and simplification, a system of linear equations of the following type is obtained.

$$\begin{aligned} a_{11}\, \bar{V}^1_{rI} + a_{12}\, \bar{V}^1_{rII} &= b_1 \\ a_{11}\, \bar{V}^1_{rI} + a_{12}\, \bar{V}^1_{rII} &= b_2 \\ a_{31}\, \bar{V}^1_{rII} + a_{32}\, \bar{V}^1_{rII} &= b_3 \end{aligned} \qquad \text{III.7}$$

where

$$a_{11} = - \chi_I + \tfrac{1}{2}[\chi_{III} + \chi_{IV} + (\chi_{III} - \chi_{IV}) \cos 2\sigma)]$$

$$a_{12} = a_{21} = \tfrac{1}{2} (\chi_{III} - \chi_{IV}) \sin 2\sigma$$

$$a_{22} = - \chi_{II} + \tfrac{1}{2} [\chi_{III} + \chi_{IV} - (\chi_{III} - \chi_{IV}) \cos 2\sigma]$$

$$a_{31} = (\bar{e}_1, \Omega_{12}, \bar{i}_{II}) - \chi_I \bar{V}_I^{12}$$

$$a_{32} = (\bar{e}_1, \Omega_{12}, \bar{i}_{II}) - \chi_{II} \bar{V}_{II}^{12}$$

$$b_1 = (\bar{e}_1, \Omega_{12}, \bar{i}_I) - \tfrac{1}{2} \bar{V}_I^{12} \{\chi_{III} + \chi_{IV} + (\chi_{III} - \chi_{IV}) \cos 2\sigma\}$$

$$- \tfrac{1}{2} \bar{V}_{II}^{12} (\chi_{III} - \chi_{IV}) \sin 2\sigma$$

$$b_2 = (\bar{e}_1, \Omega_{12}, \bar{i}_{II}) - \tfrac{1}{2} \bar{V}_I^{12} \{(\chi_{III} - \chi_{IV}) \sin 2\sigma\} -$$

$$- \tfrac{1}{2} \bar{V}_{II}^{12} \{(\chi_{III} + \chi_{IV}) - (\chi_{III} - \chi_{IV}) \cos 2\sigma\}$$

$$b_3 = \bar{e}_1 \cdot (\Omega_2 \times \bar{V}_e^1 - \Omega_1 \times \bar{V}_e^2)$$

$$\bar{V}_e^1 = \Omega_1 \times \bar{R}_1 \text{ and } \bar{V}_e^2 = \Omega_2 \times \bar{R}_1 + \Delta \times \Omega_2.$$

When the contact is in a line, the system of linear equations must hold good for the different directions of $\bar{V}_r^1$. The system must be consistent but the values of $\bar{V}_{rI}^1$ and $\bar{V}_{rII}^1$ are not unique. This is possible if the rank of the matrix,

$$\begin{bmatrix} a_{11} & a_{12} & b_1 \\ a_{21} & a_{22} & b_2 \\ a_{31} & a_{32} & b_3 \end{bmatrix}$$

is equal to 1.

It follows, therefore, that

$$\frac{a_{11}}{a_{21}} = \frac{a_{12}}{a_{22}} = \frac{b_1}{b_2} \qquad \text{III.8}$$

$$\frac{a_{21}}{a_{31}} = \frac{a_{22}}{a_{32}} = \frac{b_2}{b_3} \qquad \text{III.9}$$

Since $a_{12} = a_{12}$, for above equations

$$\frac{a_{11}}{a_{21}} = \frac{a_{12}}{a_{22}} = \frac{a_{31}}{a_{32}} = \frac{b_1}{b_2} \qquad \text{III.10}$$

$$\frac{a_{21}}{a_{31}} = \frac{b_2}{b_3} \qquad \text{III.11}$$

From equations (III.10) one can get only two independent equations, because

$$b_1 = a_{31} - \bar{V}_I^{12}\, a_{11} - \bar{V}_{II}^{12}\, a_{12} \qquad \text{III.12}$$

$$b_2 = a_{32} - \bar{V}_I^{12}\, a_{12} - \bar{V}_{II}^{12}\, a_{22} \qquad \text{III.13}$$

Using equation (III.11) and the relation

$$\frac{a_{11}}{a_{21}} = \frac{a_{12}}{a_{22}} = \frac{a_{31}}{a_{32}} \quad ,$$

one gets three equations for the determination of χ_{III}, χ_{IV} and σ of the following form

$$\tan 2\sigma = \frac{2F}{\chi_I - \chi_{II} + G} \qquad \text{III.14}$$

$$\chi_{III} + \chi_{IV} = \chi_I + \chi_{II} + S \qquad \text{III.15}$$

$$\chi_{III} - \chi_{IV} = \frac{\chi - \chi_{II} + G}{\cos 2\sigma} \qquad \text{III.16}$$

where,

$$F = \frac{a_{31}\, a_{32}}{b_3 + \bar{V}_I^{12}\, a_{31} + \bar{V}_{II}^{12}\, a_{32}}$$

$$G = \frac{a_{31}^2 - a_{32}^2}{b_3 + \bar{V}_I^{12}\, a_{31} + \bar{V}_{II}^{12}\, a_{32}}$$

$$S = \frac{a_{31}^2 + a_{32}^2}{b_3 + \bar{V}_I^{12}\, a_{31} + \bar{V}_{II}^{12}\, a_{32}}$$

Appendix IV

RANGES OF PARAMETERS

In this appendix, the ranges of parameters for which results have been obtained in the report [22] are given. In that report following parameters are assumed constant,

pressure angle of the cutter, α_o - 20°,

addendum factor , f_o - 1 ,

radial clearance factor , c_o - 0.25,

correction factor of cutter , ξ_o - 0.

The following table shows the ranges of the parameter.

Type of gear	Phenomena	Ranges														
		Σ			β			i_{12}			A*			Z_1		
		min	max	step	min	max	step	min	max	step	min	max	step	min	max	step
Tapered	undercutting	105°	165°	15°	0°	25°	5°	1	10	1	0	.50	.05	17	30	1
	Pointing	105°	135°	15°	0°	25°	5°	1	10	1	0	.50	.05	17	30	1
Face	undercutting	90°	90°	-	0	25	5°	1	10	1	0	.5	.05	17	30	1
	Pointing	90°	90°	-	0	25	5°	1	10	1	0	.5	.05	17	30	1

The report also covers the intermediate results of calculations of surface durability rating, contact stress contact zone and effect of independent design parameters on surface durability ratings.

spalling ?

REFERENCES

1. G. Sanborn and B. Bloomfield "Effect of axis angle on tapered gear design" Gear design and application, edited by N.P.Chironis, McGraw Hill, 1967. P-83

2. Victor Francis and Joseph Silvagi "Face gear design factors" Gear design and application edited by N.P. Chironis, McGraw Hill , 1967. P-88

3. B. Bloomfield "Designing face gears" Machine design, Vol. 29, No. 4, p. 127, April 1947.

4. B. Bloomfield "Alignment charts for face gears" Product Engineering, p. 189, July 1952.

5. B.S. Bhadoria "Design parameters of orthogonal offset and on-center face gears" M. Tech. Thesis, Dept. of Mechanical Engg., I.I.T. Kanpur, 1970.

6. E. Buckingham "Analytic mechanics of gears" Dover Publications, Inc. N.Y. 1949.

7. B. Bloomfield "Designing tapered gears" Machine design, Vol. 20, No. 3, p. 125, March 1948.

8. F.L. Litvin "Theory of toothed gearing" Science Publishers, Moscow, 1968 (in Russian).

9. K.I. Gochman "Improved general theory of meshing" Odessa, 1886 (In Russian).

10. N.I. Kolchin "Analiticheski rachhot ploskikh i proctranstvemikh zatseplenu" Mashgiz, Moscow, 1949 (In Russian).

11. J. Chakraborty and B.S. Bhadoria "Design parameters of face gears" Jnl. Mechanisms, Vol. 6, p. 435 - 445, 1971.

12. J. Chakraborty and B.S. Bhadoria "Some studies on hypoid face gears" Paper 1M7/ASME/AGMA/IFTOMM. International Symposium on Gearing and transmission, Oct. 11 - 13, 1972, Sash Fransisco.

13. J. Chakraborty andD. Palit "Contact ratio of worm gears' ASME Publication 70 Mech - 49, 6th Conference of Mechanism.

14. E.J. Wellaues "Load rating of gears" Gear hand book, edited by D.W. Dudley, McGraw Hill, N.Y. 1962.

15. L.V. Krostelev "Curvatures mutually enveloping surfaces in space gearing" Collections of transmission in machines, Mashgig, Moscow 1963.

16. A.M. Pavlov "Determination of curvatures of mutually enveloping surfaces for space gears" Trudi LPI, leningrad, No. 211, 1960.

17. F.L. Litvin "The relation between the curvatures of tooth surface in space meshing" ZAMM, Vol. 49, No. 11, p. 685-690, 1969.

18. A. Dyson "A general theory of kinematics and geometry of gears in 3-D", Clarendon Press, Oxford, 1969.

19. M.L. Baxter "Basic theory of gear tooth action and generation" Gear hand book, edited by D.W. Dudley, McGraw Hill, N.Y. 1962.

20. O. Sarry "Mathematical background of Speriod gearing" Industrial mathematics, No. 7, 1956.

21. D. Palit "Investigation of some kinematic characteristics of cylindrical worm gear" M. Tech. Thesis, Dept. of Mech. Engg., I.I.T. Kanpur, 1969.

22. B.S. Bhadoria and J. Chakraborty "Design parameters of tapered gears in mesh with skew helical pinions" Technical report, Dept. of Mechanical Engg., I.I.T.Kanpur, 1973.

23. P.M. Dean "Gear tooth proportions" Gear hand book, edited by D.W. Dudley, McGraw Hill, N.Y. p. 545, 1962.

24. P.K.Rayabskiya "Differential geometry" Gonte, 1956, (In German).

25. B.F. Bregi "Gear finishing by shaving, honing and lapping" Gear hand book, edited by D.W. Dudley, McGraw Hill,N.Y. 1962.

26. S. Timoshenko and J.N. Goodier " Theory of elasticity" McGraw Hill. N.Y. 1951.

27. T.A. Harris "Rolling bearing analysis" John Willey and Sons, Inc., 1966.

28. Echnron, Hasbargen and Weigand "Ball and roller bearings" K.G. Heyden & Co., London, 1958.

29. W. Coleman "Gear design considerations" Inter disciplinary approach to the lubrication of concentrated contacts, edited by PMKU, Proceedings of NASA Symposium, Troy, N.Y. July 15-17, 1969.

30. R.W.Snidle and J.F. Archard "Lubrication of elliptical contacts" Inst. of Mech. Engrs., Tribology Convention, Gothenburg, Sweden, May 1969.